



HAL
open science

On induction machine faults detection using advanced parametric signal processing techniques

Youness Trachi

► **To cite this version:**

Youness Trachi. On induction machine faults detection using advanced parametric signal processing techniques. Other. Université de Bretagne occidentale - Brest, 2017. English. NNT : 2017BRES0103 . tel-01868185

HAL Id: tel-01868185

<https://theses.hal.science/tel-01868185>

Submitted on 5 Sep 2018

HAL is a multi-disciplinary open access archive for the deposit and dissemination of scientific research documents, whether they are published or not. The documents may come from teaching and research institutions in France or abroad, or from public or private research centers.

L'archive ouverte pluridisciplinaire **HAL**, est destinée au dépôt et à la diffusion de documents scientifiques de niveau recherche, publiés ou non, émanant des établissements d'enseignement et de recherche français ou étrangers, des laboratoires publics ou privés.



université de bretagne
occidentale

UNIVERSITE
BRETAGNE
LOIRE

THÈSE / UNIVERSITÉ DE BRETAGNE
OCCIDENTALE

sous le sceau de l'Université Bretagne Loire

pour obtenir le titre de

DOCTEUR DE L'UNIVERSITÉ DE BRETAGNE
OCCIDENTALE

Mention : Génie Electrique

École Doctorale des Sciences pour l'Ingénieur

présentée par

Youness TRACHI

Préparée au sein de la FRE CNRS 3744 IRDL

Institut de Recherche Dupuy de Lôme

On induction machine faults
detection using advanced
parametric signal
processing techniques

Thèse soutenue le 22 Novembre 2017

devant le jury composé de :

Claude DELPHA

Maître de Conférences – HDR, Université Paris-Sud / *rapporteur*

Demba DIALLO

Professeur, Université Paris-Sud / *président*

Mohamed EL BADAoui

Professeur, Université de Saint Etienne / *Rapporteur*

Emmanuel SCHAEFFER

Maître de Conférences, Université de Nantes / *examineur*

Tianzhen WANG

Professor, Shanghai Maritime University, Chine / *examineur*

Elhoussin ELBOUCHIKHI

Enseignant-Chercheur, ISEN Yncréa Ouest, Brest / *co-encadrant*

Mohamed BENBOUZID

Professeur, Université de Bretagne Occidentale / *directeur de thèse*

Abstract

This Ph.D. thesis aims to develop a reliable and cost-effective condition monitoring and faults detection architectures for induction machines. These architectures are mainly based on advanced parametric signal processing techniques. To analyze and detect faults, a parametric stator current model under stationary conditions has been considered. It is assumed to be multiple sinusoids with unknown parameters in noise. This model has been estimated using parametric techniques such as subspace spectral estimators and maximum likelihood estimator. A fault severity criterion based on the amplitude evaluations has been proposed to determine the induction machine severity. A novel faults detector based on hypothesis testing has been also proposed. This detector is mainly based on the generalized likelihood ratio test detector with unknown signal and noise parameters. The proposed parametric techniques have been evaluated using experimental stator current signals issued from induction machines under two considered faults: bearing and broken rotor bars faults. Experimental results show the effectiveness and the detection ability of the proposed parametric techniques.

List of Publications

The PhD thesis main results haven been published in the following international journals and conferences:

International journal papers:

1. **Y.Trachi**, E. Elbouchikhi, V. Choqueuse and M.E.H. Benbouzid, "A Novel Induction Machine Fault Detector Based on Hypothesis Testing", IEEE Transactions on Industry Applications, vol.: 53, n° 3, pp. 3039–3048, May/June 2017.
2. **Y.Trachi**, E. Elbouchikhi, V. Choqueuse and M.E.H. Benbouzid, "Induction machines fault detection based on subspace spectral estimation", IEEE Transactions on on Industrial Electronics, vol.: 63, n° 9, pp. 5641–5651, September 2016.

International conference papers:

1. **Y.Trachi**, E. Elbouchikhi, V. Choqueuse and M.E.H. Benbouzid, "Induction machine faults detection based on a constant false alarm rate detector", in Proceedings of the 2016 IEEE IECON, Florence (Italy), pp. 6359-6363, October 2016.
2. **Y.Trachi**, E. Elbouchikhi, V. Choqueuse and M.E.H. Benbouzid, "Stator current analysis by subspace methods for fault detection in induction machines", in Proceedings of the 2015 IEEE IECON, Yokohama (Japan), pp. 3479-3484, November 2015.
3. E. Elbouchikhi, V. Choqueuse, **Y.Trachi** and M.E.H. Benbouzid, "Induction machine bearing faults detection based on Hilbert-Huang transform", " in Proceedings of the 2015 IEEE ISIE, Buzios-Rio de Janeiro (Brazil), pp. 843-848, June 2015.



Table of Contents

List of Figures	ix
List of Tables	xiii
Introduction	1
1 Condition Monitoring and Fault Detection of Induction Machines:	
State of the Art	5
1.1 Introduction	7
1.2 Induction machine faults	7
1.2.1 Construction	7
1.2.2 Faults: types, causes, and effects	8
1.2.2.1 Stator faults	8
1.2.2.2 Broken rotor bars	9
1.2.2.3 Bearing faults	9
1.2.2.4 Air gap eccentricity	11
1.3 Maintenance Methods of Induction Machines	11
1.3.1 Corrective maintenance	12
1.3.2 Preventive maintenance	12
1.3.3 Predictive Maintenance	15
1.4 Existing Condition Monitoring Techniques	16
1.4.1 Oil Analysis	17
1.4.2 Vibration Monitoring	17
1.4.3 Acoustic Monitoring	18
1.4.4 Temperature Monitoring	19
1.4.5 Torque monitoring	20
1.4.6 Motor Current Signature Analysis	21

TABLE OF CONTENTS

1.5	Induction machine faults modeling	22
1.5.1	Finite element modeling	22
1.5.2	Magnetic equivalent circuit modeling	23
1.5.3	MMF and permeance wave modeling	23
1.5.4	Multiple Coupled Circuit modeling	24
1.5.5	dq modeling	25
1.6	Advanced feature extraction techniques for induction machine fault analysis	25
1.6.1	Power spectrum estimation	25
1.6.1.1	Nonparametric techniques	26
1.6.1.2	Higher order spectra analysis	30
1.6.1.3	Parametric techniques	30
1.6.2	Demodulation techniques	33
1.6.2.1	Monodimensional techniques	34
1.6.2.2	Multidimensional techniques	36
1.6.3	Advanced feature extraction techniques for induction machines in non-stationary environments	38
1.7	Induction machine fault detection techniques	40
1.7.1	Artificial intelligence techniques	40
1.7.1.1	Expert Systems	40
1.7.1.2	Fuzzy logic	41
1.7.1.3	Artificial Neural Networks	42
1.7.1.4	Support Vector Machine	44
1.7.1.5	Genetic Algorithms	44
1.7.1.6	Hybrid Approaches	46
1.7.2	Statistical decision theory	46
1.8	Conclusion	47
2	Stator Current Parameters Estimation and Fault Severity Analysis	49
2.1	Introduction	50
2.2	Stator Current Model	50
2.2.1	Stator Current Model in Stationary Conditions	50
2.2.2	Stator Current Frequency Model	52

TABLE OF CONTENTS

2.2.3	Stator Current Parameters Estimation	53
2.3	Subspace Spectral Estimation Techniques	56
2.3.1	Covariance Matrix	56
2.3.2	MUSIC Estimators	57
2.3.3	ESPRIT Estimators	60
2.3.4	Modified ESPRIT	62
2.4	Model Order Estimation	66
2.4.1	Model Order Estimation (Nonparametric Approach)	67
2.4.2	Model Order Selection (Parametric Approach)	69
2.5	Proposed Fault Detection Methodology	70
2.5.1	Proposed Fault Severity Criterion	70
2.5.2	Condition Monitoring Architecture	71
2.6	Simulations Results	72
2.6.1	Subspace Techniques Performances	73
2.6.2	Model Order Selection Performances	75
2.6.3	Fault Severity Criterion Performances	76
2.7	Conclusion	77
3	Induction Machine Fault Detection based on the Generalised Likelihood Ratio Test	79
3.1	Introduction	81
3.2	Statistical Decision Theory	81
3.2.1	Simple Binary Hypothesis Testing	81
3.2.2	Bayes Criterion	83
3.2.3	Minmax Criterion	88
3.2.4	Neyman-Pearson Criterion	89
3.2.5	Receiver Operating Characteristics	91
3.3	Composite Hypothesis Testing	93
3.3.1	BLRT Approach for Composite Hypothesis Testing	93
3.3.2	GLRT Approach for Composite Hypothesis Testing	95
3.4	Proposed Induction Machine Faults Detector	97
3.4.1	Problem Formulation	97
3.4.2	GLRT of the Stator Current Model	98

TABLE OF CONTENTS

3.4.3	Performance of the Proposed Faults Detector	100
3.4.4	Proposed Induction Machine Faults Detection Architecture . . .	103
3.5	Simulations Results	103
3.5.1	Simulations Parameters	103
3.5.2	ROC curves and Histogram	104
3.5.3	Influences of SNR , N , and P_{Fa}	105
3.6	Conclusion	105
4	Experimental Validation	109
4.1	Introduction	110
4.2	Experimental Setup Description	110
4.2.1	Setup Description for Bearing Faults	111
4.2.2	Setup Description for Broken Rotor Bars	111
4.3	Experimental Results for Bearing Faults	111
4.3.1	Spectral Estimation Techniques	112
4.3.2	Demodulation Techniques	114
4.3.3	Fault Severity Analysis	117
4.3.4	GLRT-Based Faults Detection	119
4.4	Experimental Results for Broken Rotor Bars	120
4.4.1	Spectral Estimation Techniques	120
4.4.2	Demodulation Techniques	121
4.4.3	Fault Severity Detection	124
4.4.4	GLRT-Based Faults Detection	125
4.5	Conclusion	127
5	Conclusions and Recommendations for Future Research	129
	References	131



List of Figures

1.1	Induction machines construction [1].	8
1.2	Distributions of induction motor faults [2].	9
1.3	Bearing structure with main dimensions.	10
1.4	Different types of eccentricity.	12
1.5	Failure data modeling process [3].	13
1.6	Maintenance decision making process [3].	14
1.7	Condition diagnosis monitoring framework [4].	16
1.8	Family of periodogram-based techniques.	27
1.9	The choose of the demodulation technique [5].	33
1.10	Analytic signal estimation [5].	34
1.11	Synchronous demodulator [6].	35
1.12	Hilbert transform-based demodulation.	36
1.13	Bedrosian theorem conditions.	36
1.14	Basic architecture of a rule-based expert system [7, 8].	41
1.15	Block diagram of the fuzzy diagnostic system based diagnostic system [8, 9].	43
2.1	Plot of $J(\mathbf{x}, \mathbf{\Omega}, \boldsymbol{\theta})$ for five frequencies with the frequency structure given in (2.3) with $f_s = 50Hz$, $f_c = 4Hz$, and $k = \{0, 1, 2\}$	55
2.2	Proposed condition monitoring architecture of induction machines.	72
2.3	Stator current spectrum based on MUSIC estimators and BIC for a healthy and faulty induction machines with severity 4.	73
2.4	Stator current spectrum based on ESPRIT estimators and BIC for a healthy and faulty induction machines with severity 4.	74

LIST OF FIGURES

2.5	Stator current spectrum based on Modified ESPRIT estimators and BIC for a healthy and faulty induction machines with severity 4.	74
2.6	MSE for frequency estimation.	75
2.7	SNR and samples number influences on the model order selection based on eigenvalues of the covariance matrix.	75
2.8	SNR and samples number influences on the model order selection based on penalized likelihood metric.	76
2.9	Severity and samples number influences in FSC value with $SNR = 30$	76
3.1	Probability density functions under \mathcal{H}_0 and \mathcal{H}_1	88
3.2	Risk \mathcal{R} versus $P(\mathcal{H}_1)$	89
3.3	Example of ROC curve.	91
3.4	ROC curves with $m = 0.1$ and $N = 100$	92
3.5	Proposed fault detection architecture of induction machines.	104
3.6	ROC curves and histogram of the estimated $\mathcal{T}(\mathbf{x})$	105
3.7	GLRT performance with respect to N and SNR	106
3.8	Evolution of P_D with respect to N for several desired fault alarm probability.	106
4.1	Machinery fault simulator.	110
4.2	The stator current for healthy and faulty induction machines.	112
4.3	Spectral analysis by Welch periodogram using Hanning window ($N = 2000$) for a healthy and faulty induction machines with bearing faults.	112
4.4	Stator current spectrum based on the subspace techniques and BIC criterion for a healthy and faulty induction machines with bearing faults (severity4).	113
4.5	Synchronous demodulation for a healthy and faulty induction machines with bearing faults (severity4).	114
4.6	Hilbert transform-based demodulation for a healthy and faulty induction machines with bearing faults (severity4).	115
4.7	Teager energy operator-based demodulation for a healthy and faulty induction machines with bearing faults (severity4).	115
4.8	CT-based demodulation for a healthy and faulty induction machines with bearing faults (severity4).	116

4.9	ML-based demodulation for a healthy and faulty induction machines with bearing faults (severity4).	116
4.10	PCA-based demodulation for a healthy and faulty induction machines with bearing faults (severity4).	117
4.11	Fault severity criterion value versus bearing fault degrees using demodulation techniques.	117
4.12	Fault severity criterion value versus bearing fault degrees of induction machines.	118
4.13	Fault severity criterion value versus N (samples number) for bearing faults using TLS ESPRIT, for healthy and faulty induction machines with bearing faults.	118
4.14	GLRT criterion with different N for a healthy machine and faulty induction machines with different considered severities of bearing faults ($P_{Fa} = 10^{-3}$).	119
4.15	The stator current for healthy and faulty induction machines.	120
4.16	The stator current for healthy and faulty induction machines.	121
4.17	Spectral analysis by Welch periodogram using Hanning window ($N = 4096$) for a healthy and faulty induction machines with broken rotor bar faults.	121
4.18	Stator current spectrum based on the subspace techniques and BIC criterion for a healthy and faulty induction machines with three broken rotor bars.	122
4.19	Synchronous demodulation for a healthy and faulty induction machines with three broken rotor bars.	123
4.20	Hilbert transform-based demodulation for a healthy and faulty induction machines with three broken rotor bars.	123
4.21	Teager energy operator-based demodulation for a healthy and faulty induction machines with three broken rotor bars.	124
4.22	CT-based demodulation for a healthy and faulty induction machines with three broken rotor bars.	124
4.23	ML-based demodulation for a healthy and faulty induction machines with three broken rotor bars.	125

LIST OF FIGURES

4.24 PCA-based demodulation for a healthy and faulty induction machines with three broken rotor bars.	125
4.25 Fault severity criterion for different BRB fault degrees. In this figure, 0 corresponds to healthy induction machine and other values correspond to BRB number.	126
4.26 Fault severity criterion value for different N (samples number) for bearing faults using TLS ESPRIT, for healthy and faulty induction machines with broken rotor bars.	126
4.27 GLRT criterion with different N for a healthy machine and faulty induction machine with different considered severities of broken rotor bars ($P_{Fa} = 10^{-3}$).	127



List of Tables

2.1	Simulation parameters $L = 5$	73
3.1	The four possible case of a binary hypothesis test.	82
3.2	Simulation parameters ($L=5$).	103
4.1	Bearing fault severity versus hole diameter.	111

LIST OF TABLES



Introduction

Induction machines also called asynchronous machines are the most used in electromechanical energy conversion systems thanks to their advantages such as simple construction, ruggedness, efficiency, high reliability and low cost. Their applications include: renewable energy systems, variable speed applications. These electromechanical machines are subjected to several faults that can be categorized into electrical faults and mechanical faults. These faults may lead to fatal consequences such as cost expensive downtime and maintenance. Then, developing a condition monitoring and fault diagnosis techniques are challenging topics of industrial applications. Condition monitoring systems permit to detect and analyze faults at an early stage to avoid the substantial cost penalties. Fault diagnosis systems consist of the three following process: fault detection (i.e. taking notice of the fault appearance at a certain time instant), fault isolation (i.e. determining the nature and the place of its occurrence), and fault analysis or identification (i.e. recognition of the size and nature of the fault variability) [10]. Fault diagnosis systems can determine: the occurrence of faults, the fault type, the fault severity, and the next fault would occur.

In the literature, condition monitoring and fault diagnosis systems can be classified into three main techniques: signal-based techniques (mechanical vibration analysis, shock pulse monitoring, temperature measurement, acoustic noise analysis, electromagnetic field monitoring through inserted coil, instantaneous output power variation analysis, infrared analysis, gas analysis, oil analysis, radio-frequency emission monitoring, partial discharge measurement, motor current signature analysis, and statistical analysis of relevant signals), model-based techniques (neural network, fuzzy logic analysis, genetic algorithm, artificial intelligence, finite-element magnetic circuit equivalents, and linear-circuit-theory-based mathematical models), machine-theory-based fault analysis, simulations-based fault analysis (finite-element analysis, and time-step coupled finite element state space analysis) [11–14]. Regarding induction machine fault indicators,

INTRODUCTION

stator current-based techniques are the satisfactory and the promising techniques in the industrial applications due to several advantages: easy-access, the ease of implementation, the information richness, and the ability to detect electrical and mechanical faults. In fact, stator current measurements do not require an additional sensors or data acquisition devices.

Regarding the literature review of the advanced feature extraction techniques for induction machine fault analysis, it can be distinguished between two main conditions: stationary and non-stationary environments. For stationary environments, there are three main categories of feature extraction techniques: power spectrum (second order spectrum) estimation, demodulation techniques, and higher order spectra analysis. There are mainly two types of power spectrum estimation: nonparametric methods (Periodogram and its extension) and parametric methods (maximum likelihood estimator and subspace techniques). Demodulation techniques can be categorized into monodimensional techniques (synchronous demodulator, Teager energy operator, and Hilbert transform) and multidimensional techniques (Concordia transform, maximum likelihood approach, principal component analysis, and empirical mode decomposition and its extensions). For non-stationary environments, feature extraction techniques can be classified into the following categories: parametric techniques, nonparametric techniques (time-frequency and time-scale presentations), and demodulation techniques (Hilbert-Huang transform).

These PhD thesis focuses on the induction machines faults detection using parametric stator current model under stationary conditions. The objective then is to propose practical schemes using the advanced signal processing and statistical analysis techniques that exploit stator current measurements. A stator current model parameters estimators is investigated in these works. These estimators use the particular stator current frequency structure under faulty conditions to determine the machine state using a fault severity criterion. The corresponding estimations can be also exploited to define faults detector using statistical decision theory.

Contributions of this thesis can be summarized as follows

- A model order estimator is proposed that associates the order-selection rule with the maximum likelihood method.

- A new fault severity analysis has been proposed to measure and determine the state of induction machines. This analysis can detect the faults degree even in the presence of harmonic components. The major advantages of this fault analysis criterion are its low computational complexity and its ability to automatically detect faults without need of an expert for interpreting the stator current spectrum.
- A novel induction machine faults detector based on the hypothesis testing has been also proposed. Indeed, a composite hypothesis testing with nuisance parameters is considered.

This manuscript is organized as follows

- **Chapter I** gives the state of the art for condition monitoring and faults detection of induction machines. It presents the main faults that can occur under different operating conditions. This chapter describes the basic maintenance in the industry applications. It reviews also the existing condition monitoring techniques. A literature review of the induction machine faults modeling is also presented. It describe the most popular advanced feature extraction techniques and the existing faults detection techniques.
- **Chapter II** presents the stator current parameters estimation under stationary conditions. It starts with a description of the stator current model to define the problem of the parameters estimation. Three main estimations are considered in this chapter: model order selection, frequency estimation, amplitudes and phases estimation. This chapter proposes a fault severity analysis using amplitude estimates. Simulations results are presented to analyze performances of the proposed parametric techniques.
- **Chapter III** presents the different decision rules of the statical decision theory. Two cases are considered in this chapter, simple and composite binary hypothesis testing. It describes the way that allows analyzing the detector performances in the binary hypothesis testing context. In this chapter, the faults detection problem is referred to composite hypothesis testing with unknown signal and noise parameters. It proposes the generalized likelihood ratio test detector of the proposed stator current model and its performances according to the detection and

INTRODUCTION

the false alarm probabilities. Finally, performances are evaluated using synthetic signals.

- **Chapter IV** shows experimental results for two induction machines: healthy and faulty machines. Two faults are considered in this chapter: bearing and broken rotor bars faults. These faults are investigated according to several feature extraction techniques such as demodulation techniques, nonparametric techniques, and parametric techniques. This chapter shows also the performances of the proposed parametric detector.
- **Chapter V** concludes this manuscript and proposes directions for further works.

Condition Monitoring and Fault Detection of Induction Machines: State of the Art

Contents

1.1	Introduction	7
1.2	Induction machine faults	7
1.2.1	Construction	7
1.2.2	Faults: types, causes, and effects	8
1.3	Maintenance Methods of Induction Machines	11
1.3.1	Corrective maintenance	12
1.3.2	Preventive maintenance	12
1.3.3	Predictive Maintenance	15
1.4	Existing Condition Monitoring Techniques	16
1.4.1	Oil Analysis	17
1.4.2	Vibration Monitoring	17
1.4.3	Acoustic Monitoring	18
1.4.4	Temperature Monitoring	19
1.4.5	Torque monitoring	20
1.4.6	Motor Current Signature Analysis	21
1.5	Induction machine faults modeling	22
1.5.1	Finite element modeling	22
1.5.2	Magnetic equivalent circuit modeling	23
1.5.3	MMF and permeance wave modeling	23
1.5.4	Multiple Coupled Circuit modeling	24
1.5.5	dq modeling	25

1. CONDITION MONITORING AND FAULT DETECTION OF INDUCTION MACHINES: STATE OF THE ART

1.6	Advanced feature extraction techniques for induction machine fault analysis	25
1.6.1	Power spectrum estimation	25
1.6.2	Demodulation techniques	33
1.6.3	Advanced feature extraction techniques for induction machines in non-stationary environments	38
1.7	Induction machine fault detection techniques	40
1.7.1	Artificial intelligence techniques	40
1.7.2	Statistical decision theory	46
1.8	Conclusion	47

1.1 Introduction

This chapter aims to review the various induction machine condition monitoring and faults detection techniques. It reviews induction machine faults, their causes, and their effects. It presents also maintenance methods and existing condition monitoring techniques. A brief review of the induction machine fault modeling is also given. Existing advanced feature extraction techniques for induction machine fault analysis in stationary and nonstationary environments are also studied. Finally, it reviews the main induction machine faults detection and diagnosis techniques.

1.2 Induction machine faults

This section focuses on the construction of induction machines to understand their physical realization. It also reviews the main induction machine faults, causes, and consequences. It presents four mainly faults that can appear in the operating condition: stator faults, broken rotor bars, bearing faults, and air-gap eccentricities.

1.2.1 Construction

Induction machines mainly consist of the following elements (see Fig.1.1):

- The Stator is the outer stationary part of induction machines. It consists of three main parts: stator frame, stator core, stator winding or field winding. The stator frame is the outer most part in machines who's the main function is to support the stator core and the field winding. The stator core allows carrying alternating flux. The stator winding is simply the stationary winding that has a very low resistance and the winding is also insulated from the frame.
- The Rotor is the rotating part of induction machines. These machines are classified according to their rotor. There are two types of induction machine rotors: squirrel cage rotor and slip ring rotor or wound rotor or phase wound rotor. The rotor is connected to the mechanical load through the shaft.
- Other parts such as: end-flanges, bearings, steel shaft, cooling fan, and terminal box.

1. CONDITION MONITORING AND FAULT DETECTION OF INDUCTION MACHINES: STATE OF THE ART

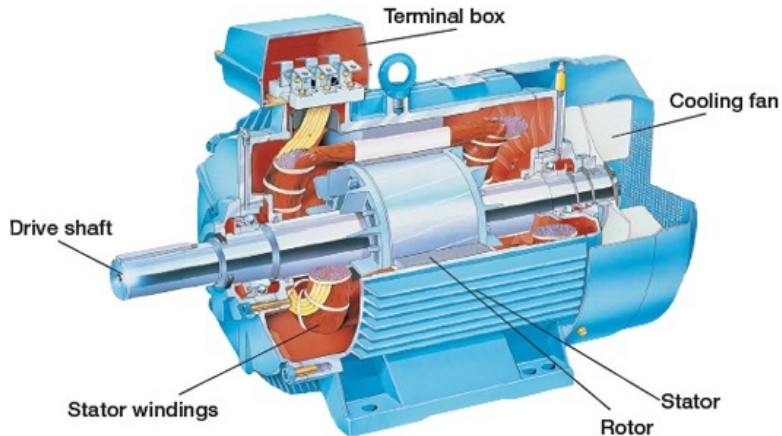


Figure 1.1: Induction machines construction [1].

1.2.2 Faults: types, causes, and effects

Induction machines are subjected to many fault types. In the literature, these faults can be categorized into electrical faults and mechanical faults. Electrical faults include unbalance supply voltage or current, single phasing, reverse phase sequence, earth fault, overload, inter-turn short-circuit fault, and broken rotor bars [15]. Besides, mechanical faults are the most frequent faults in induction machines. These faults include mass unbalance, air gap eccentricity, bearing damage, rotor winding failure, and stator winding failure [14]. The most studied faults in the literature are: bearing faults, stator faults, broken rotor bars, and eccentricity faults. Distributions of induction motor faults according to IEEE and EPRI studies are given in Fig. 1.2 [2].

1.2.2.1 Stator faults

Stator faults can be classified as the lamination or frame fault (core defect, circulation current, or ground, etc.) and the stator winding fault (winding insulation damage, displacement of conductors, etc.) [14]. These faults are due to various stresses: mechanical (due to movement of stator coil and rotor striking the stator), electrical (due to the supply voltage transient), thermal (due to thermal overloading), and environmental (environment too hot, too cold, or too humid) [13]. Stator fault frequencies are given by [14, 16]

$$f_{sf} = f_s \left| \frac{m}{p} (1 - s) \pm k \right| \quad (1.1)$$

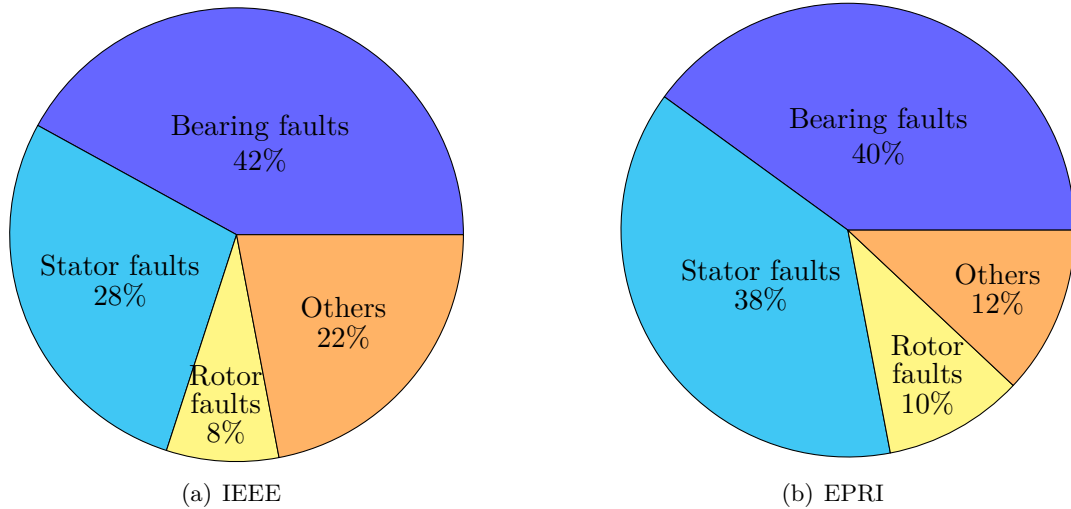


Figure 1.2: Distributions of induction motor faults [2].

where f_s is the supply frequency in Hz, s is the slip, p is the number of pole pairs, $m \in \mathbb{N}...$ and $k = 1, 3, 5, \dots$

1.2.2.2 Broken rotor bars

Broken rotor bars (BRB) are the most frequent faults in the rotor. These faults occur when bars are partially cracked or completely broken. These faults can be caused by various stresses [12, 17, 18]: thermal (due to thermal overload), mechanical (caused by loose laminations, fatigued parts, or bearing faults), magnetic (caused by electromagnetic forces, unbalanced magnetic pull), dynamic (due to shaft torques), and environmental (due to contamination, abrasion of rotor material). These faults result in an unbalanced rotor flux and additional faulty frequency components appear in the stator current spectrum [18]. These frequencies are given by [19]

$$f_{brb} = f_s |1 \pm 2ks| \quad (1.2)$$

where $k \in \mathbb{N}^*$.

1.2.2.3 Bearing faults

Bearing faults are the most frequent faults in induction machines [20]. The bearing consists mainly of outer raceway, inner raceway, balls, and the cage which assures

1. CONDITION MONITORING AND FAULT DETECTION OF INDUCTION MACHINES: STATE OF THE ART

equidistance between the balls. Bearing faults can be classified according to the affected element: outer raceway fault, inner raceway fault, balls fault, and cage fault. Several factors can lead to bearing faults: excessive loads, excessive temperature rise, corrosion, contamination, lubricant failure, and misalignment of bearings [12, 15]. The remarkable effects of these faults are: rise in temperature, increase in vibration. Moreover, these faults can introduce mechanical oscillations and eccentricity faults.

For each type of bearing faults, a characteristic frequency f_c can be associated [20, 21]. Their expressions for the four considered fault types are given by [20, 21]

$$\begin{cases} f_o = \frac{N_b}{2} f_r \left(1 - \frac{D_b}{D_c} \cos \alpha \right) \\ f_i = \frac{N_b}{2} f_r \left(1 + \frac{D_b}{D_c} \cos \alpha \right) \\ f_b = \frac{D_c}{D_b} f_r \left(1 - \frac{D_b^2}{D_c^2} \cos^2 \alpha \right) \\ f_{ca} = \frac{1}{2} f_r \left(1 - \frac{D_b}{D_c} \cos \alpha \right) \end{cases} \quad (1.3)$$

where f_o is the outer raceway fault frequency, f_i the inner raceway fault frequency, f_b the ball fault frequency, f_{ca} the cage fault frequency, N_b the number of balls, D_b the ball diameter, D_c the bearing pitch diameter, and α the contact angle of the balls on the races. Bearing structure with main dimensions are given in Fig. 1.3.

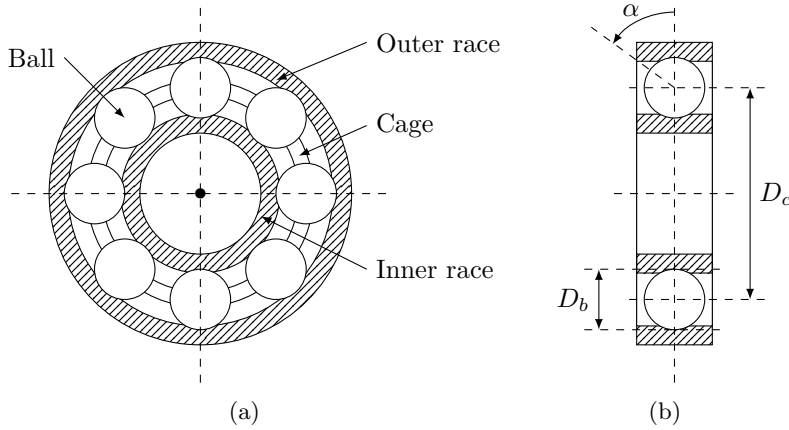


Figure 1.3: Bearing structure with main dimensions.

1.2.2.4 Air gap eccentricity

Air gap eccentricity is a mechanical fault that is defined as an unbalanced air-gap between the rotor and stator of electrical machines. Three eccentricity types can be distinguished: static eccentricity, dynamic eccentricity, and mixed eccentricity. The static eccentricity appears when the position of the minimum air gap remains fixed in space. Besides, dynamic eccentricity appears when the rotation axis of the rotor does not overlap its geometric axis, so that the position of the minimum air gap changes with time. The mixed eccentricity appear when the static and the dynamic eccentricities occur. The three cases are shown in Fig. 1.4.

These faults are due to several factors such as: manufacturing tolerance, an oval stator core, incorrect bearing positioning, and bearing wear. Effects of these faults are: unbalanced magnetic pull, decrease in rotor speed, and appearance of fault frequency components in the stator current. Eccentricity faults affect particular characteristic frequency components in the machine such as air-gap magnetic field, torque, speed, and stator currents. For each eccentricity fault, a fault frequency can be associated [22, 23]:

$$f_{ecc} = f_s \left| \left(nR \frac{1-s}{p} \pm k \right) \pm \left(n_d \frac{1-s}{p} \pm 2n_{sat} \right) \right| \quad (1.4)$$

where R is the number of rotor slots, p is the number of fundamental pole pairs, n_d is the eccentricity order ($n_d = 0$ for static eccentricity, $n_d = 1$ for dynamic eccentricity), n is any positive integer, n_{sat} models magnetic saturation ($n_{sat} = 0, 1, 2, \dots$, and k is the order of harmonics. In case of mixed eccentricity, the fault frequency is given by

$$f_{ecc} = f_s \left| 1 \pm n \frac{1-s}{p} \right| = f_s \pm n f_r \quad (1.5)$$

where f_r is the mechanical rotational frequency.

1.3 Maintenance Methods of Induction Machines

Maintenance methods of induction machines can be mainly divided into three types: corrective maintenance, preventive maintenance, and predictive maintenance [24].

1. CONDITION MONITORING AND FAULT DETECTION OF INDUCTION MACHINES: STATE OF THE ART

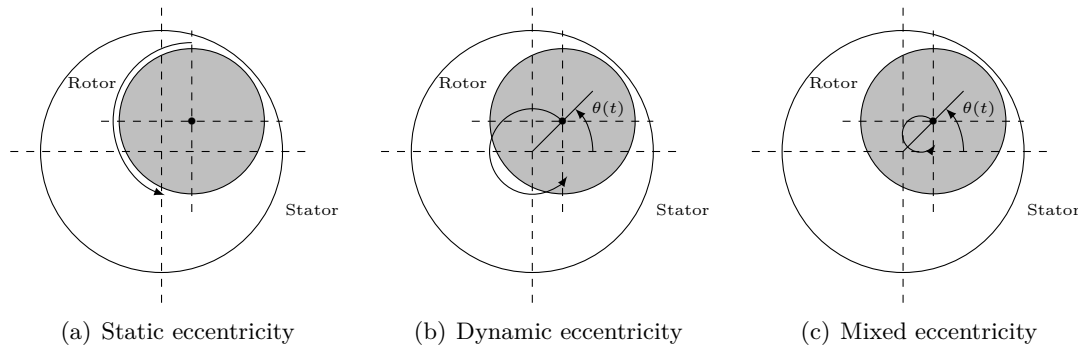


Figure 1.4: Different types of eccentricity.

1.3.1 Corrective maintenance

Corrective maintenance also known as run-to-failure, breakdown or reactive maintenance is used to correct, identify, isolate, and rectify faults [3]. The main purpose of this maintenance type is to bring the item back to a functioning state as soon as possible, either by repairing or replacing the failed item or by switching in a redundant item [25]. The positive aspects of this maintenance are: low maintenance costs during operation, and components will be used for a maximum lifetime [26]. However, disadvantages of this method are: high risk in consequential damages resulting in extensive downtime, maintenance scheduling is not possible, spare part logistics is complicated, It is likely to have long delivery periods for parts, high one-time maintenance cost [26].

1.3.2 Preventive maintenance

Preventive maintenance (PM) also known as time-based maintenance (TBM) or periodic-based maintenance is a technique that can detect and correct incipient faults at an early stage before they introduce breakdowns of installations. It is based on the two processes: failure data analysis/modeling (Fig. 1.5) and maintenance decision making (Fig. 1.6).

The purpose of the first process is to statistically investigate the failure characteristics of the equipment based on the set of failure time data gathered [3]. In this process, there are three distribution models that can be used: the Weibull distribution model, normal distribution model, and Lognormal distribution model. Thanks to analysis of this statistical model, a failure characteristics of the equipment can be identified, in-

1.3 Maintenance Methods of Induction Machines

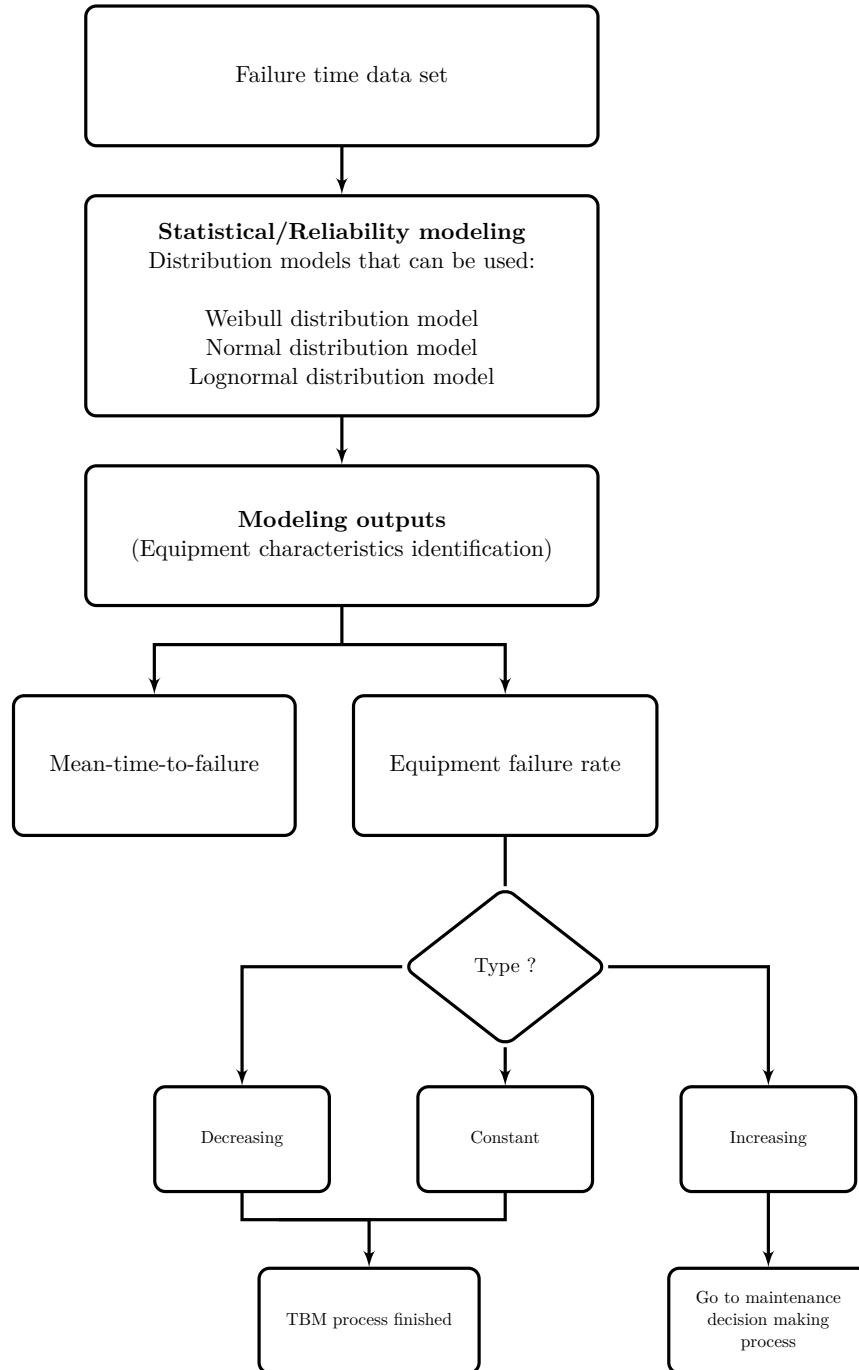


Figure 1.5: Failure data modeling process [3].

cluding the mean-time-to-failure (MTTF) estimation and the trend of the equipment failure rate based on bathtub curve process [3]. The purpose of the second process is to

1. CONDITION MONITORING AND FAULT DETECTION OF INDUCTION MACHINES: STATE OF THE ART

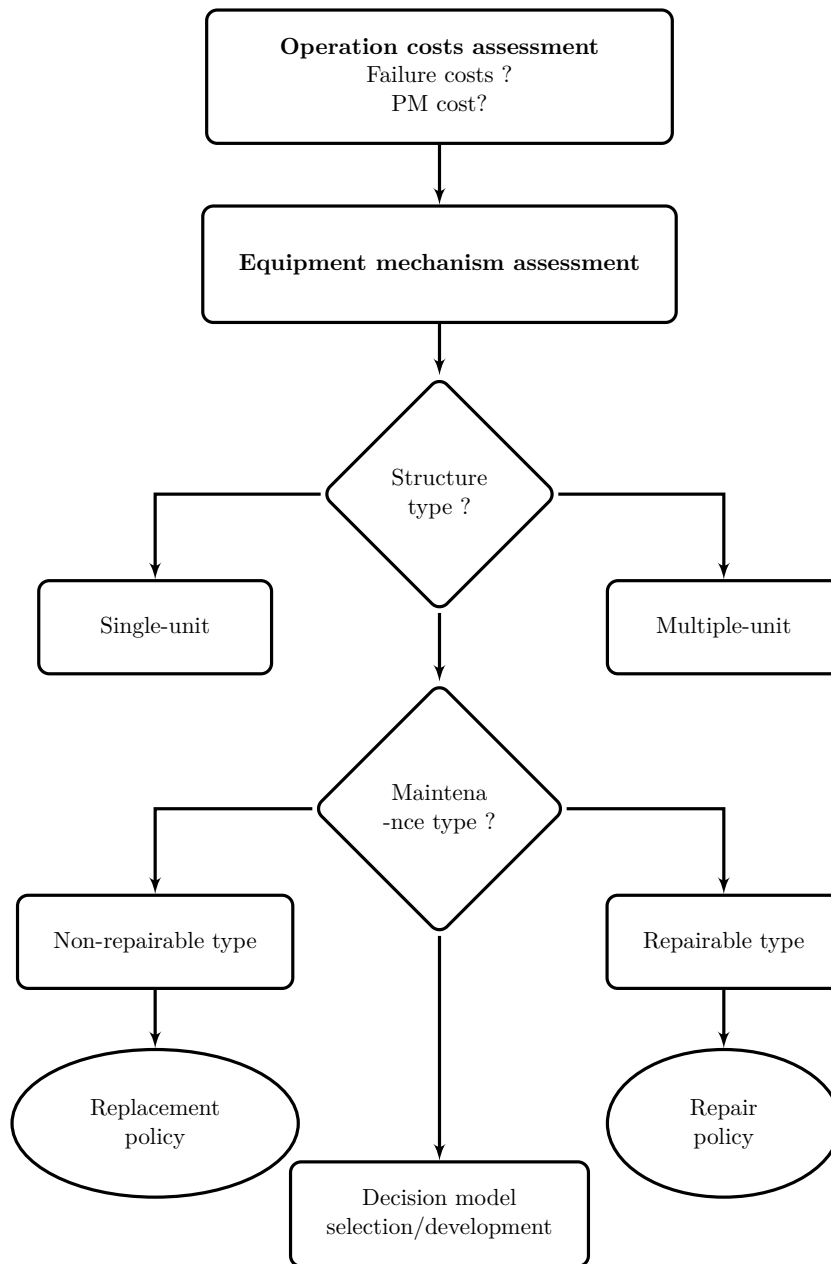


Figure 1.6: Maintenance decision making process [3].

determine the optimal maintenance policies that aim to provide optimum system reliability or availability and safety performance at the lowest possible maintenance cost [3]. The maintenance decision making process is composed of two main assessments: operational cost assessment and the equipment mechanism assessment. The operational

cost assessment can calculate two costs: PM cost and failure cost. The equipment mechanism assessment aims to classify the structure type of the equipment as either non-repairable or repairable. The PM is characterized by: its low expected downtime and its easiness of spare part logistics [26]. Unfortunately, costs of this maintenance are higher (compared to corrective maintenance) and components will not be used for the maximum lifetime [26]. An overview of the preventive maintenance applications can be found in [3].

1.3.3 Predictive Maintenance

Predictive maintenance also called condition-based maintenance (CBM) is used to predict when maintenance should be performed and to prevent unexpected equipment failures. It is based on two processes: condition monitoring process and maintenance decision making. The condition monitoring process is the heart of the predictive maintenance for which signals are continuously monitored using certain types of sensors or other appropriate indicators. This process can be carried out in two ways: on-line and off-line. On-line processing is carried out during the running state of the equipment (operating state), while off-line processing is performed when the equipment is not running. Maintenance decision making under the predictive maintenance program can be classified into two: diagnosis and prognosis. It is characterized by: its low expected downtime, its easiness of spare part logistics, and components will be used close to their full lifetime [26]. Unfortunately, the reliable information about the remaining lifetime of the components, and an additional condition monitoring hardware and software are required [26].

A comparison between TBM and the predictive maintenance is available in [3]. According to this paper, more than 98% equipment failures are preceded by certain signs, conditions, or indications that such a failure was going to occur. The application of CBM appears more realistic compared to TBM. Compared to TBM, the CBM has many advantages such as: data availability and accuracy [3]. As a conclusion, the CBM seems a solution to analyze and detect induction machine faults in industrial applications and research on CBM is still necessary.

1.4 Existing Condition Monitoring Techniques

The generalized theory of condition monitoring is illustrated in Fig. 1.7. It is composed five steps: data acquisition, data analysis, feature selection, decision making, and condition diagnosis. Condition monitoring systems are generally based on measurements of signals containing the fault signature. Then, the question is what fault indicator can be used to analyze induction machine faults. These indicators can be classified into mechanical (vibrations and acoustic), electromechanical (current, voltage, electromagnetic flux leakages, torque, and power), thermal (temperature) and chemical (oil and gas leakages) [8, 27, 28]. According to these indicators, several condition monitoring techniques have been proposed to analyze induction machine faults. Therefore, these techniques can be categorized as vibration monitoring, temperature monitoring, oil debris analysis, acoustic emission monitoring, and current, voltage, or power monitoring.

This section reviews and summarizes existing techniques in induction machine condition monitoring. General reviews of induction machines condition monitoring and faults diagnosis techniques are available in [11–13, 17, 29–32].

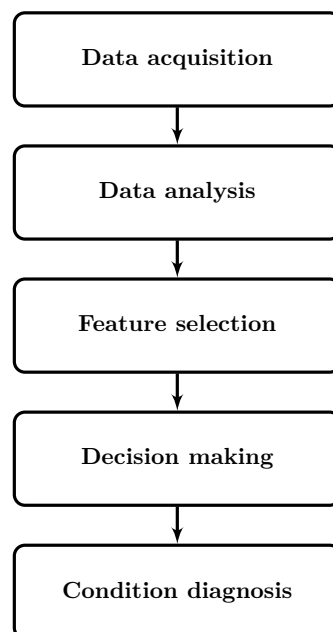


Figure 1.7: Condition diagnosis monitoring framework [4].

1.4.1 Oil Analysis

Oil analysis is a cost-effective machine condition monitoring technique that involves monitoring oil that lubricates parts of the machine for any debris that may be present. Oil analysis can be roughly categorized into the following three fluid analysis: property analysis, fluid contamination analysis, wear debris analysis [33, 34]. Oil analysis has several benefits in short term and in long term. In short term, this technique can minimize unscheduled maintenance operations and gives the evaluation prior to shutdowns. In long term, the OCM can support of warranty claims on new equipment installations and identifies extreme operating conditions which the equipment was not designed to accommodate [35]. Oil analysis can be integrated with other condition monitoring techniques (such as vibration, sonic, thermography, etc) to reduce the maintenance costs [35]. [34] and [36], the authors have proposed a condition monitoring technique based on the correlation between vibration and wear debris analysis for predicting and diagnosing machine failures.

1.4.2 Vibration Monitoring

Vibration monitoring is based on the principle that most faults generate additional vibrations in electrical machines. In fact, vibrations are small and constant for healthy machines compared to faulty machines. The main sources of vibrations in electrical machines are: the attractive magnetic force between rotor and stator, slot harmonics, saturation harmonics, the response of the stator end windings to the electromagnetic forces on the conductors, rotor eccentricity and the flexible rotor [37]. It is noticed also that the mechanical load can have eccentricity or it can induce vibration due to its mechanical structure or the load can process materials that give shocks to the motor axis or to the stator frame [37].

Applications of induction machine vibration monitoring can be found in [38–40]. The major weakness of this technique is its high cost due to additional sensors. These sensors are difficult to access during induction machine operation and are inevitably subject to failures that could cause additional problems with system reliability and additional operating and maintenance costs [24]. Furthermore, the acquisition of vibration signals requires a significant investment.

1. CONDITION MONITORING AND FAULT DETECTION OF INDUCTION MACHINES: STATE OF THE ART

1.4.3 Acoustic Monitoring

Acoustic monitoring is performed by measuring and analyzing the acoustic noise spectrum generated by the induction machine [15]. It is based on the sound measurements. When faults appear in induction machines, their acoustic noise spectrums change. The noise spectrum not only depends on size, geometry and structure of the induction machines but also on the measurement position [30]. It also depends on the source of noise. Acoustic monitoring has a strong relationship with the vibration monitoring to detect incipient faults in industrial applications. The sound wave is generated by vibrating objects and can be defined as mechanical interference with the finite speed of advancing through the media. These waves have small amplitude, adiabatic oscillation are characterized by a wave speed, wavelength, frequency and amplitude [41]. The main sources of noise in induction machines are: the electromagnetic source, the mechanical source, and the aerodynamic source [41]. The electromagnetic noise source is the electromagnetic field that exerts a force on the stator core. The vibration of the stator thereby affects the surrounding air. The vibration of the tiny molecules in the air is propagated to the sound sensors [42]. The main mechanical sources of the noise are: alignment, inaccurate machining of parts, running speed, number of rolling elements carrying the load, mechanical resonance frequency of the outer ring, lubrication conditions, and temperature [41]. In fact, Mechanical noise is mainly due to bearings, their defects, ovality, sliding contacts, bent shaft, rotor unbalance, shaft misalignment, couplings, etc. In principle, the mechanical source of noise has a mixed character [41]. The basic aerodynamic noise source is the cooling by air, water, or oil. A review of noise in electrical machines can be found in [43].

This technique has been used to analyze the rotor eccentricity effects of induction machines [44]. In [44], authors have described a technique to calculate variations of noise components in the eccentricity fault condition. This technique takes into account the variation of the magnetic force waves, the mechanical behavior, and the sound radiation resulting from the surface vibrations in the faulty condition. Applications of acoustic monitoring for induction machine condition monitoring can be found in [45, 46]. The main drawback of acoustic monitoring is its high cost since the sensors and data acquisition equipments are more expensive than other techniques [24]. It has been demonstrated also that acoustic spectra can not show clear sidebands and their

differences between normal and BRB fault as vibration and current spectra [30, 47]. Moreover, this technique may not be practical in the noisy environment.

1.4.4 Temperature Monitoring

Limits to the rating of induction machines are set by the maximum permissible temperature for insulation [8]. Temperature measurements are therefore important in the induction machine condition monitoring. There are three approaches to measure temperature [8]: local temperature measurements, distributed temperature measurements, and the use of thermal images. These measurements are done using: resistance temperature detection, thermistors, thermocouples, quartz thermometers, fiber-optic temperature sensing and infrared thermography. Resistance temperature detectors (RTD) use the resistance change of a metal to indicate temperature change [8]. Advantages of these detectors are: their good accuracy, their precision, and their linearity over a wide operating range. A major drawback of RTD is their low sensitivity [8]. Thermistors differ from RTD in that the material used in a thermistor is generally a ceramic or polymer. There are two opposite fundamental types of thermistors: the negative temperature coefficient exhibit a decrease in electrical resistance when subjected to an increase in body temperature and the positive temperature coefficient exhibit an increase in electrical resistance when subjected to an increase in body temperature. Thermistors are easy to use and are highly sensitive so can detect small changes in temperature very easily. Thermistors cannot be used at very high temperatures. Thermocouples use Seebeck effect whereby a current circulates around a circuit formed using two dissimilar metal conductors forming electrical junctions, when the metal junctions are held at different temperatures [8]. Thermocouples are interchangeable and can measure a wide range of temperatures. The main limitation of thermocouples is their poor accuracy.

Local temperature measurements are done using embedded temperature detectors, resistance temperature detectors, or thermocouples [48]. The choice of location requires careful consideration during specification. For example, temperature detectors embedded in the stator winding need to be located close to its hottest part, which may be in the slot or end-winding portions. For a machine with asymmetrical cooling, they should be located at the hottest end of the machine [8]. Distributed temperature mea-

1. CONDITION MONITORING AND FAULT DETECTION OF INDUCTION MACHINES: STATE OF THE ART

measurements are obtained using thermocouples. This can be found from the measurement of the internal and external temperature rises [8].

Thermal images fed with suitable variables to monitor the temperature of the perceived hottest spot in the machine. Thermal images are obtained using the infrared thermography (IRT) that the thermography data can be taken based an infrared camera without any contact with the machine under test. IRT is based on infrared radiation measurements which are converted into temperature data. Afterward, the temperature data are transformed into electrical signals [49]. This technique can detect faults especially when assessing the rotor condition [50]. This technique can be fused with another techniques to analyze faults in induction machines. A fusion of IRT and motor current signature analysis (MCSA) is used to detect induction machine faults [51]. In this application, IRT is used as complementary tool for MCSA based on the image segmentation to detect faults.

The major drawback of temperature monitoring is that the measured temperature depends on multiple factors: environment temperature, stator current heating, and physical phenomena that can contribute in increasing temperature in electrical machines. Therefore, it is complicated to simply use this technique without a further analysis [24].

1.4.5 Torque monitoring

Torque monitoring is a condition monitoring technique based on torque oscillations. It exploits fault signatures such as oscillations that can appear in the air-gap torque. These signatures are generally modeled by amplitude and frequency modulations [52]. In fact, air-gap torque represents the combined effects of all flux linkages and currents in both the stator and the rotor of the entire machine [53].

The major disadvantage of this method is its need of a torque transducer which increases the cost and complexity. To avoid this limitation, a special method called Vienna monitoring has been proposed in [54, 55] to estimate the electromagnetic torque for any induction machine drive and in particular to variable speed inverter supply conditions. It is based on outputs of both current and voltage models. The Vienna monitoring method compares between these outputs and a reference model, which represents a healthy machine . This comparison allows detecting faults [55]. Vienna monitoring has been applied also in [56, 57] to analyze rotor faults. However, this

method seems not much attractive, because it requires two different measurements (currents and voltages) and hence it demands excess costs [30]. Torque monitoring has been applied to detect induction machine faults in [53, 58–61]. In [53], authors suggest a condition monitoring technique based on air-gap torque observations to monitor rotor and stator faults in induction machines. A novel approach based on torque monitoring and finite element method analysis has been proposed in [60] to detect BRB faults of induction machines.

1.4.6 Motor Current Signature Analysis

Stator current-based condition monitoring has received more and more attention in academia and industry due to their non-intrusive character and economic advantages [62]. The most used current-based technique is the motor current signature analysis (MCSA). It has received a great deal of attention in the recent years to develop a non-invasive, a lower-cost, and a reliable technology that fully exploit the benefits of induction machines condition monitoring [63–65]. This technique remains the most used condition monitoring in industry applications thanks to several advantages such as the easy-access, the ease of implementation, the information richness, and the ability to detect electrical and mechanical faults. In fact, it do not require additional sensors or data acquisition devices. Therefore, current-based condition monitoring and fault detection techniques have great economic benefits than other fault indicator based techniques.

An approach to use stator current and motor efficiency as indicators for bearing faults is proposed in [66]. In fact, authors propose to analyze the decrease in induction machine efficiency as alarm of incipient faults and as an evaluation of the extent of energy waste resulting from the lasting of the fault condition before the breakdown of the machine. A comparison results of BRB fault analysis using three different condition monitoring techniques is presented in [47]. This paper compares stator current, vibration and acoustic techniques. It can be concluded from this paper that the MCSA is the most sensitive technique to detect BRB faults while the vibration technique is the sensitive technique to detect mechanical faults. The acoustic monitoring can be used as a supplementary technique in the presence of strong noise and interferences.

1.5 Induction machine faults modeling

Induction machine modeling is one of the most challenging task to represent and simulate electromechanical phenomena and variables that can appear in the various machine operating conditions. It is also useful to analyze and test performances of condition monitoring and fault detection techniques. These mathematical methods exploit essentially electromechanical phenomena appearing in machines for healthy-state and faulty-state. In the literature, induction machine modeling can be classified into four categories: magnetomotive force (MMF) and permeance wave models, multiple coupled circuit also called winding function approach models [67], d-q models, magnetic equivalent circuit models, and finite element models [68, 69]. A review of induction machine fault modeling is available in [69]. This review gives a general description of each modeling type and their ability to model different faults.

1.5.1 Finite element modeling

To calculate the airgap magnetic flux density, a finite element methods (FEM) can be used [70–73]. FEM is used to determine the parameters of induction machines such as magnetic coupling method and winding and extended winding function methods that give more accurate results than analytical approach [74]. This method is a numerical technique that approximates solutions of Maxwell equations to model electromagnetic phenomena appearing in electrical rotating machines. The Maxwell equations are given by

$$\begin{cases} \operatorname{div} \vec{D} = \rho \\ \operatorname{div} \vec{B} = 0 \\ \operatorname{rot} \vec{E} = -\frac{\partial \vec{B}}{\partial t} \\ \operatorname{rot} \vec{H} = \vec{j} + \frac{\partial \vec{D}}{\partial t} \end{cases} \quad (1.6)$$

where $\operatorname{div}(\cdot)$ is the divergence operator and $\operatorname{rot}(\cdot)$ is the rotational operator. \vec{E} , \vec{D} , \vec{j} , \vec{H} , \vec{B} , \vec{A} and ρ , denote the electric field strength, the electric flux density, the current density, the magnetic field strength, the magnetic flux density, the vector magnetic potential, and the volume charge density, respectively.

The advantages of the finite element method are its ability to handle the most general type of machine geometries, the relative motion effects due to the movement of the rotor, and nonlinear iron saturation effects [75]. In fact, this technique provides

detailed information about nonlinear effects. This numerical technique provides also waveform of electromechanical variables but not analytical models. The main limitation of the finite element method for this application is that complete, coupled, transient electric machine models are at present limited to two dimensions, due to practical constraints of computing resources. Therefore, three-dimensional phenomena such as stator winding end turns, rotor cage end rings, slot skewing, and axial flux cannot be modeled precisely [75]. An another drawback of these methods, their time-intensive calculations [52]. These methods can be investigated also in condition monitoring of induction machines by analyzing variations of electromechanical variables such as currents, flux, torque, and speed for healthy and faulty induction machines [76]. FEM has been proposed to model and analyze several faults such as stator shorted turn [74, 77–79], broken rotor bars [79–85], and eccentricity faults [60, 86–90].

1.5.2 Magnetic equivalent circuit modeling

Magnetic equivalent circuit (MEC) modeling also called as permeance network modeling or flux tube modeling is based on the representation of the equivalent magnetic circuit for each part of the induction machine. Each magnetic circuit contains a magnetic flux Φ , magnetic reluctance \mathcal{R} , and magneto-motive forces (MMFs) \mathcal{F} . These circuits are then connected to each others taking into account the direction of the magnetic flux [91]. Parameters of MEC are obtained using the geometric calculations or FEM. It can provide acceptably accurate solutions with reasonable computational effort [92]. Indeed, MEC is fast compared to FEM. An another advantage of this method is non-linearities can be implemented easily. However, MEC has several drawbacks such as it is restricted to very special geometries, the flux paths must be known to build up the model, and MMFs computations are troublesome [93]. This method has been used to model several faults like rotor faults [94–96], stator faults [95, 96], and eccentricity faults [97].

1.5.3 MMF and permeance wave modeling

Consequences of mechanical faults are mainly studied using MMF and permeance wave method [98–100]. The basic idea in the MMF and permeance wave method is when a asymmetry appearing in the airgap of induction machines produce additional frequency components in the flux density and force waves. It is a simpler and flexible

1. CONDITION MONITORING AND FAULT DETECTION OF INDUCTION MACHINES: STATE OF THE ART

magnetic field analysis method to determine the magnetic fluxes and forces in the air gap [52]. In fact, this method allows calculating the magnetic flux density in the airgap of induction machines. The models given by this approach is valid only in stationary conditions and also when the supply frequency and the speed transients are considered slow compared to the electrical transients. Modeling by this method consists to study four fault effects of electromechanical variables: airgap permeance, airgap flux density, stator current, and torque. This approach has been used extensively in the literature for both synchronous and induction machine modeling because of its convenience and flexibility [75]. This technique is most successful in predicting frequencies and pole numbers of vibration-producing magnetic force waves and less effective in predicting the vibration amplitudes. Therefore, this method can be used to simulate mechanical faults of induction machines and to test performances of the advanced processing techniques using in the induction condition monitoring and fault detection techniques.

MMF and permeance wave method has two benefits: its simplicity and its obvious relationship to physical phenomena [52]. However, this technique cannot provide the exact harmonic amplitudes of the airgap magnetic fields and not takes into account the coupling phenomena appearing between stator and rotor [52, 75]. However, since the purpose is to give an analytical models of electromechanical variables under faulty conditions that can be exploited to analyze and detect faults using advanced signal processing and statistical analysis techniques, MMF and permeance wave approach seems a suitable solution to analyze mechanical faults [52, 101]. This method has been investigated to model bearing faults [20], eccentricity faults [102], and load torque oscillations [52].

1.5.4 Multiple Coupled Circuit modeling

Multiple coupled modeling (MCM) technique is the most detailed and complete model used to analyze the performance of the rotor and stator faults [103]. Models obtained by this method take into account effects of non-sinusoidal airgap MMF produced by both the stator and the rotor currents. It mainly exploits the variations of induction machine parameters to model faults. Benefits of this technique are: its lower complexity and its ability to model both rotor and stator faults. To estimates inductance matrices in this method, four methods have been proposed: winding function, modified winding

1.6 Advanced feature extraction techniques for induction machine fault analysis

function, extended $2D$ modified winding function, and inductance look up table methods. The MCM has been proposed to model various induction machine fault types such as broken rotor bars [104–117], stator faults [104, 105, 108, 115, 117–122], airgap eccentricities [123–126] and bearing faults [127].

1.5.5 dq modeling

dq modeling technique is a mathematical model which can transform (a, b, c) reference to dq reference according to a frame (stationary, rotor, and synchronously rotating reference frames). Description of the detailed and the preferred frames to model induction machine are given in [128, 129]. This technique is based on the assumption that both the stator and the rotor windings and MMF are sinusoidally distributed [69]. However, these variables are non-sinusoidally distributed. To overcome this limitation, a modified dq reference has been proposed in [130], that take into account non-sinusoidal distributions. This method has been investigated to model rotor faults [131–134], stator faults [133, 135], and eccentricity faults [133].

1.6 Advanced feature extraction techniques for induction machine fault analysis

In induction machine faults analysis, it can be distinguished between two main conditions: stationary and nonstationary environments. Stationary signals are not changed in their statistics over time. These signals can be divided into deterministic and random signals. Deterministic signals are a special class of stationary signals that can be characterized by mathematical models. Non-stationary signals are changed in their statistics over time. They are divided into continuous and transient types.

Advanced feature extraction techniques for induction machines in stationary environments are classified into three main categories: power spectrum (second order spectrum) estimation, demodulation techniques, and higher order spectra analysis.

1.6.1 Power spectrum estimation

A large and growing body of literature has focused on the power spectrum estimation also called power spectral density estimation to analyze and detect induction machine

1. CONDITION MONITORING AND FAULT DETECTION OF INDUCTION MACHINES: STATE OF THE ART

faults [136–153]. Therefore, several advanced spectral estimation techniques using stator currents have been proposed to detect these faults. There are mainly two types of power spectrum estimation (PSE): nonparametric methods and parametric methods (also known as model-based methods). In estimation theory context, there are three main parameters to choose the good estimator: bias, variance, consistency. The bias is the difference between the mean (the first order statistics) or expected value of an estimate $\hat{\theta}$ and its true value θ . The variance is the expectation of the squared deviation of a random variable from its mean or expected value. Consistency is when the bias and the variance both tend to zero as the limit tends to infinity or the number of observations become large. Therefore, a good estimator is a consistent estimator with small variance and small bias. If the bias is equal to zero is called unbiased estimator [154].

1.6.1.1 Nonparametric techniques

Nonparametric techniques estimate the power spectrum directly from the measurements. These methods constitute the classical means for power spectral density (PSD) estimation. These methods include the conventional periodogram and its extensions [149–153].

Periodogram: The periodogram is a nonparametric power spectrum technique that is based on the discrete Fourier transform (TFD) of the autocorrelation function (i.e. the second order statistics) of stationary discrete-time process $x[n]$. The periodogram can be defined as a squared TFD of $x[n]$ divided by the samples number N :

$$\hat{P}_x(f) = \frac{1}{N} \left| \sum_{n=0}^{N-1} x[n] e^{-j2\pi f n / F_s} \right|^2 \quad (1.7)$$

where F_s is the sampling frequency and N is the samples number. In practice, the periodogram is implemented using the fast Fourier transform (FFT). This is because that the FFT algorithm is computationally efficient and produces reasonable results for a large data of signal processes. The family of periodogram-based techniques is given in Fig.1.8.

Unfortunately, the periodogram presents several problems: it is biased and inconsistent estimator (its variance does not decrease with growing N) [155]. The most

1.6 Advanced feature extraction techniques for induction machine fault analysis

prominent limitation of periodogram-based techniques is that of frequency resolution (its ability to distinguish the spectral responses of two or more signals) [155]. Its frequency resolution is defined by

$$\Delta f = \frac{F_s}{N} \quad (1.8)$$

It is a key element to analyze performances of spectral estimation techniques. In practice, the fact of choosing a finite-length N of an infinite signal $x[n]$ is similar to multiplying this signal with a rectangular windows. Then the bias of the Periodogram is expressed as

$$E\{\hat{P}_x(f)\} = \frac{1}{F_s} \int_{-F_s/2}^{F_s/2} \frac{\sin^2(N\pi(f-f')/F_s)}{N\sin^2(\pi(f-f')/F_s)} P_{xx}(f') df' \quad (1.9)$$

The variance then, can be expressed as

$$Var(\hat{P}_x) = \begin{cases} \hat{P}_x^2, & 0 < f < \frac{F_s}{2} \\ 2\hat{P}_x^2, & f = 0 \vee f = \frac{F_s}{2} \end{cases} \quad (1.10)$$

In statistical terms, this estimator is not a consistent PSD estimator (because its variance not tend to zero as the data length tends to infinity).

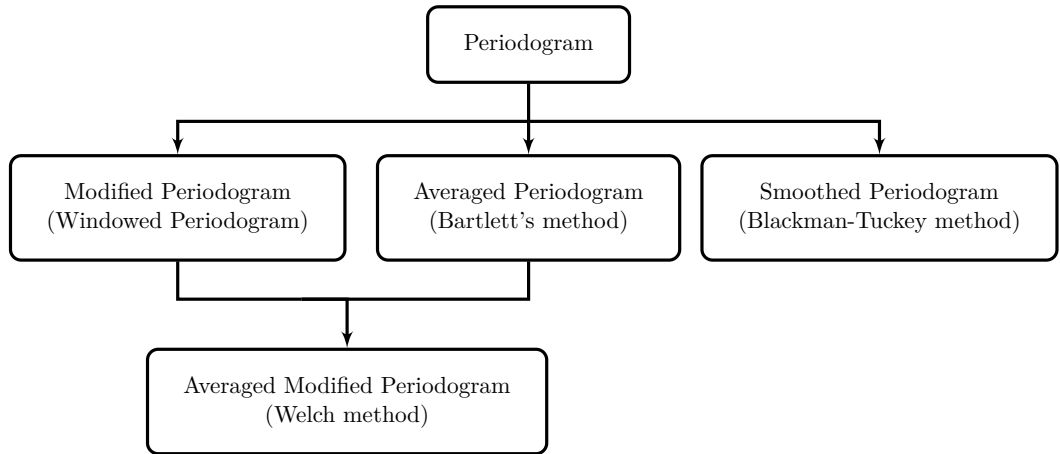


Figure 1.8: Family of periodogram-based techniques.

Modified Periodogram: The modified periodogram is proposed to smooth the edges of the signal with a N -length window $w[n]$. This operation has the effect of reducing

1. CONDITION MONITORING AND FAULT DETECTION OF INDUCTION MACHINES: STATE OF THE ART

the height of the sidelobes or spectral leakage. It uses a non-rectangular window and therefore has to be scaled to account for the loss of power due to the window. This scaling is required to make the Modified Periodogram asymptotically unbiased (estimator becomes unbiased in the limit when the number of data points goes to infinity). Furthermore, it has reduced the bias but it is still a biased estimator and its variance that roughly equals that of the periodogram $\hat{P}_x(f)$. This periodogram type is defined by

$$\hat{P}_m(f) = \frac{1}{NU} \left| \sum_{n=0}^{N-1} x[n]w[n]e^{-\frac{j2\pi fn}{F_s}} \right|^2 \quad (1.11)$$

where $w[n]$ is the non-rectangular window and U denotes the scaling factor defined by

$$U = \frac{1}{N} \sum_{n=0}^{N-1} |w[n]|^2 \quad (1.12)$$

For large values of N , U is chosen independent of the window length.

Averaged Periodogram: The averaged periodogram also called as a Bartlett's periodogram is an improved periodogram-based technique that can reduce the variance of the periodogram in exchange for a reduction of resolution. This method reduces also the fluctuation of the $\hat{P}_x(f)$ by splitting up the available data of N observations into $K = N/L$ subsections of L observations each. Then, spectral densities of produced K periodograms are then averaged. The Bartlett periodogram is defined by

$$\hat{P}_a(f) = \frac{1}{K} \sum_{k=1}^K \hat{P}_{x,k}(f) \quad (1.13)$$

where K denotes the considered realizations and $\hat{P}_{x,k}(f)$ the periodogram of k -th realization $x_k[n]$. Then, its variance decreases by a factor K compared to the variance of $\hat{P}_x(f)$

$$Var(\hat{P}_a(f)) = \frac{1}{K} Var(\hat{P}_x) \quad (1.14)$$

The main problem of this method is the tradeoff between the variance and the resolution.

Averaging-modified Periodogram: The averaging-modified periodogram also called as a Welch's periodogram is a combined technique between the averaged periodogram

1.6 Advanced feature extraction techniques for induction machine fault analysis

and the modified periodogram. It tends to decrease the variance compared to $Var(\hat{P}_x)$ of the entire data record. It is based on three main steps in this order: partition the data sequence into K segments, computation the modified periodogram for each segment k of length N , average the modified periodograms. Then, the Welch periodogram is given by

$$\hat{P}_{a,m}(f) = \frac{1}{K} \sum_{k=1}^K \hat{P}_{m,k}(f) \quad (1.15)$$

where $\hat{P}_{m,k}(f)$ denotes the modified periodogram for k -th segment.

Blackman-Tukey method: The Blackman-Tukey method also called Smoothed periodogram is a method to reduce the variance that corresponds to a locally weighted average of the periodogram [156]. The smoothed periodogram is defined by

$$\hat{\phi}_{BT}(f) = \sum_{k=-(N-1)}^{N-1} w[k] \hat{r}_B[k] e^{-\frac{j2\pi f k}{F_s}} \quad (1.16)$$

where $w[k]$ is a lag window and $\hat{r}_B[k]$ denotes an estimate of the covariance $r_B[k] = E\{x[n]x^*[n-k]\}$. There are two ways to estimate $r_B[k]$:

$$\hat{r}_B[k] = \frac{1}{N-k} \sum_{n=k+1}^N x[n]x^*[n-k] \quad 0 \leq k \leq N-1 \quad (1.17a)$$

and

$$\hat{r}_B[k] = \frac{1}{N} \sum_{n=k+1}^N x[n]x^*[n-k] \quad 0 \leq k \leq N-1 \quad (1.17b)$$

Estimators (1.17a) and (1.17b) are called the standard unbiased and biased estimators of $r_B[k]$, respectively. Estimator (1.17b) is the most used [156]. A particular case of the Blackman-Tukey class of spectral estimators is the Daniell estimator which corresponds to a rectangular spectral window[156]:

$$W(f) = \begin{cases} \frac{1}{\beta} & f \in \left[-\frac{\beta}{2}, \frac{\beta}{2}\right] \\ 0 & \text{Otherwise} \end{cases} \quad (1.18)$$

Therefore, the variance in periodogram can be reduced by four common methods: modified, averaged, averaged-windowed, and smoothing periodograms that are easy to compute using FFT algorithm with some zero padding for purposes of interpolating the spectral estimate [157]. However, these techniques have several drawbacks since their

1. CONDITION MONITORING AND FAULT DETECTION OF INDUCTION MACHINES: STATE OF THE ART

frequency resolution is limited and long data measurements are required. Prominent conclusions from these non-parametric techniques are that there is always a compromise in the bias-variance trade-off because both of these errors cannot be minimised simultaneously [154, 156, 158]. In fact, these classical estimators of PSD are still inconsistent and biased estimators and have limited ability to resolve closely frequency components. Nevertheless, these estimators can be a useful tool for spectral estimation in situations where SNR is high, and especially if the data is long. In addition, these nonparametric techniques of PSD estimation can be also useful in applications where there is little or no information about the signal in question [156, 158].

1.6.1.2 Higher order spectra analysis

Higher order spectra (HOS), also known as polyspectra techniques have been also proposed to analyze induction machine faults [8, 159–176]. Particular cases of these techniques are: the third-order-spectrum (also known as bispectrum) and the fourth-order-spectrum (also known as trispectrum) [177]. The main advantages of HOS are: additive Gaussian noise is automatically suppressed, Nonminimum phase systems can be identified, information due to deviations from Gaussianity can be extracted, and nonlinear systems can be detected and identified [164]. These spectral estimation techniques have disadvantages such as a high-computational overhead, and their interpretation is complex [164].

1.6.1.3 Parametric techniques

Several parametric techniques have been developed for PSE to overcome drawbacks of nonparametric methods. These parametric methods for PSE are based on parametric models to represent the signal and then to estimate model parameters from the available signal data. Parametric methods for spectral estimation are divided into two classes: parametric for continuous spectra and parametric for line spectra [158].

Parametric techniques for continuous spectra: The parametric techniques for continuous spectra include the linear prediction techniques. The linear prediction techniques contain several algorithms like the Pisarenko and Prony methods. Pisarenko method is an estimation technique for which signal is assumed be a sum of sinusoids in white noise. It is based on the eigendecomposition of the autocorrelation matrix.

1.6 Advanced feature extraction techniques for induction machine fault analysis

Pisarenko harmonic decomposition is computationally efficient but its performance degrades at low SNRs. The Prony method is a high-resolution spectral analysis method. This method approximates a sampled waveform as a linear combination of complex conjugate exponentials [178, 179]. The positive aspects of Prony method are: parameter estimates are less biased than those obtained from the Pisarenko method and can resolve delays to better than half the nonparametric methods limit. The main drawback of Prony method is its resolution which is poor at low SNR scenarios. Prony method is known by its sensitivity to noise and its long computational time especially for high order signals models. The Prony analysis has been proposed to diagnose broken rotor bars in [114]. This study reveals improvements of diagnostics using Prony method than nonparametric techniques. In [178], authors propose to use the modified Prony method to detect the air-gap eccentricity faults in induction motors. These linear prediction methods are specifically designed for continuous PSD, where the frequency content does not vary abruptly. Unfortunately, these methods are not suited for fault frequency estimation because the fault signature introduces specific frequencies close to the fundamental frequency.

Parametric techniques for line spectra: The parametric techniques for line spectra include Maximum Likelihood Estimator (MLE) and subspace techniques called also high-resolution techniques. The applications of MLE-based spectral estimations for machine fault detection are available in [145–147]. Indeed, in [145, 146, 148], a model order and spectral estimations based on MLE are proposed to detect induction machine fault frequency signatures. In stator current analysis, subspace techniques have been proposed to avoid the computational complexity inherent to multidimensional optimization of MLE [136–144, 180]. The subspace techniques include minimum norm, singular value decomposition (SVD), MUSIC (Multiple Signal Classification) and ESPRIT (Estimation of Signal Parameters via Rotational Invariance Techniques) approaches. The first advantage of MUSIC approach is its better resolution than parametric techniques for continuous spectra. Another advantage, it yields asymptotically unbiased parameter estimates. The serious criticism of this approach is its failing to resolve closely spaced signals at low SNRs. Moreover, it has a high computational burden. Minimum Norm has lower computational cost, and better resolution, than the MUSIC algorithm. It optimizes the separation of the spurious roots in root-MUSIC.

1. CONDITION MONITORING AND FAULT DETECTION OF INDUCTION MACHINES: STATE OF THE ART

The main drawback of main norm is exhibits spurious peaks, and merging of spectral peaks at low SNR values. Advantages of TLS-ESPRIT [181]: produces less biased estimates, more accurate than conventional ESPRIT, manifests superior performance than the Pisarenko and minimum norm methods. Disadvantages of TLS-ESPRIT: requires an accurate estimate of the number of signals, has higher computational cost than conventional ESPRIT. A condition monitoring based on the traditional SVD, short-time matrix series and singular value ratio has been investigated to detect bearing faults[182]. An another application based on SVD and Hankel matrix has been proposed in [183] to detect bearing faults. In induction machine condition monitoring, the problem of frequency estimation using subspace techniques has received a lot of attention in the electrical engineering community. In [137], the authors propose to use the spectral-MUSIC or Root-MUSIC for frequency estimation. An application of high-resolution spectral analysis for identifying multiple combined faults in induction motors can be found in [144]. The major contribution of [144] is the development of a condition-monitoring strategy that allows accurate and reliable assessments of the presence of specific fault conditions in induction motors with single or multiple combined faults. The proposed condition monitoring strategy is based on the combination between a finite impulse response filter bank to separate the original current and vibration signals into different fault-related bandwidths and the spectral-MUSIC to detect frequencies of the stator current. This methodology can detect two faults: bearing and broken rotor bars faults. A modified version of the MUSIC algorithm has been developed in [141] to estimate the stator current spectrum. In this paper, a fault detection criterion has been also proposed to detect faults. This criterion does not take into account the harmonic structure of the stator current. Another application of high-resolution frequency estimation method for three-phase induction machine fault detection can be found in [184]. The proposed Zoom-MUSIC in [184] is used to detect broken rotor bars fault using spectrum analysis in induction machine under different loads and in steady-state condition. This proposed technique allows reducing the computational complexity focusing on frequencies close to the fundamental frequency. In this case, the model order is obtained by the Frequency Signal Dimension Order (FSDO) estimator proposed in [185]. The application of high-resolution parameter estimation method to identify broken rotor bar faults in induction motors has been proposed recently in [138]. The authors in [138] propose two algorithms Zoom-MUSIC and Zoom-ESPRIT to estimate

1.6 Advanced feature extraction techniques for induction machine fault analysis

frequencies in order to reduce the long computation times required by classical subspace techniques from short data signals with low Signal-to-Noise Ratio (SNR). In this case, the model order is obtained by the FSDO estimator proposed in [186]. In [138], a fault detection criterion based on false alarm and detection probabilities is proposed to detect faults. Finally, a stator current analysis by subspace methods for fault detection in induction machines has been proposed in [136]. Two subspace techniques: Root-MUSIC and ESPRIT are presented and a fault severity criterion with a fault severity criterion.

1.6.2 Demodulation techniques

It has been demonstrated that mechanical faults causes amplitude and frequency modulations of the stator currents [5]. In this context, several studies have investigated on demodulation techniques [5, 65, 187–199]. These techniques are mainly classified into two categories: monodimensional and multidimensional techniques [5]. Figure 1.9 depicts how to choose the demodulation technique according to the signal type.

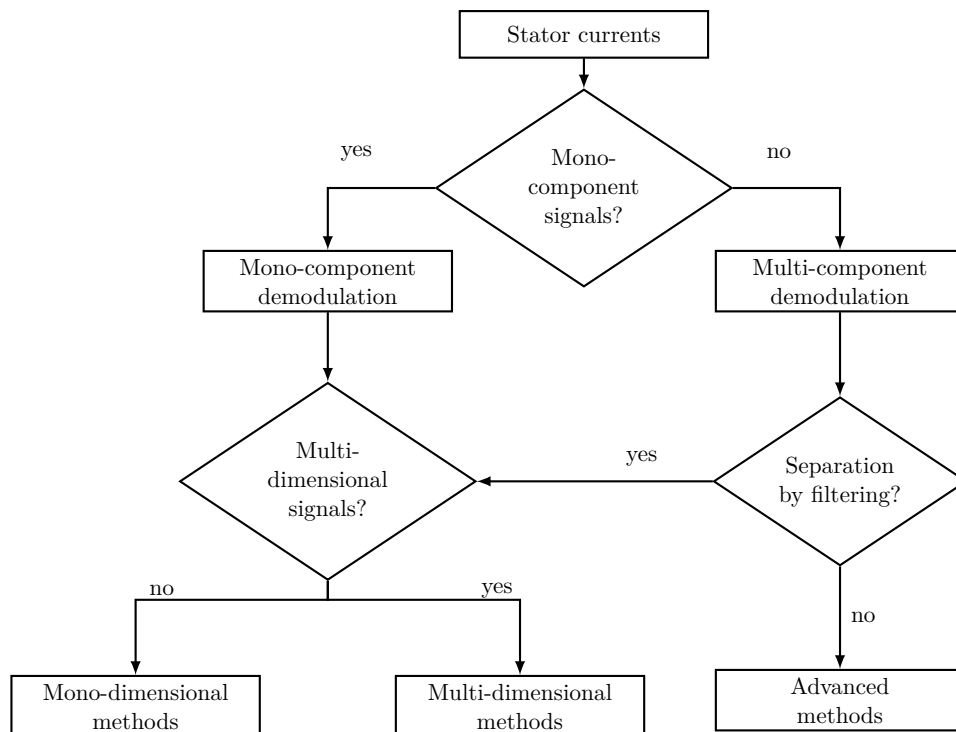


Figure 1.9: The choose of the demodulation technique [5].

1. CONDITION MONITORING AND FAULT DETECTION OF INDUCTION MACHINES: STATE OF THE ART

1.6.2.1 Monodimensional techniques

Monodimensional techniques include the synchronous demodulator [187, 190, 194, 195], the Teager energy operator [189, 200, 201], and Hilbert transform [191–194, 196, 198, 202, 203].

A monodimensional signal in noise is defined as

$$x[n] = a[n] \cos(\phi[n]) + b[n] \quad (1.19)$$

where $a[n] > 0$ is the instantaneous amplitude (IA), $\phi[n]$ is the instantaneous phase (IP), and $b[n]$ denotes the noise component. This signal can be expressed in term of the corresponding direct (real part) and quadrature (imaginary part) components

$$\begin{cases} y_1[n] = a[n] \cos(\phi[n]) \\ y_2[n] = a[n] \sin(\phi[n]) \end{cases} \quad (1.20)$$

The corresponding analytic signal is defined by

$$z[n] = y_1[n] + jy_2[n] = a[n] \exp(j\phi[n]) \quad (1.21)$$

The analytic signal estimation is given in Fig.1.10

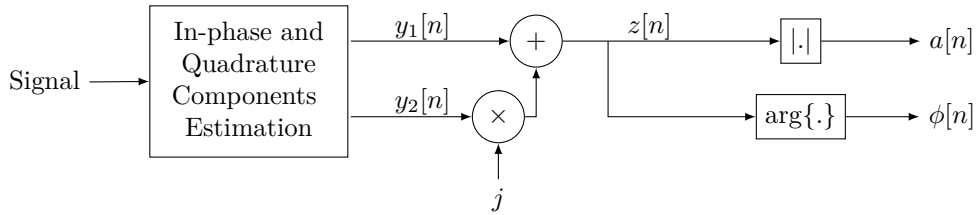


Figure 1.10: Analytic signal estimation [5].

Therefore, the instantaneous amplitude and phase are estimated from the analytic signal by

$$\begin{cases} a[n] = |z[n]| \\ \phi[n] = \arg\{z[n]\} \end{cases} \quad (1.22)$$

where $|\cdot|$ and $\arg\{\cdot\}$ denote the modulus and the argument of the complex signal $z[n]$, respectively. Then, the instantaneous frequency (IF) can be estimated using the

1.6 Advanced feature extraction techniques for induction machine fault analysis

backward finite differences

$$\hat{f}[n] = \frac{F_s}{2\pi} (\phi[n] - \phi[n-1]) \quad (1.23)$$

where F_s is the sampling rate.

Synchronous demodulator: The synchronous demodulator is a AM and PM demodulation technique for monodimensional technique. The demodulation is performed by multiplying the analyzed signal with two reference signals $\cos(2\pi f_0 n/F_s)$ and $\sin(2\pi f_0 n/F_s)$. The principle is illustrated in Fig.1.11. Estimations of IA and IP are obtained using (1.21) and (1.22).

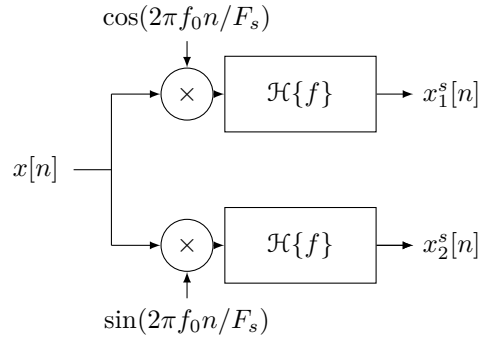


Figure 1.11: Synchronous demodulator [6].

Teager energy operator: The Teager energy operator (TEO) is a IA and IF demodulation techniques for monocomponent signal that estimates them without using the analytical signal $z[n]$. It directly estimates from the $x[n]$ using the discrete-time TEO

$$\Psi(x[n]) = x^2[n] - x[n+1]x[n-1] \quad (1.24)$$

IA and IF can be estimated using the energy separation algorithm

$$a[n] \approx \sqrt{\frac{\Psi(x[n])}{1 - \left(1 - \frac{\Psi(x[n] - x[n-1])}{2\Psi(x[n])}\right)^2}} \quad (1.25a)$$

and

$$f[n] \approx \frac{1}{2\pi} \arccos\left(1 - \frac{\Psi(x[n] - x[n-1])}{2\Psi(x[n])}\right) \quad (1.25b)$$

1. CONDITION MONITORING AND FAULT DETECTION OF INDUCTION MACHINES: STATE OF THE ART

Hilbert transform: The Hilbert transform is a linear operator for which analytic signal can be derived if the Bedrosian theorem is verified from the signal $x[n]$ according to Fig.1.12

$$\begin{cases} y_1^h[n] = x[n] \\ y_2^h[n] = x[n] * h[n] \end{cases} \quad (1.26)$$

where $*$ denotes the convolution operator and $h[n]$ denotes the impulse response of the Hilbert filter

$$h[n] = \begin{cases} \frac{2}{\pi} \frac{\sin^2(\frac{\pi n}{2})}{n} & , n \neq 0 \\ 0 & , n = 0 \end{cases} \quad (1.27)$$

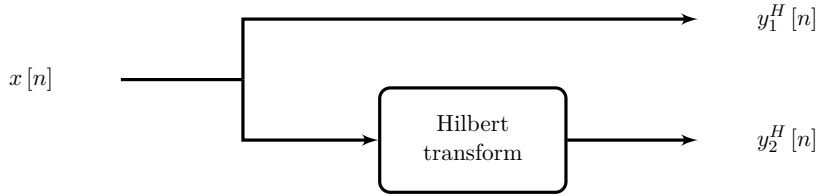


Figure 1.12: Hilbert transform-based demodulation.

In fact, the Bedrosian theorem is verified when the spectra of the $a[n]$ and $\cos(\phi[n])$ are disjoint. Figure 1.13 illustrates the Bedrosian theorem conditions.

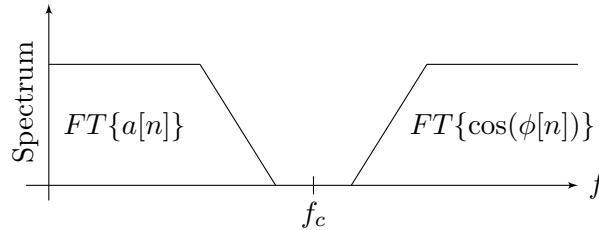


Figure 1.13: Bedrosian theorem conditions.

1.6.2.2 Multidimensional techniques

Multidimensional techniques include the Concordia transform [65, 197, 198, 202, 204] and the principal component analysis [40, 205, 206]. Empirical Mode Decomposition(EMD) or the Ensemble EMD (EEMD) have been proposed to analyze faults for multicomponents signals [174, 207–214]. A review of condition monitoring of induction motors based on stator currents demodulation is available in [5].

1.6 Advanced feature extraction techniques for induction machine fault analysis

Three phase stator current under general conditions (fault, unbalance,...etc) can be modeled as

$$x_k [n] = d_k a [n] \cos (\phi [n] + \psi_k) + b_k [n] \quad (1.28)$$

where d_k and ψ_k represent the amplitude and phase unbalance, respectively and $k = \{0, 1, 2\}$. A multidimensional demodulation technique is a linear transform that allows passing from n -dimensional subspace to p -dimensional subspace ($n > p$). In three phase systems, this linear transform can be expressed mathematically as

$$\begin{bmatrix} y_1 [n] \\ y_2 [n] \end{bmatrix} = \mathbf{H} \begin{bmatrix} x_0 [n] \\ x_1 [n] \\ x_2 [n] \end{bmatrix} \quad (1.29)$$

where \mathbf{H} is the 2×3 matrix.

Concordia transform: The concordia transform is a multidimensional demodulation technique for three electrical signals [198] that the matrix \mathbf{H} is defined by

$$\mathbf{H}^c = \sqrt{\frac{2}{3}} \begin{bmatrix} \frac{\sqrt{2}}{3} & \frac{-1}{\sqrt{6}} & \frac{-1}{\sqrt{6}} \\ 0 & \frac{1}{\sqrt{2}} & \frac{-1}{\sqrt{2}} \end{bmatrix} \quad (1.30)$$

This transform assumes that the three phase systems are balanced ($d_0 = d_1 = d_2 = 1$ and $\psi_k = 0$). This assumption is the main drawback of this method.

Maximum likelihood approach: The maximum likelihood approach is a powerful statistical technique for estimating unknown parameters [180] that the matrix \mathbf{H} is defined by

$$\mathbf{H}^{ML} = \frac{1}{M} \begin{bmatrix} d_1^2 + d_2^2 & -d_1 d_2^2 & -d_1^2 + d_2 \\ \frac{d_1^2 - d_2^2}{\sqrt{3}} & \frac{d_1}{\sqrt{3}} (d_2^2 + 2) & -\frac{d_2}{\sqrt{3}} (d_1^2 + 2) \end{bmatrix} \quad (1.31)$$

where $M = d_1^2 + d_2^2 + d_1^2 d_2^2$

Principal component analysis: Principal component analysis (PCA) is a statistical tool that transforms a number of correlated signals into a small number of principal components [152].

1. CONDITION MONITORING AND FAULT DETECTION OF INDUCTION MACHINES: STATE OF THE ART

Empirical Mode Decomposition: The Empirical Mode Decomposition (EMD) has been originally proposed by Huang[215]. The EMD algorithm is defined by the following steps:

- Identification of all extrema of $x[n]$.
- Interpolation between minima (resp. maxima) ending up with some envelope $e_{min}[n]$ (resp. $e_{max}[n]$).
- Computation of the mean:

$$m[n] = \frac{e_{min}[n] + e_{max}[n]}{2} \quad (1.32)$$

- Extraction of the detail:

$$d[n] = x[n] - m[n] \quad (1.33)$$

- Iteration on the residual $m[n]$.

The EMD algorithm presents some drawbacks as border effects, mode mixing or uncertain stopping criterion. Some noised assisted methods have been developed to overcome these problems such as the Complete Ensemble Empirical Mode Decomposition (CEEMD) or the Ensemble Empirical Mode Decomposition (EEMD) [216].

1.6.3 Advanced feature extraction techniques for induction machines in non-stationary environments

It has been demonstrated that the Fourier transform-based techniques cannot not provide simultaneous time and frequency localization and are not very useful for analyzing time-variant, non-stationary signals. Then, the problem of stator current spectral estimation in non-stationary environments has received a great deal of attention. Therefore, several techniques have been proposed to analyze faults. These techniques can be classified into three categories: parametric techniques, nonparametric techniques, and demodulation techniques. Nonparametric techniques include time-scale and time-frequency presentations [20, 102, 217–223]. Parametric techniques include non-stationary MLE and nonstationary subspace techniques [224]. A demodulation

1.6 Advanced feature extraction techniques for induction machine fault analysis

technique called Hilbert-Huang Transform has been proposed to analyze faults in non-stationary environments [153, 225]. It based on Hilbert transform and Empirical Mode Decomposition techniques.

Several advanced combined techniques have been proposed to analyze faults in start-up and steady-state regimes [226]. A fusion between two techniques: the Complete Ensemble Empirical Mode Decomposition (CEEMD) and the MUSIC is proposed in [226]. In this case, the proposed methodology allows identifying time evolution of the faulty frequencies in start-up and steady-state regimes from the short data record signal buried in noise, as it is the case for inverter-fed induction motors. Another technique has been proposed in [227] to detect incipient broken rotor bar in induction motors using high-resolution spectral analysis based on the start-up current analysis. This technique is based on the short-time MUSIC algorithm that provides high-resolution and the time-frequency pseudo-representation. The proposed methods can graphically show the physical effect of a broken or partially-broken rotor bar. An application of the ESPRIT and the Simulated Annealing Algorithm (SAA) has been proposed to detect broken rotor bar fault in induction motors with short-time measurement data in [143]. These proposed techniques can correctly identify the parameters of the broken rotor bars characteristic components with short-time measurement data. Another fusion between two techniques: the Hilbert transform and the ESPRIT for detecting rotor fault in induction motors at low slip has been proposed in [142]. This fusion combines two main characteristics: ability to avoid spectral leakage and to achieve high-frequency resolution even with a short measurement time. A comparative study and the evaluation of various condition monitoring methods used for induction machines, with the aim of early detection of one partially-broken rotor bar by steady-state current spectrum analysis and different supply conditions is proposed in [228]. The techniques considered in this study are the Fast Fourier transform (FFT), Wavelet and FFT, MUSIC, Empirical Mode Decomposition (EMD) and FFT, and EMD associated with MUSIC. Broken rotor bar detection in variable speed drive-fed induction motors at start-up by high-resolution spectral analysis has been proposed in [229]. In this case, the time-frequency spectrum is able to graphically show a different pattern for the healthy and faulty conditions.

1.7 Induction machine fault detection techniques

Early fault detection helps to reduce the maintenance-cost in the induction machine-based applications. In the literature, the existing techniques for induction machine fault detection based on stator currents can be categorized into two subclasses: artificial intelligence and detection theory.

1.7.1 Artificial intelligence techniques

Artificial intelligence (AI) techniques are ways that imitate the intelligent humans think to develop expert systems and to implement human intelligence in machines. The main steps of an AI-based diagnostic mechanism are signature extraction, fault identification, and fault severity evaluation [13]. These techniques include: Expert Systems (ES), Artificial Neural Network (ANN), Support Vector Machine (SVM), Fuzzy Logic (FL), Genetic Algorithms (GA) and hybrid techniques [230, 231]. Reviews of artificial intelligence applications for induction machine fault detection are available in [232–234]. However, these techniques present several drawbacks such as its required initial training phase and their performances depend on the used feature extraction techniques.

1.7.1.1 Expert Systems

Expert Systems also known as knowledge-based systems are computer programs that emulate the reasoning process of a human expert or perform in an expert manner in a domain for which no human expert exists [235]. They solve problems using heuristic knowledge rather than precisely formulated relationships, in forms that reflect more accurately the nature of most human knowledge. These systems consist of a knowledge bases, an inference mechanism, and human/expert system interface [232, 236]. There are three different types of ES: rule-based diagnostic, model-based diagnostic, and on-line diagnostic expert systems [237].

The rule-based diagnostic is the most commonly used technique for developing ES [238]. The basic architecture of this type is depicted in Fig. 1.14. The user interacts with the system through a user interface which may use menus, natural language or any other style of interaction. Then an inference engine is used to reason with both the expert knowledge (extracted from expert) and data specific to the particular problem

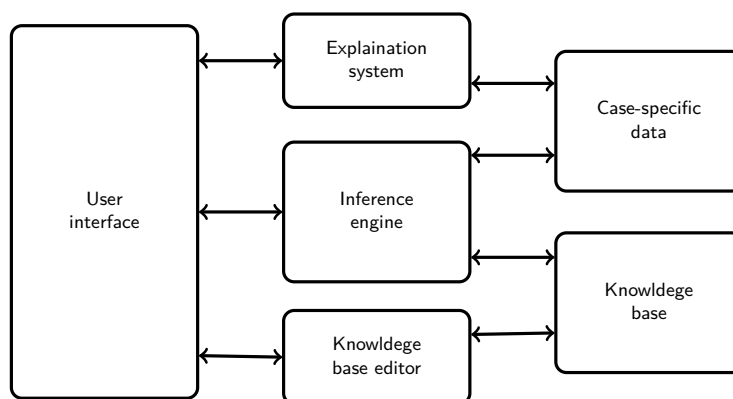


Figure 1.14: Basic architecture of a rule-based expert system [7, 8].

being solved. The case specific data includes both data provided by the user and partial conclusions (along with certainty measures) based on this data. Almost all expert systems have also an explanation subsystem, which allows the program to explain its reasoning to the user. Some systems also have a knowledge base editor which help the expert or knowledge engineer to easily update and check the knowledge base [7].

The main limitations of the early diagnostic expert systems are the: inability to represent accurately time-varying and spatially varying phenomena, inability of the program to detect specific gaps in the knowledge base, difficulty for knowledge engineers to acquire knowledge from experts reliably, difficulty for knowledge engineers to ensure consistency in the knowledge base, and inability of the program to learn from its errors [239]. Performances of ES are depended on the information stored in the knowledge phase. The inference manages the use of knowledge bases. In industry, applications of ES include classification, diagnosis, monitoring, process control, design, scheduling and planning, and generation of options [240]. Applications of ES in condition monitoring and fault diagnosis of induction machines are available in [241, 242].

1.7.1.2 Fuzzy logic

Fuzzy logic systems (FLS) are reminiscent of human thinking processes and natural language enabling decisions to be made based on vague information. It is a nonlinear mapping of an input data (feature) vector into a scalar output, i.e., it maps numbers into numbers. Fuzzy set theory and fuzzy logic establish the specifics of the nonlinear mapping [243]. The richness of FLS is that there are enormous numbers of possibilities

1. CONDITION MONITORING AND FAULT DETECTION OF INDUCTION MACHINES: STATE OF THE ART

that lead to lots of different mappings [243]. Figure 1.15 shows the block diagram of a fuzzy logic based diagnostic system [9]. The knowledge acquisition consists of the construction of the membership functions which describe the monitored quantities and of the construction of the rule base that correlates these quantities to the various types of system working states (normal, faulty and pre-faulty working state) [9]. This can be made using an off-line built the database obtained from three sources of knowledge: the expert knowledge, the historical data and the analytical knowledge. Expert knowledge is acquired by interviewing the expert operator and can be represented as fuzzy conditional statements. Historical data (process history and fault statistics) is usually available as service notes collected by monitoring the behaviour of the system under diagnosis over time [9]. Analytical knowledge based on computer simulation of the system under diagnosis, if the mathematical model, even complex, is available. This knowledge is obtained by observing any parameter change under the influence of each simulated fault and then by expressing this information as fuzzy conditional statements [9].

FLS can contribute with: well-developed fuzzy logic theory, humanlike reasoning mechanisms, using linguistic terms, accommodating commonsense knowledge, ambiguous knowledge, imprecise but rational knowledge, universal approximation techniques, robustness, fault tolerance, and low cost of development and maintenance [244]. The main characteristics of a fuzzy logic diagnosis system performance are [245]: automatic interpretation of relations among the test (observation results) and possible situations, pointing out the process condition, detailed explanation of how the particular conclusion has been reached, indication of the possible causes of failures, description of the possible consequences, and recommendation for process maintenance and repair under new circumstances. Applications of induction machine fault detection using FL are available in [246–252].

1.7.1.3 Artificial Neural Networks

Artificial Neural Networks (ANN) are the most popular AI techniques used to detect faults in induction machines. These techniques are inspired from computational model of the brain [253, 254]. Artificial neurons are interconnected by edges, forming a neural network. Networks receive input, internal processes take place such as activations of

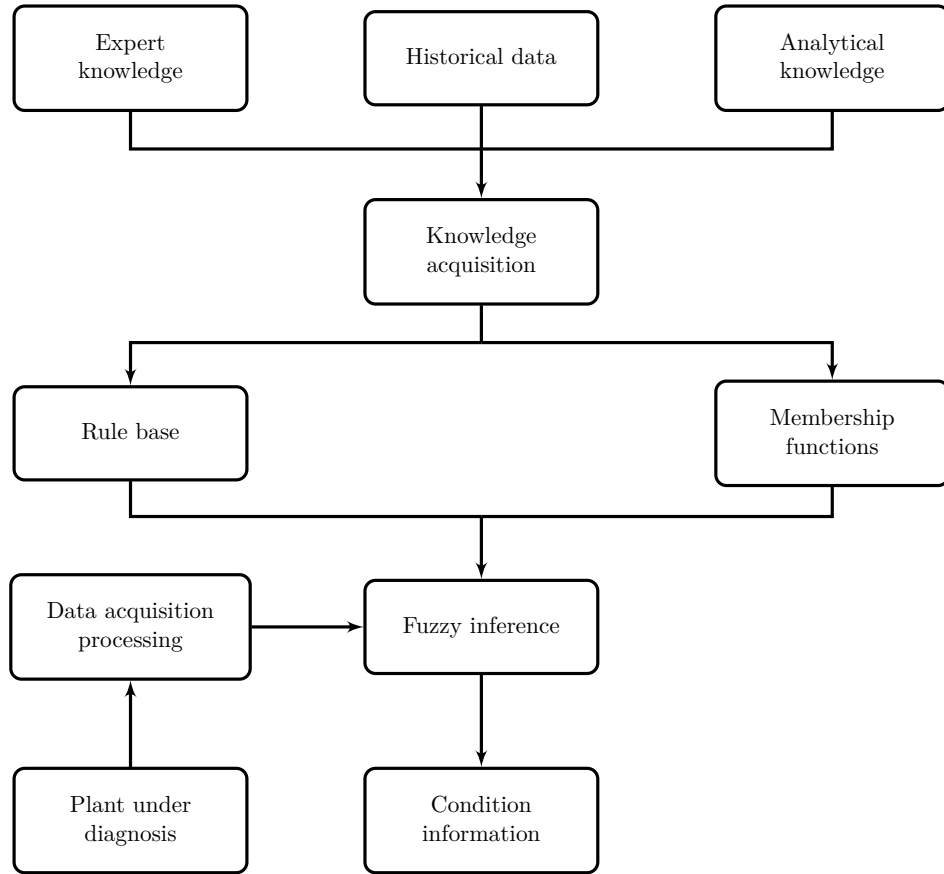


Figure 1.15: Block diagram of the fuzzy diagnostic system based diagnostic system [8, 9].

the neurons, and the network yields output [255]. ANN can learn supervised or unsupervised. For supervised learning, the most commonly used neural network structure is the multilayer perceptrons (MLP) trained using the back-propagation algorithm. In this configuration, neurones are grouped into layers. The first layer and the last layer constitute the input and the output layers. The remaining layers represent the hidden layers [256, 257]. Unsupervised learning networks proceed through the learning stage without the provision of input of data classifications. They require less training iterations as they do not require exact optimization [8].

ANN can contribute with: learning from data, modeling empirical behavior of humans, universal approximation techniques, good generalization, methods for extracting knowledge from data, methods for data analysis, associative memories and pattern-matching techniques, massive parallelism, and robustness [244]. The major advantage

1. CONDITION MONITORING AND FAULT DETECTION OF INDUCTION MACHINES: STATE OF THE ART

of ANN is their ability to represent complex, nonlinear relationships and to self-learn the pattern recognition of those relationships [8]. In [258], a fast and accurate motor condition monitoring and early fault detection system using 1D convolutional neural networks is proposed. An applications of induction machine fault detection using ANN are available in [204, 212, 214, 259–269].

1.7.1.4 Support Vector Machine

Support Vector Machine (SVM) is a classification technique based on developed statistical learning theory. The SVM is fundamentally a two-class classifier but in practice, problems involve classes greater than 2. Various methods have therefore been proposed for combining multiple two-class SVMs in order to build a multiclass classifier [270]. These methods convert n -class classification problem into n two-class problems. There have several SVM variants: least squares SVM, linear programming SVM, robust SVM, Bayesian SVM, and committee machines [271]. Advantages of SVM over ANN classifiers are as follows: maximization of generalization ability, no local minima, and robustness to outliers [271]. SVM presents several disadvantages such as: the long training time, its extension to multiclass problems and the need of parameters selection. The long training time is due to the fact that the number of variables is equal to the number of training data. Extension to multiclass problems is not straightforward, and there are several formulations.

Several studies based on SVM have been proposed in the literature [272–280]. A SVM-based decision to detect mechanical faults using an improved combination of Hilbert and Park transformations is proposed in [276]. This combination allows creating two fault signatures: Hilbert modulus current space vector and Hilbert phase current space vector. These two signatures are exploited as inputs for learning and testing SVM.

1.7.1.5 Genetic Algorithms

Genetic Algorithms (GA) are an iterative search heuristic based on the process of natural selection. They are a family of computational models inspired by natural evolution [281]. These algorithms encode a potential solution to a specific problem on a simple chromosome-like data structure, and apply recombination operators to these structures in such a way as to preserve critical information [281]. GA belong to

1.7 Induction machine fault detection techniques

the larger class of evolutionary algorithms and they combine randomized information exchange methods, which incorporate the survival of the fittest strategy, to find optimal solutions to the problem [282]. In fact, GA are employed to solve optimization problems efficiently. The three most important aspects of using GA are the: definition of the objective function, implementation of the genetic representation, and implementation of the genetic operators.

To apply GA, six steps are needed: initialization, selection, crossover, mutation, reproduction, termination. In practice, the standard GA has the following steps: choose the initial population, assign a fitness function, perform elitism, perform selection, perform crossover, and perform mutation. GA begins with the initialization that the population of chromosomes is chosen according to the problem nature. It typically contains several hundreds or thousands of possible solutions. Often, the initial population is generated randomly, allowing the entire range of possible solutions. The selection operator is the process that determines which solutions are to be preserved and allowed to reproduce and which ones deserve to die out. The primary objective of the selection operator is to emphasize the good solutions and eliminate the bad solutions in a population while keeping the population size constant. There are different techniques to implement selection operator in GA: tournament selection, roulette wheel selection, proportionate selection, rank selection, steady state selection, etc. The crossover operator is used to vary the programming of a chromosome or chromosomes from one generation to the next. It is analogous to reproduction and biological crossover, upon which GA are based. Cross over is a process of taking more than one parent solutions and producing a child solution from them. There are several crossover techniques: single-point crossover, two-point crossover, uniform crossover, half uniform crossover, three parent crossover, crossover for ordered chromosomes. The mutation operator is the occasional introduction of new features in the solution strings of the population pool to maintain diversity in the population. It is analogous to biological mutation. The main purpose of the mutation operator is preserving and introducing diversity. Mutation should allow the algorithm to avoid local minima by preventing the population of chromosomes from becoming too similar to each other, thus slowing or even stopping evolution. There are several mutation types: insert, inversion, scramble, swap, flip, interchanging, reversing, uniform, and creep mutations [283].

1. CONDITION MONITORING AND FAULT DETECTION OF INDUCTION MACHINES: STATE OF THE ART

An induction machine fault detection using a GA is proposed in [284]. In this application, the GA are used to keep the amplitude of all faulty lines and fuzzy logic approach to conclude to the load level operating system and to inform the operator of the rotor fault severity. Turn faults detection technique using the GAs is proposed in [285]. GA is proposed in this paper to performe a fault identification method.

1.7.1.6 Hybrid Approaches

To diagnose faults, several hybrid approaches have been proposed in the literature [286–293]. Among hybrid approaches, Neuro-Fuzzy Systems (NFS) have received a great of attention to overcome the knowledge acquisition bottleneck faced by humans while designing the knowledge base of a traditional fuzzy expert system. The neural network training techniques of NFS can handle the information retrieval from data using optimization techniques. The fuzzy system representation on the other hand provides the intuitive understanding of the resulting system and establishes the possibility of integrating expert knowledge. Since the two approaches have a different knowledge representation, their combination can be a persuasive way to fuse information from different sources, namely human experts and experimental data. NFS can generate new rules from data or they can refine existing rules by adapting parameters within them.

1.7.2 Statistical decision theory

The decision based on the detection theory allows making an optimal decision in order to identify which hypothesis is true without need for a training database. Popular criteria defining the detection procedure with unknown signal and noise parameters are the Bayesian and the Neyman-Pearson approaches. The Bayesian approach is a detector to composite hypothesis testing. Unknown parameters are considered as realizations of random variables and are assigned a prior Probability Density Function (PDF) [294]. Unfortunately, this approach requires multidimensional integration with a dimension equal to the unknown parameter dimension. The Neyman-Pearson approach involves a maximization of the probability of detection P_D for a given probability of false alarm P_{Fa} [295]. It is based on the likelihood ratio test of the PDFs under a binary hypothesis. The threshold of this test is chosen from the false alarm constraint P_{Fa} . When the likelihood ratio depends on unknown parameters, these parameters are replaced by

their estimates using the MLE. This solution is known as the Generalized Likelihood Ratio Test (GLRT). Applications of Fault-detection procedures based on hypothesis testing can be found in [138, 296].

1.8 Conclusion

This chapter has described the basic concept and the common faults of induction machines. These faults can be classified into two main classes: mechanical and electrical faults. In term of maintenance, three types have been described: the corrective, the preventive, and the predictive maintenances. According to several literature reviews, the predictive maintenance is the most promising technique to detect and analyze faults. In this predictive context, several faults indicators are exploited to develop condition monitoring techniques. Existing techniques are mainly categorized as vibration monitoring, temperature monitoring, oil debris analysis, acoustic emission monitoring, and current, voltage, or power monitoring. It has been demonstrated that stator current-based condition monitoring has several advantages over other techniques in terms of low cost, easy access, easy implementation, and ability to detect faults. In operating conditions, it can be distinguished between two main conditions: stationary and nonstationary environments. In nonstationary environments, the existing advanced feature extraction techniques can be classified into three categories: parametric techniques, nonparametric techniques, and demodulation techniques. In stationary environments, techniques can be also classified into three main categories: power spectrum estimation, demodulation techniques, and higher order spectra analysis.

This chapter has reviewed the state of the art of the existing induction machine condition monitoring and fault detection techniques. Taking into account benefits and drawbacks of each described technique in stationary environments, parametric techniques seem to be the most suitable approaches for induction machines conditions monitoring using the stator current. In addition, the detection theory seems to be the candidate of choice for fault detection.

**1. CONDITION MONITORING AND FAULT DETECTION OF
INDUCTION MACHINES: STATE OF THE ART**

Stator Current Parameters Estimation and Fault Severity Analysis

Contents

2.1	Introduction	50
2.2	Stator Current Model	50
2.2.1	Stator Current Model in Stationary Conditions	50
2.2.2	Stator Current Frequency Model	52
2.2.3	Stator Current Parameters Estimation	53
2.3	Subspace Spectral Estimation Techniques	56
2.3.1	Covariance Matrix	56
2.3.2	MUSIC Estimators	57
2.3.3	ESPRIT Estimators	60
2.3.4	Modified ESPRIT	62
2.4	Model Order Estimation	66
2.4.1	Model Order Estimation (Nonparametric Approach)	67
2.4.2	Model Order Selection (Parametric Approach)	69
2.5	Proposed Fault Detection Methodology	70
2.5.1	Proposed Fault Severity Criterion	70
2.5.2	Condition Monitoring Architecture	71
2.6	Simulations Results	72
2.6.1	Subspace Techniques Performances	73
2.6.2	Model Order Selection Performances	75
2.6.3	Fault Severity Criterion Performances	76
2.7	Conclusion	77

2. STATOR CURRENT PARAMETERS ESTIMATION AND FAULT SEVERITY ANALYSIS

2.1 Introduction

To analyze and detect faults, the problem is equivalent to a model parameters estimation of multiple sinusoids. Several techniques have been proposed to address this problem. The Nonlinear Least Squares Estimator (NLSE) is the natural one. When noise is assumed to be white Gaussian, NLSE is equivalent to the Maximum Likelihood Estimator (MLE). The MLE estimator is an asymptotically optimal estimator but it requires the maximization of a multidimensional and multimodal cost function. Among techniques that can approach performances of the MLE, subspace techniques have the ability to distinguish closely spaced frequencies. Subspace techniques are therefore ways to separate frequencies including components close to the fundamental frequency f_s and harmonics (multiple of f_s). Once frequencies are estimated, amplitudes and phases are obtained using MLE that is equivalent to a Linear Least-Squares Estimator (LSE). Then, a fault severity criterion can be derived from amplitudes that can determine the machine state.

The present chapter is organized as follows: First, a stator current model in stationary environments is presented. This model is used to describe the problem of stator current model parameters estimation. This problem is solved using several estimation techniques such as subspace spectral estimation techniques for frequency estimation, LSE for amplitudes and phases estimation, information theoretic criteria to select the model order. Then, a fault severity detection methodology is proposed. Finally, simulation results of the proposed techniques are given in the last part.

2.2 Stator Current Model

This section presents the stator current model under fault conditions in stationary environments. It gives also the stator current frequency structure that can be exploited to interpret results of the power spectrum estimation.

2.2.1 Stator Current Model in Stationary Conditions

Many signal processing methods are based on parametric models of the signals. The performance of such methods depends heavily on the chosen model structure and

on the quality of the parameter estimates [297]. Parametric models called also parametric family or finite-dimensional models are mathematical functions that represent the probability of the model producing the given data. Statistically, data model selection is to search its probability density function that is parametrized by the unknown parameters. A reasonable model of the PDF is the white Gaussian noise [298]. This choice is justified by the need to formulate a mathematically tractable model so that closed form estimators can be found [298]. Once the model is selected, efficiency and unbiased estimators are required to estimate model parameters. In fact, the bias and variance are both important measures of the quality of these estimators. These PDF-based estimators are called the classical estimators that parameters are assumed to be deterministic but unknown. There have several criteria for model selection: Akaike information criterion, the Bayes factor and/or the Bayesian information criterion, false discovery rate, Likelihood-ratio test, etc.

In electrical engineering context, the model selection is based on understanding the physical phenomena that can appear in electrical systems. It has been demonstrated that induction machine faults manifest in frequency domain by frequency signatures appearing in the stator current power spectrum. To model stator current in stationary conditions, this model is assumed to be physical, deterministic, and nonlinear. This model is based on the following assumptions:

- The received signal is modeled as a sum of L sinus components in noise.
- The phases of the exponential components are independent and uniformly distributed on the interval $[-\pi, \pi[$.
- The noise is assumed to be a white Gaussian noise with zero-mean and variance σ^2 . In practice, a noise component is added to take into account the measurement errors.

Since performances of any estimator is critically depend on the PDF assumptions, the noise assumption is motivated by the following reasons:

- The Gaussian noise assumption leads to minimize the worst-case asymptotic Cramer-Rao Bound (CRB) [299].
- The Minimum Variance Unbiased (MVU) estimator is equivalent to the mean LSE when the noise is white Gaussian [298].

2. STATOR CURRENT PARAMETERS ESTIMATION AND FAULT SEVERITY ANALYSIS

- The sum of a sufficiently large number of independent and identically random variables are approximately Gaussian distributed (Central Limit Theorem) [300].

According to the above-mentioned assumptions, the induction machine stator current in faults presence can be described by the following model

$$x[n] = \sum_{k=0}^{L-1} a_k \cos\left(2\pi f_k \times \frac{n}{F_s} + \phi_k\right) + b[n] \quad (2.1)$$

where $x[n]$ denotes the stator current samples, $b[n] \sim \mathcal{N}_c(0, \sigma^2)$ is a white Gaussian noise, L represents the model order, F_s is the sampling frequency, a_k , f_k , and ϕ_k are amplitude, frequency, and initial phase of the k^{th} component, respectively.

At time $n = 0, 1, 2, 3, \dots, N - 1$, the observed stator current vector \mathbf{x} , defined as $\mathbf{x} = [x(0) \ \dots \ x(N-1)]^T$, can be expressed by the following separable nonlinear model

$$\mathbf{x} = \mathbf{H}(\boldsymbol{\Omega}) \boldsymbol{\theta} + \mathbf{b} \quad (2.2)$$

where

- $\boldsymbol{\theta} = [\Re(\mathbf{v}) \ -\Im(\mathbf{v})]^T$ is a $2L \times 1$ column vector that contains the information on the sinusoids amplitudes and phases, and $\mathbf{v} = [a_0 e^{j\phi_0} \ a_1 e^{j\phi_1} \ \dots \ a_{L-1} e^{j\phi_{L-1}}]$.
- $\mathbf{H}(\boldsymbol{\Omega}) = [\Re(\mathbf{B}(\boldsymbol{\Omega})) \ \Im(\mathbf{B}(\boldsymbol{\Omega}))]$ is a $N \times 2L$ matrix depending on the frequencies $\boldsymbol{\Omega} = [f_0 \ \dots \ f_{L-1}]$, where $\mathbf{B}(\boldsymbol{\Omega}) = [\mathbf{a}(f_0) \ \mathbf{a}(f_1) \ \dots \ \mathbf{a}(f_{L-1})]$, and $\mathbf{a}(f) = [1 \ e^{j2\pi f \times \frac{1}{F_s}} \ \dots \ e^{j2\pi f \times \frac{N-1}{F_s}}]^T$.
- $\mathbf{b} = [b[0] \ \dots \ b[N-1]]^T$ is a $N \times 1$ column vector containing the noise samples.
- The symbol $(.)^T$ refers to the matrix transpose.

This model is linear in $\boldsymbol{\theta}$ but nonlinear in $\boldsymbol{\Omega}$. If frequencies are estimated, a linear least squares can estimate amplitudes and phases.

2.2.2 Stator Current Frequency Model

In stationary environment, the stator current spectrum of induction machines without faults contains only the fundamental frequency and harmonics. In the international standard IEC 038 of electrical engineering, frequencies of the stator current spectrum

may have a small variation up to 1% of the fundamental frequency value [301]. In case of fault presence, the spectrum also contains frequencies called fault frequencies according to the following relationship [302]

$$f_f = f_s \pm kf_c \quad (2.3)$$

where f_s is the supply fundamental frequency, f_c is the fault characteristic frequency, and $k \in \mathbb{N}^*$. Therefore, based on the assumed stator current model, the problem of faults analysis is then a classical problem of estimating the multiple sinusoids in Gaussian noise.

2.2.3 Stator Current Parameters Estimation

When a parametric model is considered, the objective is often the estimation and/or the detection. The main purpose of any parametric modeling is often to adjust parameters of a selected model function such that the model optimizes some criterion. Generally, it is based on the measured signal fitting with a minimum possible error. In signal processing, this task is called model parameters estimation [297]. Once the stator current model has specified, the problem becomes on of determining an optimal estimator. Regarding the stator current model, the problem is a estimation of multiple sinusoids with unknown parameters in the Gaussian noise. This problem has attracted a great intention in signal processing community. It is called spectral line analysis or line spectrum analysis that the main goal is extracting information on sinusoidal signals in noise. This estimation problem has been studied in numerous applications: sonar, radar, underwater surveillance, communications, geophysical exploration, speech analysis, nuclear physics and other fields [303]. The multiple sinusoids is a non linear model with unknown parameters that generates a non linear least squares problem. Then, the natural estimator to estimate parameters of this model is the Nonlinear Least Squares Estimator (NLSE) [158, 298] since the optimal minimum variance unbiased (MVU) estimator is analytically difficult to obtain it or may not exist [298]. In fact, The NLSE is usually applied in situations where a precise statistical characterization of the data is unknown or where an optimal estimator cannot be found or may be too complicated to apply in practice. Estimations of NLSE are obtained by the squared deviations minimization between stator current measurements and the assumed stationary model

2. STATOR CURRENT PARAMETERS ESTIMATION AND FAULT SEVERITY ANALYSIS

[158, 298]. These estimation problems using NLSE can be expressed by the following cost function

$$\{\hat{\boldsymbol{\Omega}}, \hat{\boldsymbol{\theta}}\} = \arg \min_{\{\boldsymbol{\Omega}, \boldsymbol{\theta}\}} \|\mathbf{x} - \mathbf{H}(\boldsymbol{\Omega}) \boldsymbol{\theta}\|^2, \quad (2.4)$$

where $\{\boldsymbol{\Omega}, \boldsymbol{\theta}\}$ denote the unknown stator current model parameters. Note that, when the noise is assumed to be white and Gaussian, this estimator corresponds to the Maximum Likelihood Estimator (MLE). MLE is the most commonly used parametric estimation method thanks to it is asymptotically unbiased (i.e the estimate becomes unbiased in the limit when the number of data points goes to infinity) and efficient (i.e. its mean-squared error satisfies the Cramer-Rao bound) estimator [298]. The main drawback of the MLE is its computation cost since the estimation of the frequencies requires the maximization of a multidimensional and multimodal cost function [145, 146].

The exact MLE requires to select model order but when it is assumed to be known, model parameters are found by maximizing $\ln p(\mathbf{x}, \boldsymbol{\Omega}, \boldsymbol{\theta})$ with respect to $\boldsymbol{\Omega}, \boldsymbol{\theta}$.

$$\{\hat{\boldsymbol{\Omega}}, \hat{\boldsymbol{\theta}}\} = \operatorname{argmax} \ln p(\mathbf{x}, \boldsymbol{\Omega}, \boldsymbol{\theta}) \quad (2.5)$$

where $p(\mathbf{x}, \boldsymbol{\Omega}, \boldsymbol{\theta})$ is the probability density function (PDF) of the data \mathbf{x} that is given by

$$p(\mathbf{x}, \boldsymbol{\Omega}, \boldsymbol{\theta}) = \frac{1}{(2\pi\sigma^2)^{\frac{N}{2}}} \times \exp\left(\frac{-1}{2\sigma^2} (\mathbf{x} - \mathbf{H}(\boldsymbol{\Omega}) \boldsymbol{\theta})^T (\mathbf{x} - \mathbf{H}(\boldsymbol{\Omega}) \boldsymbol{\theta})\right) \quad (2.6)$$

The maximization in (2.5) is equivalent to the minimization of the following cost function [298]

$$J(\mathbf{x}, \boldsymbol{\Omega}, \boldsymbol{\theta}) = (\mathbf{x} - \mathbf{H}(\boldsymbol{\Omega}) \boldsymbol{\theta})^T (\mathbf{x} - \mathbf{H}(\boldsymbol{\Omega}) \boldsymbol{\theta}) \quad (2.7)$$

The optimization of the previous cost function requires a multidimensional grid search over the possible frequencies since the multidimensional likelihood function is a highly nonlinear function of the frequencies and has many local maxima, even in the absence of noise [304]. This problem becomes so worse when the model order increases [304]. The multimodal nature of the MLE can be seen in Fig.2.1. This estimation problem can be divided into three separate estimations: frequency, phase and amplitude estimations. To estimate frequencies, the MLE requires the maximization of a multidimensional and multimodal cost function. Despite these problems of the exact MLE, an estimator called mean likelihood has been proposed in [304] that can be implemented with a

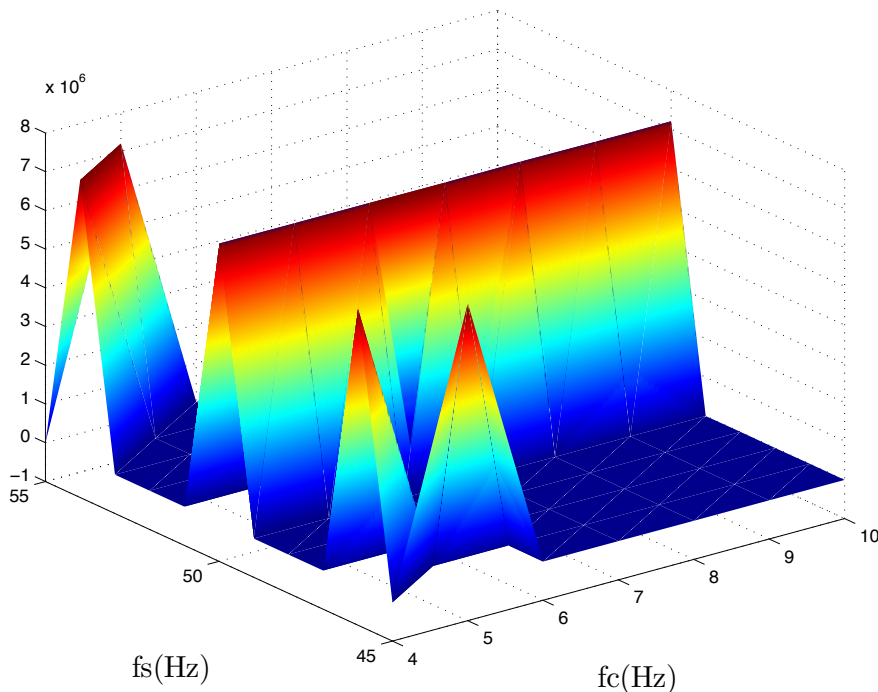


Figure 2.1: Plot of $J(\mathbf{x}, \boldsymbol{\Omega}, \boldsymbol{\theta})$ for five frequencies with the frequency structure given in (2.3) with $f_s = 50\text{Hz}$, $f_c = 4\text{Hz}$, and $k = \{0, 1, 2\}$.

moderate amount of computation. This estimator considers the normalized likelihood function (NLF) as a probability density function. In this approach, frequencies can be obtained as the mean value of the NLF. In the literature, many methods have been developed to address this issue. The list of references for spectral line analysis can be found in [303]. Among these proposed techniques that can approach performances of the MLE, the subspace techniques called also high-resolution methods have been proposed [136–144, 180]. The subspace techniques are based on the eigendecomposition of the covariance matrix of measurements data \mathbf{x} . Once the frequencies are estimated, the signal model then becomes linear in $\boldsymbol{\theta}$ and MLE becomes a linear Least Squares Estimator (LSE). In this case, the MLE of phases and amplitudes is given by

$$\hat{\boldsymbol{\theta}} = \left(\mathbf{H}^T \left(\hat{\boldsymbol{\Omega}} \right) \mathbf{H} \left(\hat{\boldsymbol{\Omega}} \right) \right)^{-1} \mathbf{H}^T \left(\hat{\boldsymbol{\Omega}} \right) \mathbf{x} \quad (2.8)$$

2. STATOR CURRENT PARAMETERS ESTIMATION AND FAULT SEVERITY ANALYSIS

2.3 Subspace Spectral Estimation Techniques

This section proposes subspace spectral estimation techniques to avoid limitations of the MLE. These techniques are an attractive alternative to the ML-based estimation methods since they can attain nearly the same estimation performance for time-series as the NLS estimator without being based on the intractable cost function [305]. The term subspace-based refers to separating two distinct subspaces: the signal subspace and the noise subspace. To separate these subspaces, an eigendecomposition of the covariance matrix \mathbf{R}_x is required.

2.3.1 Covariance Matrix

According to chosen stator current model, it can be seen that in the absence of noise, the N -dimensional vector \mathbf{x} belongs to L -dimensional subspace but in case when the noise is present, it is not the case [306]. Therefore, the N -dimensional vector \mathbf{x} belongs to P -dimensional subspace that can differentiate between two main subspaces: signal and noise subspaces. To separate these subspaces, an eigendecomposition of the covariance matrix $\mathbf{R}_x = E[\mathbf{x}[n]\mathbf{x}^H[n]]$ is used. This matrix \mathbf{R}_x has two main properties: it is orthogonally diagonalizable and their eigenvalues are positive and real. The covariance matrix eigendecomposition can be written as follows

$$\mathbf{R}_x = \mathbf{U}\mathbf{\Lambda}\mathbf{U}^H = \sum_{k=1}^P \lambda_k \mathbf{u}_k \mathbf{u}_k^H \quad (2.9)$$

where $P \succ L$ is the eigenvalues number, $\mathbf{\Lambda} = \text{diag}[\lambda_1, \dots, \lambda_L]$, and $\mathbf{U} = [\mathbf{u}_{L+1}, \dots, \mathbf{u}_P]$. The eigenvalues λ_m are real and positive, arranged in descending order and the corresponding eigenvectors \mathbf{u}_k are orthonormal. Thus, the covariance matrix can be written as a sum of the signal and the noise covariance matrices

$$\mathbf{R}_x = \mathbf{R}_s + \mathbf{R}_n = \begin{bmatrix} \mathbf{S} & \mathbf{G} \end{bmatrix} \begin{bmatrix} \mathbf{\Lambda}_s & 0 \\ 0 & \mathbf{\Lambda}_n \end{bmatrix} \begin{bmatrix} \mathbf{S} & \mathbf{G} \end{bmatrix}^H, \quad (2.10)$$

where \mathbf{R}_s denotes the signal covariance matrix, \mathbf{R}_n is the noise covariance matrix, $\mathbf{\Lambda}_s = \text{diag}[\lambda_1 \dots \lambda_L]$ and $\mathbf{\Lambda}_n = \text{diag}[\lambda_{L+1} \dots \lambda_P]$ are diagonal matrices containing eigenvalues of the signal and the noise subspaces arranged in descending order, respectively (\mathbf{S} and \mathbf{G} are the associated orthonormal eigenvectors, respectively).

2.3 Subspace Spectral Estimation Techniques

Since \mathbf{R}_x is orthogonally diagonalizable, the signal and noise subspaces are orthogonal to each other. Therefore, the orthogonality between signal and noise subspaces ($\mathbf{S}^H \mathbf{S} = \mathbf{I}$ and $\mathbf{G}^H \mathbf{G} = \mathbf{I}$), can be explained by the following expressions

$$\begin{aligned} \mathbf{P}_G \mathbf{S} &= 0, \\ \mathbf{P}_S \mathbf{G} &= 0, \end{aligned} \tag{2.11}$$

where $\mathbf{P}_S = \mathbf{S} \mathbf{S}^H$ and $\mathbf{P}_G = \mathbf{G} \mathbf{G}^H$ are the projection operators onto signal and noise subspaces, respectively.

In practice, the theoretical covariance matrix \mathbf{R}_x and its eigendecomposition are not known but can be estimated from observations as follows

$$\hat{\mathbf{R}}_x = \frac{1}{N} \sum_{p=M-1}^{N-1} \mathbf{x}_p \mathbf{x}_p^H \tag{2.12}$$

where $\mathbf{x}_p = [x(p), \dots, x(p - M + 1)]^T$.

2.3.2 MUSIC Estimators

MUSIC estimators are subspace methods based on the noise subspace [158] that exploit the orthogonality between noise and signal subspaces. This method is given by algorithm 1. Frequencies are determined as the minimizing arguments of the following cost function

$$f(\theta) = \text{Tr} \left(\mathbf{H}_c(\boldsymbol{\Omega}_c) \mathbf{H}_c^H(\boldsymbol{\Omega}_c) \mathbf{G} \mathbf{G}^H \right). \tag{2.13}$$

where $\mathbf{H}_c(\boldsymbol{\Omega}_c) = \mathbf{B}(\boldsymbol{\Omega}_c)$ is a $N \times 2L$ matrix depending on the frequencies $\boldsymbol{\Omega}_c = [-\boldsymbol{\Omega} \quad \boldsymbol{\Omega}]$. Using trace properties, and properties of \mathbf{G} , we can write

$$\hat{\boldsymbol{\Omega}}_c = \arg \min_{\{f\}} \left\| \mathbf{a}^H(f) \hat{\mathbf{G}} \right\|_F^2, \tag{2.14}$$

where $\|\cdot\|_F$ denotes the Frobenius norm. Depending on how the minimizing arguments of $f(\theta)$ are searched for, there exist two kinds of MUSIC implementations: Spectral-MUSIC and Root-MUSIC [307].

The Spectral-MUSIC finds the minimizing arguments of $f(\theta)$ by a one-dimensional

2. STATOR CURRENT PARAMETERS ESTIMATION AND FAULT SEVERITY ANALYSIS

Algorithm 1 Spectral MUSIC.

Require: N -data samples $x[n]$

1. Estimate the model order L
2. Estimate the covariance matrix \mathbf{R}_x
3. Evaluate the eigendecomposition $\mathbf{R}_x = \mathbf{U}\mathbf{\Lambda}\mathbf{U}^H$
4. Separate the signal and the noise subspaces

$$\mathbf{R}_x = \mathbf{S}\mathbf{\Lambda}_s\mathbf{S}^H + \mathbf{G}\mathbf{\Lambda}_n\mathbf{S}^H \quad (2.16)$$

5. Use eigenvectors of the noise subspace to plot the pseudo-spectrum function:

$$\mathcal{P}(f) = \frac{1}{\|\mathbf{a}^H(f)\widehat{\mathbf{G}}\|_F^2} \quad (2.17)$$

6. Find L peaks of the pseudo-spectrum function to obtain frequencies.
 7. Return frequencies.
-

search algorithm as follows

$$\widehat{\Omega}_c = \arg \max_{\{f\}} \frac{1}{\|\mathbf{a}^H(f)\widehat{\mathbf{G}}\|_F^2}, \quad (2.15)$$

Frequency estimation is obtained by finding the L -highest local maxima of the (2.15) called pseudo-spectrum function. In the case when $\widehat{\mathbf{G}}$ contains a one vector, the MUSIC estimator is equivalent to Pisarenko method.

The Root-MUSIC finds the minimizing arguments of $f(\theta)$ by polynomial rooting to avoid searching for peaks [307, 308]. This estimator converts this pseudo-spectrum function into a polynomial representation that is given by

$$Q(z) = \mathbf{a}^H\left(\frac{1}{z^*}\right)\mathbf{G}\mathbf{G}^H\mathbf{a}(z), \quad (2.21)$$

where $\mathbf{a}(z) = [1 \quad z \quad \dots \quad z^{M-1}]^T$ is a column vector and $z = e^{\frac{j2\pi f}{F_s}}$. The root-MUSIC algorithm requires to find the roots of the complex polynomial function $z^{M-1}Q(z)$ for

2.3 Subspace Spectral Estimation Techniques

Algorithm 2 Root MUSIC.

Require: N -data samples $x[n]$

1. Estimate the model order L
2. Estimate the covariance matrix \mathbf{R}_x
3. Evaluate the eigendecomposition $\mathbf{R}_x = \mathbf{U}\mathbf{\Lambda}\mathbf{U}^H$
4. Separate the signal and the noise subspaces

$$\mathbf{R}_x = \mathbf{S}\mathbf{\Lambda}_s\mathbf{S}^H + \mathbf{G}\mathbf{\Lambda}_n\mathbf{S}^H \quad (2.18)$$

5. Constitute the complex polynomial function

$$Q(z) = \mathbf{a}^H \left(\frac{1}{z^*} \right) \mathbf{G}\mathbf{G}^H \mathbf{a}(z), \quad (2.19)$$

6. Estimates frequencies according to

$$\hat{f}_k = \frac{\arg(\hat{z}_k)}{2\pi} \times F_s, \quad (2.20)$$

where \hat{z}_k are closest to the unit circle.

7. Return frequencies.
-

frequency estimation

$$Q(z) = z^{-(M-1)} \begin{bmatrix} z^{M-1} & \dots & z & 1 \end{bmatrix} \mathbf{G}\mathbf{G}^H \begin{bmatrix} 1 \\ z \\ \vdots \\ z^{M-1} \end{bmatrix}. \quad (2.22)$$

Thus, the root-MUSIC algorithm finds the roots of $\tilde{Q}(z)$, that is a complex polynomial function given by

$$Q(z) = z^{-(M-1)} \tilde{Q}(z), \quad (2.23)$$

where $\tilde{Q}(z)$ is a $2(M-1)$ degree polynomial in z the roots of which come in pairs, since, by construction, if z_0 is a root, then $\frac{1}{z_0^*}$ is a root. Once the polynomial $\tilde{Q}(z)$ is obtained, the frequency estimation can be determined by calculating the $2(M-1)$ roots of $\tilde{Q}(z)$, then keeping the L stable roots that are closest to the unit circle. The

2. STATOR CURRENT PARAMETERS ESTIMATION AND FAULT SEVERITY ANALYSIS

relationship between L roots and frequencies is given by

$$\hat{f}_k = \frac{\arg(\hat{z}_k)}{2\pi} \times F_s, \quad (2.24)$$

where \hat{z}_k denotes the k^{th} root of $\tilde{Q}(z)$. Note that many programming language contain functions for root finding. Root-MUSIC has the same asymptotic performance as spectral-MUSIC [308]. Since the search procedure in spectral MUSIC is replaced by solving the roots of a polynomial in root-MUSIC, the computational cost is significantly reduced [307]. Thus, it is preferable to use only the root-MUSIC estimator for practical applications.

2.3.3 ESPRIT Estimators

The key element of ESPRIT is to use the rotational property between staggered subspaces for frequency estimation [309, 310]. Two extensions of ESPRIT methods are considered: Least-Squares (LS) ESPRIT and Total Least-Squares (TLS) ESPRIT. ESPRIT Estimators, an invertible transformation \mathbf{T} to estimate frequencies. This transformation can be formulated by

$$\mathbf{S} = \mathbf{H}_c(\boldsymbol{\Omega}_c) \mathbf{T} \quad (2.25)$$

where \mathbf{T} is non-singular linear transformation

Let $\mathbf{H}_1(\boldsymbol{\Omega}_c) = \begin{bmatrix} \mathbf{I}_{M-1} & 0 \end{bmatrix} \mathbf{H}_c(\boldsymbol{\Omega}_c)$ and $\mathbf{H}_2(\boldsymbol{\Omega}_c) = \begin{bmatrix} 0 & \mathbf{I}_{M-1} \end{bmatrix} \mathbf{H}_c(\boldsymbol{\Omega}_c)$ be un-staggered and staggered of the matrix \mathbf{A} , respectively. So, we can demonstrate the following equality

$$\mathbf{H}_2(\boldsymbol{\Omega}_c) = \mathbf{H}_1(\boldsymbol{\Omega}_c) \boldsymbol{\psi} \quad (2.26)$$

where $\boldsymbol{\psi} = \text{diag}(e^{-j2\pi f_{L-1}}, \dots, e^{-j2\pi f_0}, e^{j2\pi f_0}, e^{j2\pi f_1}, \dots, e^{j2\pi f_{L-1}})$ contains the unknown frequencies.

Let $\mathbf{S}_1 = \begin{bmatrix} \mathbf{I}_{M-1} & 0 \end{bmatrix} \mathbf{S}$ and $\mathbf{S}_2 = \begin{bmatrix} 0 & \mathbf{I}_{M-1} \end{bmatrix} \mathbf{S}$ be un-staggered and staggered signal subspaces, respectively. According to the previous equations, we can write

$$\begin{cases} \mathbf{S}_1 = \mathbf{A}_1 \mathbf{T}, \\ \mathbf{S}_2 = \mathbf{A}_2 \mathbf{T}. \end{cases} \quad (2.27)$$

2.3 Subspace Spectral Estimation Techniques

From equations (2.26) and (2.27), we obtain

$$\mathbf{S}_2 = \mathbf{S}_1 \mathbf{T}^{-1} \mathbf{\Omega}_c \mathbf{T} = \mathbf{S}_1 \mathbf{\Phi}, \quad (2.28)$$

where $\mathbf{\Phi} = \mathbf{T}^{-1} \mathbf{\Omega}_c \mathbf{T}$ is the relation between the two subspaces rotations. Indeed, eigenvalues of $\mathbf{\Phi}$ must be equal to diagonal elements of $\mathbf{\Omega}_c$ and columns of \mathbf{T} are eigenvectors of $\mathbf{\Phi}$. There have two solutions to find eigenvalues of $\mathbf{\Phi}$: LS and TLS.

In the LS ESPRIT, we estimate frequencies by using eigenvalues of $\mathbf{\Phi}_{LS}$ that are given by

$$\mathbf{\Phi}_{LS} = \left(\mathbf{S}_1^H \mathbf{S}_1 \right)^{-1} \mathbf{S}_1^H \mathbf{S}_2. \quad (2.29)$$

This method is given in Algo.4. This LS solution is obtained by minimizing the estimation error on \mathbf{S}_1 according to

$$(\mathbf{S}_2 + \mathbf{E}_2) = \mathbf{S}_1 \mathbf{\Phi} \quad (2.30)$$

We can do better by using the TLS ESPRIT that is obtained by minimizing estimation errors on \mathbf{S}_1 and \mathbf{S}_2 . This method is given in Algo.4. In this technique, we estimate frequencies by using the Singular Value Decomposition (SVD) of $\begin{bmatrix} \mathbf{S}_1 & \mathbf{S}_2 \end{bmatrix} = \mathbf{L} \mathbf{\Sigma} \mathbf{V}^H$ [309], where \mathbf{L} is a matrix of left singular vectors, $\mathbf{\Sigma}$ is a matrix consisting of singular values on the main diagonal ordered in descending magnitude, and \mathbf{V} is a matrix of right singular vectors. The matrix \mathbf{V} is an $(2L \times 2L)$ unitary matrix, which can be partitioned into $(L \times L)$ quadrants according to

$$\mathbf{V} = \begin{bmatrix} \mathbf{V}_{11} & \mathbf{V}_{12} \\ \mathbf{V}_{21} & \mathbf{V}_{22} \end{bmatrix}. \quad (2.40)$$

In the TLS solution, we estimate frequencies by using eigenvalues of $\mathbf{\Phi}_{TLS}$ that are given by

$$\mathbf{\Phi}_{TLS} = -\mathbf{V}_{11} \mathbf{V}_{22}^{-1}. \quad (2.41)$$

In practice, we can estimate signal frequencies using the following expression

$$\hat{f}_k = \frac{\arg(v_k)}{2\pi} \times F_s, \quad (2.42)$$

where v_k are eigenvalues of $\hat{\mathbf{\Phi}}_{LS}$ or $\hat{\mathbf{\Phi}}_{TLS}$.

2. STATOR CURRENT PARAMETERS ESTIMATION AND FAULT SEVERITY ANALYSIS

Algorithm 3 LS-ESPRIT.

Require: N -data samples $x[n]$

1. Estimate the model order L
2. Estimate the covariance matrix \mathbf{R}_x
3. Evaluate the eigendecomposition $\mathbf{R}_x = \mathbf{U}\mathbf{\Lambda}\mathbf{U}^H$
4. Separate the signal and the noise subspaces

$$\mathbf{R}_x = \mathbf{S}\mathbf{\Lambda}_s\mathbf{S}^H + \mathbf{G}\mathbf{\Lambda}_n\mathbf{S}^H \quad (2.31)$$

5. Compute unstaggered and staggered signal subspaces

$$\begin{cases} \mathbf{S}_1 = \begin{bmatrix} \mathbf{I}_{M-1} & 0 \end{bmatrix} \mathbf{S} \\ \mathbf{S}_2 = \begin{bmatrix} 0 & \mathbf{I}_{M-1} \end{bmatrix} \mathbf{S} \end{cases} \quad (2.32)$$

6. Calculate eigenvalues of $\mathbf{\Phi}_{LS}$

$$\mathbf{\Phi}_{LS} = (\mathbf{S}_1^H \mathbf{S}_1)^{-1} \mathbf{S}_1^H \mathbf{S}_2. \quad (2.33)$$

7. Estimate frequencies

$$\hat{f}_k = \frac{\arg(v_k)}{2\pi} \times F_s, \quad (2.34)$$

where v_k are eigenvalues of $\hat{\mathbf{\Phi}}_{LS}$

8. Return frequencies.
-

In the practice, TLS-ESPRIT involves slightly more computations, it is generally preferred over the LS-ESPRIT thanks to its performance for frequency estimation [309]. Thus, it is preferable to use only the TLS-ESPRIT estimator for practical applications.

2.3.4 Modified ESPRIT

All previously described techniques assume the data are complex valued. Unfortunately, this is not necessarily the case for several applications. These approaches are applicable also to real-valued data for which the model order is assumed to be a double number of complex-valued sinusoidal signals. It has been demonstrated that the Modified ESPRIT called also R-ESPRIT for frequency estimation performs much better

Algorithm 4 TLS-ESPRIT.

Require: N -data samples $x[n]$

1. Estimate the model order L
2. Estimate the covariance matrix \mathbf{R}_x
3. Evaluate the eigendecomposition $\mathbf{R}_x = \mathbf{U}\mathbf{\Lambda}\mathbf{U}^H$
4. Separate the signal and the noise subspaces

$$\mathbf{R}_x = \mathbf{S}\mathbf{\Lambda}_s\mathbf{S}^H + \mathbf{G}\mathbf{\Lambda}_n\mathbf{S}^H \quad (2.35)$$

5. Compute unstaggered and staggered signal subspaces

$$\begin{cases} \mathbf{S}_1 = \begin{bmatrix} \mathbf{I}_{M-1} & 0 \end{bmatrix} \mathbf{S} \\ \mathbf{S}_2 = \begin{bmatrix} 0 & \mathbf{I}_{M-1} \end{bmatrix} \mathbf{S} \end{cases} \quad (2.36)$$

6. Compute the eigendecomposition of $[\mathbf{S}_1 \ \mathbf{S}_2] = \mathbf{V}\mathbf{\Lambda}_v\mathbf{V}^H$
7. Partition \mathbf{V} into $L \times L$ submatrices

$$\mathbf{V} = \begin{bmatrix} \mathbf{V}_{11} & \mathbf{V}_{12} \\ \mathbf{V}_{21} & \mathbf{V}_{22} \end{bmatrix}. \quad (2.37)$$

8. Calculate eigenvalues of $\mathbf{\Phi}_{TLS}$

$$\mathbf{\Phi}_{TLS} = -\mathbf{V}_{11}\mathbf{V}_{22}^{-1} \quad (2.38)$$

9. Estimate frequencies

$$\hat{f}_k = \frac{\arg(v_k)}{2\pi} \times F_s, \quad (2.39)$$

where v_k are eigenvalues of $\hat{\mathbf{\Phi}}_{TLS}$

10. Return frequencies.
-

2. STATOR CURRENT PARAMETERS ESTIMATION AND FAULT SEVERITY ANALYSIS

Algorithm 5 LS-MESPRIT.

Require: N -data samples $x[n]$

1. Estimate the model order L .
2. Constitute a novel data measurements according to

$$\mathbf{x}_r(n) = \frac{1}{2} \{ \mathbf{x}_c(n) + \mathbf{x}_b(n) \} \quad (2.43)$$

3. Estimate the covariance matrix $\mathbf{R}_{\mathbf{r}\mathbf{x}}$.
4. Evaluate the eigendecomposition of $\mathbf{R}_{\mathbf{r}\mathbf{x}}$.
5. Separate the signal and the noise subspaces

$$\mathbf{R}_{\mathbf{r}\mathbf{x}} = \mathbf{S}_r \mathbf{\Lambda}_{rs} \mathbf{S}_r^T + \mathbf{G}_r \mathbf{\Lambda}_{rn} \mathbf{G}_r \quad (2.44)$$

6. Compute two $(m-2) \times m$ matrices: \mathbf{S}_{r1} and \mathbf{S}_{r2} according to

$$\begin{cases} \mathbf{S}_{r1} = \mathbf{T}_r^{(1)} \mathbf{S}_r \\ \mathbf{S}_{r2} = \mathbf{T}_r^{(2)} \mathbf{S}_r \end{cases} \quad (2.45)$$

7. Calculate eigenvalues of $\mathbf{\Phi}_r^{(LS)}$ (LS solution)

$$\mathbf{\Phi}_r^{(LS)} = \left(\mathbf{S}_{r1}^H \mathbf{S}_{r1} \right)^{-1} \mathbf{S}_{r1}^H \mathbf{S}_{r2}. \quad (2.46)$$

8. Estimate frequencies

$$\hat{f}_k = \frac{\arg(v_k)}{2\pi} \times F_s, \quad (2.47)$$

where v_k are eigenvalues of $\mathbf{\Phi}_r^{(LS)}$

9. Return frequencies.
-

2.3 Subspace Spectral Estimation Techniques

than the other existing subspace methods [311]. The proposed approach is applied to real-valued data since it allows a significant reduction in the algorithmic complexity [311]. A detailed description and performances of this method can be found in [311]. This technique has been investigated by the radar community in several applications [312–318]. This method is given in the algorithm .5.

Let

$$\mathbf{x}_r(n) = \frac{1}{2} \{\mathbf{x}_c(n) + \mathbf{x}_b(n)\} \quad (2.48)$$

where $\mathbf{x}_c(n) = [x(n) \ \dots \ x(n+m-1)]^T$ and $\mathbf{x}_b(n) = [x(n-1) \ \dots \ x(n-m)]^T$. This modified model can be expressed by the following matrix formulation

$$\mathbf{x}_r(n) = \mathbf{H}_r(\boldsymbol{\Omega}) \boldsymbol{\theta}_r(n) + \mathbf{b}_r(n) \quad (2.49)$$

where

- $\mathbf{H}_r(\boldsymbol{\Omega}) = [\mathbf{a}_r(f_0) \ \dots \ \mathbf{a}_r(f_{L-1})]$ is a $m \times L$ matrix containing frequencies, where $\mathbf{a}_r(f) = [\cos(\frac{f}{2}) \ \cos(\frac{3f}{2}) \ \dots \ \cos((m - \frac{1}{2})f)]^T$
- $\boldsymbol{\theta}_r(n) = [\cos(f_0 n + \phi_0^+) \ \dots \ \cos(f_{L-1} n + \phi_{L-1}^+)]^T$ is a $L \times 1$ column vector containing amplitudes and phases, where $\phi_k^+ = \phi_k - \pi f_k$
- $\mathbf{b}_r(n) = \frac{1}{2} \{\mathbf{b}_c(n) + \mathbf{x}_b(n)\}$ is a $m \times 1$ column vector containing the noise of the modified model, where $\mathbf{b}_c(n) = [b(n) \ \dots \ b(n+m-1)]^T$ and $\mathbf{b}_b(n) = [b(n-1) \ \dots \ b(n-m)]^T$

The covariance matrix of $\mathbf{x}_r(n)$ can be written as

$$\mathbf{R}_{\mathbf{r}\mathbf{x}} = \mathbf{S}_r \boldsymbol{\Lambda}_{\mathbf{r}\mathbf{s}} \mathbf{S}_r^T + \mathbf{G}_r \boldsymbol{\Lambda}_{\mathbf{r}\mathbf{n}} \mathbf{G}_r^T \quad (2.50)$$

where $\boldsymbol{\Lambda}_{\mathbf{r}\mathbf{s}}$ is an $L \times L$ diagonal matrix containing the L eigenvalues of $\mathbf{R}_{\mathbf{r}\mathbf{x}}$ arranged in descending order and $\boldsymbol{\Lambda}_{\mathbf{r}\mathbf{n}}$ is an $(m-L) \times (m-L)$ diagonal matrix containing the remainder eigenvalues of $\mathbf{R}_{\mathbf{r}\mathbf{x}}$ arranged in descending order. \mathbf{S}_r and \mathbf{G}_r are the associated orthonormal eigenvectors, respectively.

The key element of this approach is to identify two $(m-2) \times m$ Toeplitz matrices:

2. STATOR CURRENT PARAMETERS ESTIMATION AND FAULT SEVERITY ANALYSIS

$\mathbf{T}_r^{(1)}$ and $\mathbf{T}_r^{(2)}$ that are given by

$$\mathbf{T}_r^{(1)} = \begin{bmatrix} 0 & 1 & 0 & 0 & \dots & 0 \\ 0 & 0 & 1 & 0 & \dots & 0 \\ \ddots & \ddots & \ddots & \ddots & \ddots & \vdots \\ 0 & \dots & 0 & 0 & 1 & 0 \end{bmatrix} \quad (2.51a)$$

and

$$\mathbf{T}_r^{(2)} = \begin{bmatrix} 1 & 0 & 1 & 0 & \dots & 0 \\ 0 & 1 & 0 & 1 & \dots & 0 \\ \ddots & \ddots & \ddots & \ddots & \ddots & \vdots \\ 0 & \dots & 0 & 1 & 0 & 1 \end{bmatrix} \quad (2.51b)$$

Thus, it is easy to demonstrate that

$$\mathbf{T}_r^{(2)} \mathbf{H}_r(\Omega) = \mathbf{T}_r^{(1)} \mathbf{H}_r(\Omega) \mathbf{D}_r \quad (2.52)$$

where $\mathbf{D}_r = \text{diag}\{\cos(2\pi f_0), \dots, \cos(2\pi f_{L-1})\}$. This equality can define

$$\mathbf{T}_r^{(2)} \mathbf{S}_r = \mathbf{T}_r^{(1)} \mathbf{S}_r \Phi_r \quad (2.53)$$

where $\Phi_r = \mathbf{C}_r^{-1} \mathbf{D}_r \mathbf{C}_r$ and $\mathbf{C}_r = E[\boldsymbol{\theta}_r(n) \boldsymbol{\theta}_r^T(n)] \mathbf{H}_r^T(\Omega) \mathbf{S}_r \{\Lambda_{rn} - \frac{\sigma^2}{2} \mathbf{I}_L\}^{-1}$. To estimate frequencies for this method, a diagonalization of Φ_r leads to \mathbf{D}_r . Then, an arccos operation on the diagonal elements of \mathbf{D}_r can be made to deduce frequencies. In this case, two solutions can be distinguished following the case of ESPRIT for complex valued data: LS-MESPRIT and TLS-MESPRIT. The main advantage of this method is its reduction of operations number required to estimate frequencies and lower complexity thanks to dimension reduction of the signal subspace compared to subspace techniques based on the complex valued data. This method exhibits excellent resolution performance when the *SNR* is high [319].

2.4 Model Order Estimation

The problem of estimating the number of sinusoids has interested many fields in signal processing. This problem has been widely adopted in engineering and statistics for selecting among an ordered set of candidate models the one that better fits the observed sample data [320]. To address this problem several information theoretic criteria

(ITC) have proposed in the literature. The most commonly used criteria are the Akaike Information Criterion (AIC), and the Bayesian Information Criterion (BIC) which are the forefathers of the classes of criteria derived from Kullback-Leibler information and from Bayesian estimation [320]. Many other criteria have been also proposed to select the number of signals such as the Minimum Description Length (MDL), and the Generalized Information Criterion (GIC). The GIC embraces most common criteria such as AIC and BIC [320]. All these criteria consist of minimizing a cost function. Generally the only difference between the proposed information criteria in model order selection is in the magnitude of the penalty term coefficient. A review of information criterion can be found in [321].

2.4.1 Model Order Estimation (Nonparametric Approach)

Several model order selection criteria from information theory have been presented in the literature to estimate the number of sinusoids [321–323]. Among these criteria model order selection based on eigenvalues decomposition of the covariance matrix have been proposed to select the correct model order in the multiple sinusoids parameters estimation [186]. In this approach, the model order is determined by the eigenvalues decomposition of the covariance matrix. In [186], authors have introduced these techniques using the two common ITC techniques: AIC and MDL. The AIC is not consistent and tends to over-estimate the number of sinusoids, even at high signal-to-noise ratio (SNR) values. While the MDL method is consistent, it tends to under-estimate the sinusoids number even at low and moderate values of SNR [324]. These approaches are also known to provide good selection performance for sufficiently large number of observations [325]. In [325], authors have demonstrate that the MDL inherits enhanced robustness properties, with respect to noise eigenvalue dispersion, compared with the AIC. Recently, Mariani et al. have designed the penalties functions for AIC, GIC, and BIC in [320].

Approaches based on eigenvalues of \mathbf{R}_x are then to select one of the N following models:

$$\mathbf{R}_x^{(k)} = \sum_{m=1}^k \lambda_m \mathbf{u}_m \mathbf{u}_m^H = \sum_{m=1}^k (\lambda_m - \sigma^2) \mathbf{u}_m \mathbf{u}_m^H + \sigma^2 \mathbf{I}_N \quad (2.54)$$

where $k = 1, \dots, P$ and P is the eigenvectors number of the covariance matrix $\hat{\mathbf{R}}_x$. The model order selection problem then is to determine the dimension of the signal

2. STATOR CURRENT PARAMETERS ESTIMATION AND FAULT SEVERITY ANALYSIS

subspace. Therefore, the likelihood function can be expressed as

$$f(\mathbf{x}, \Theta^{(k)}) = \prod_{m=1}^P \frac{1}{\pi^N \det(\mathbf{R}_x^{(k)})} \exp\left(-\mathbf{x}_p^H (\mathbf{R}_x^{(k)})^{-1} \mathbf{x}_p\right) \quad (2.55)$$

where $\Theta^{(k)} = [\lambda_1, \dots, \lambda_k, \sigma^2, \mathbf{v}_1, \dots, \mathbf{v}_k]$ is a parameter vector to be estimated. Taking the logarithm and omitting terms that do not depend on the parameter vector, the log-likelihood function becomes

$$L(\Theta^{(k)}) = -N \ln(\det(\mathbf{R}_x^{(k)})) - Tr\left([\mathbf{R}_x^{(k)}]^{-1} \hat{\mathbf{R}}_x\right) \quad (2.56)$$

The maximum likelihood estimate is the value of $\Theta^{(k)}$. As in [326], the estimates of σ^2 is

$$\hat{\sigma}^2 = \frac{1}{P-k} \sum_{i=k+1}^P \hat{\lambda}_i \quad (2.57)$$

and the log-likelihood function with $\hat{\Theta}^{(k)}$ is given by

$$L(\hat{\Theta}^{(k)}) = \ln \left(\frac{\prod_{i=k+1}^P \hat{\lambda}_i^{\frac{1}{P-k}}}{\frac{1}{P-k} \sum_{i=k+1}^P \hat{\lambda}_i} \right)^{(P-k)N} \quad (2.58)$$

where $\hat{\lambda}_i$ denotes the ordered eigenvalues of the covariance matrix $\hat{\mathbf{R}}_x$. The model order can be estimated using the following criteria formulation:

$$\mathcal{JTC}(k) = -2L(\hat{\Theta}^{(k)}) + \mathcal{P}(k) \quad (2.59)$$

where $\mathcal{P}(k)$ is the penalty term coefficient which depends in the considered information theoretic criterion. Penalty functions are added in this formulation to compensate the estimation error. Each criterion is defined by its particular penalty which impacts the performance and the complexity of model order selection [320]. In [320], penalties are give by

$$\begin{cases} \mathcal{P}_{AIC}(k) = 2\phi(k) \\ \mathcal{P}_{BIC}(k) = \phi(k) \ln(N) \\ \mathcal{P}_{GIC}(k) = \phi(k) \nu \end{cases} \quad (2.60)$$

where $\phi(k) = k(2p-k) + 1$ is the number of free parameters and ν is a constant.

According to this definition, GIC is a generalized formulation of ITC. Note that, for large enough samples BIC coincides with the MDL which attempts to construct a model that permits the shortest description of the data [320]. Therefore, the model order is obtained by

$$\hat{L} = \underset{k}{\operatorname{argmin}} \{ \mathcal{JTC}(k) \} \quad (2.61)$$

Therefore, these methods are based on parametric techniques in which criteria are evaluated using eigenvalues of the covariance matrix. Recently, a modified MDL has been proposed in [327] with the help of random matrix approach. The proposed estimator is based on the improved estimation of eigenvalues and eigenvectors of the covariance matrix studied in [328]. It seems that eigenvalues are not the right quantities to be used to select the model order [329]. In fact, these techniques are considered such as a nonparametric detection of signals [330]. However, these methods are also general and do not take into account the particular structure of the considered stator current model.

2.4.2 Model Order Selection (Parametric Approach)

To overcome the limitations of the previous proposed ITC, several criteria have been proposed that associate the ITC with the exact MLE. In these approaches, the selected model minimizes a penalized likelihood metric, where the penalty is determined by the selected criterion.

The model order is obtained by minimizing the following information criteria

$$\hat{L} = \underset{l}{\operatorname{argmin}} N \ln \left(\hat{\sigma}_l^2 \right) + \eta(l, N), \quad (2.62)$$

where N is the number of samples, $\eta(l, N)$ is a penalty coefficient, which depend on information criteria, and $\hat{\sigma}_l^2$ denotes the noise variance given by

$$\hat{\sigma}_l^2 = \frac{1}{N} \sum_{n=0}^N \left| x[n] - \sum_{k=0}^{l-1} \hat{a}_k \cos \left(2\pi \hat{f}_k \times \frac{n}{F_s} + \hat{\phi}_k \right) \right|^2. \quad (2.63)$$

2. STATOR CURRENT PARAMETERS ESTIMATION AND FAULT SEVERITY ANALYSIS

For each ITC, a penalty coefficient can be associated

$$\begin{cases} \eta_{AIC}(l, N) = 2n \\ \eta_{AIC_C}(l, N) = 2n \frac{N}{N-n-1} \\ \eta_{BIC}(l, N) = n \ln(N) \\ \eta_{GIC}(l, N) = n \times \nu \end{cases} \quad (2.64)$$

where $n = 3l + 1$.

2.5 Proposed Fault Detection Methodology

This section presents an induction machine condition monitoring architecture based on the stator current model parameters estimation. It proposes also a criterion to detect faults and severities.

2.5.1 Proposed Fault Severity Criterion

The proposed fault severity criterion (FSC) is needed to measure the machine state and to detect the fault severity. This criterion is based on the evaluation of frequency component amplitudes. It is an extension of the proposed criterion in [141]. The FSC is inspired from the total harmonic distortion (THD) of a signal, which is defined as the ratio of the sum of the powers of all harmonic components to the power of the fundamental frequency. Mathematically, the FSC depends on amplitudes a_k and it can be expressed as

$$C = \frac{\sum_{k \in \theta_1} \widehat{a}_k^2}{\sum_{l \in \theta_2} \widehat{a}_l^2}, \quad (2.65)$$

where θ_1 corresponds to the integers k that belong to $[0, L - 1]$ for which $|\widehat{f}_k - n f_s| > \Delta f$ ($n \in \mathbb{N}$), θ_2 corresponds to the integers l that belong to $[0, L - 1]$ for which $|\widehat{f}_l - n f_s| < \Delta f$ ($n \in \mathbb{N}$), and $\Delta f = 10^{-2} f_s$ is the authorized variation of frequency values according to Standard IEC 038 [301].

The proposed criterion is theoretically equal to zero for healthy induction machines and increases for a faulty case. In practice, the FSC value C gives the induction machine state, which is compared with to the FSC value for healthy condition. Performance of the proposed criterion depends on the performances of model order, frequency, and amplitude estimators. This criterion can be explained by the algorithm described in

Algorithm 6 Fault Severity Criterion.

Require: N -data samples $x[n]$

- 1) Model Order Estimation.
- 2) Frequency Estimation.
- 3) Amplitude Estimation.
- 4) Compute the FSC value according to

$$\Delta f \leftarrow 10^{-2} f_s$$

$$Num \leftarrow 0$$

$$Den \leftarrow 0$$

for $k = 1$ **to** \hat{L} **do**

$$Value = \left| \hat{\mathbf{f}}_k - \left\lfloor \frac{\hat{\mathbf{f}}_k}{f_s} \right\rfloor \times f_s \right|$$

if $Value < \Delta f$ **then**

$$Den \leftarrow Den + \hat{\mathbf{a}}_k^2$$

else

$$Num \leftarrow Num + \hat{\mathbf{a}}_k^2$$

end if

end for

$$FSC \leftarrow \frac{Num}{Den}$$

algorithm 7. In this algorithm, $\lfloor \cdot \rfloor$ denotes the round function. This algorithm is characterized by its ease of implementation.

The purpose of the proposed algorithm is to calculate the FSC value that determines the state of the studied machine. Three steps are needed: model order selection, frequency estimation, and amplitude estimation. Once amplitudes are determined, we can compute the FSC ratio value. The denominator of this ratio contains the sum of squared amplitudes corresponding to the fundamental frequency and harmonics. The numerator contains the sum of the squared amplitudes corresponding to others frequencies. Therefore, a frequency evaluation is required while respecting the authorized variation according to standard IEC 038.

2.5.2 Condition Monitoring Architecture

The proposed condition monitoring architecture for induction machines is given by Fig. 3.5. It is based on the use of advanced signal processing techniques to estimate parameters of the stator current. These parameters are exploited to determine the value of the proposed FSC. This value allows evaluating the induction machine state. One of the valuable advantages of the proposed architecture is to detect faults in presence

2. STATOR CURRENT PARAMETERS ESTIMATION AND FAULT SEVERITY ANALYSIS

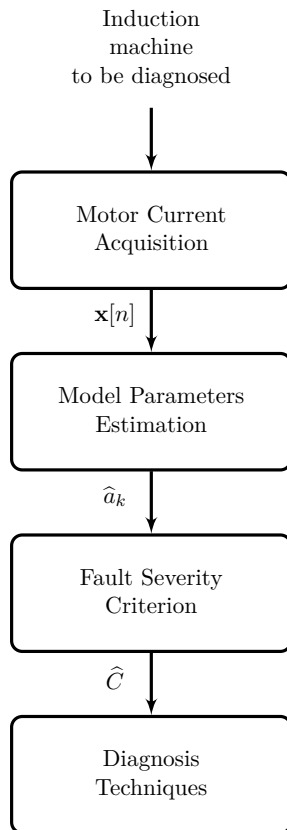


Figure 2.2: Proposed condition monitoring architecture of induction machines.

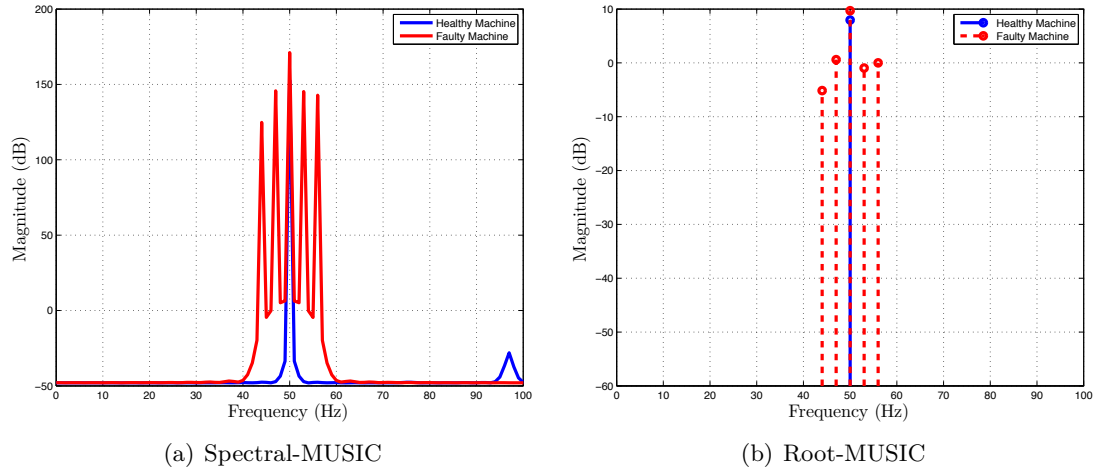
of signal parameters.

2.6 Simulations Results

This section presents simulation results that illustrate performances of the proposed techniques applied to analyze induction machine faults. These techniques are tested using synthetic signals modeled by (2.1) and the frequency structure given in (2.3) with $F_S = 1000Hz$, $f_s = 50$, $f_c = 3$, and $k = \{0, 1, 2\}$. Simulation parameters are given by Table 3.2. All simulation results using Monte Carlo Trials are obtained with 1000 trials.

Table 2.1: Simulation parameters $L = 5$.

Amplitudes	a_0	a_1	a_2	a_3	a_4
Healthy machine	0	0	2	0	0
Severity 1	0.004	0.004	2	0.004	0.004
Severity 2	0.005	0.005	2	0.005	0.005
Severity 3	0.006	0.006	2	0.006	0.006
Severity 4	0.008	0.0091	2	0.007	0.0067


Figure 2.3: Stator current spectrum based on MUSIC estimators and BIC for a healthy and faulty induction machines with severity 4.

2.6.1 Subspace Techniques Performances

Figures 2.3, 2.4, and 2.5 depict the stator current spectrum using BIC as a model order estimator. All subspace techniques can separate frequencies Ω .

To compare the proposed subspace techniques, a Mean Square Error (\mathcal{MSE}) is used that is defined by

$$\mathcal{MSE}(\Omega) = E \left[\left(\hat{\Omega} - \Omega \right)^2 \right] \quad (2.66)$$

The \mathcal{MSE} is estimated using K Monte Carlo trials by

$$\mathcal{MSE}(\Omega) = \frac{1}{K} \sum_{k=0}^K \left(\hat{\Omega} - \Omega \right)^2 \quad (2.67)$$

Figure 2.8 shows the \mathcal{MSE} of the fundamental frequency \hat{f}_s and the characteristic faulty

2. STATOR CURRENT PARAMETERS ESTIMATION AND FAULT SEVERITY ANALYSIS

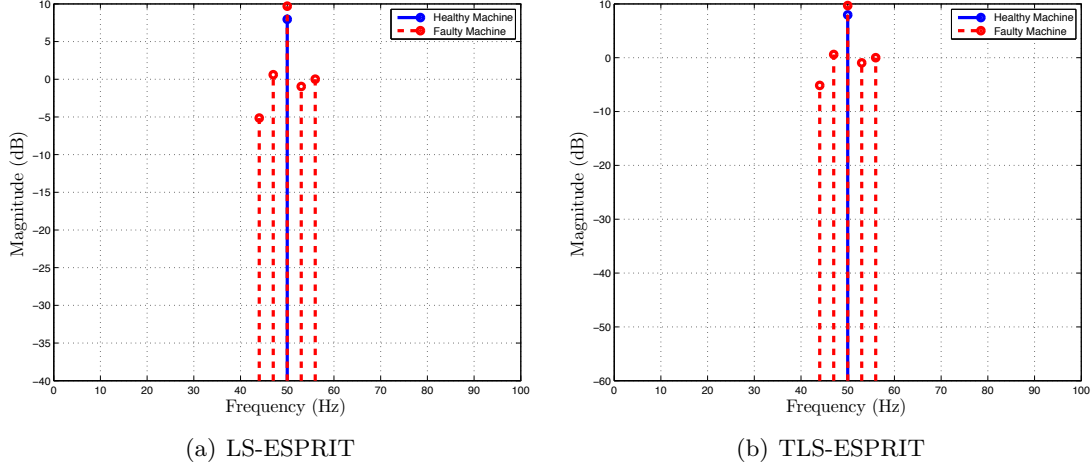


Figure 2.4: Stator current spectrum based on ESPRIT estimators and BIC for a healthy and faulty induction machines with severity 4.

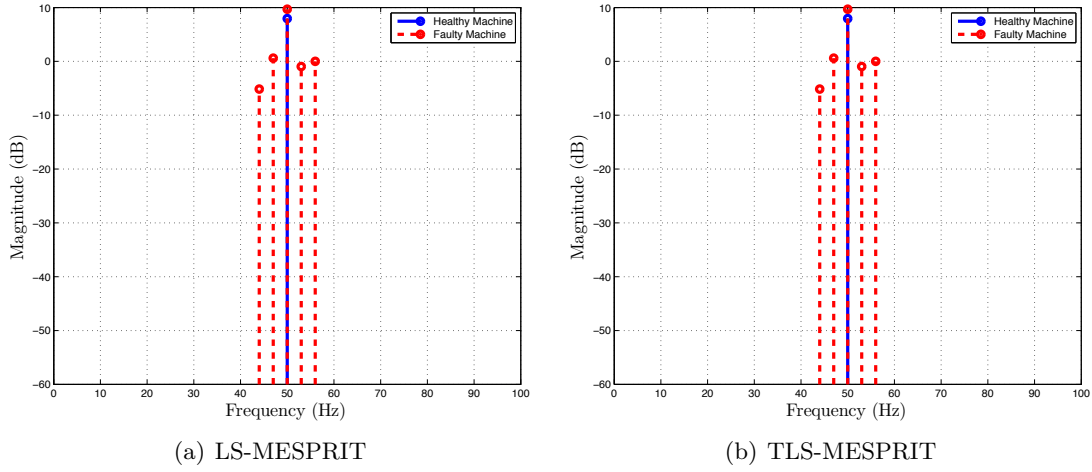


Figure 2.5: Stator current spectrum based on Modified ESPRIT estimators and BIC for a healthy and faulty induction machines with severity 4.

frequency \hat{f}_c , respectively versus the length N for different subspace spectral estimation techniques. MSE of all subspace techniques decrease when the samples number increase. Therefore, subspace spectral techniques are better as N increases. According to figs 2.8(a) and 2.8(b), the estimation of the fundamental frequency \hat{f}_s is more accurate than the estimation of the characteristic faulty frequency \hat{f}_c . An another conclusion, that the TLS-MESPRIT is the best subspace spectral estimation technique.

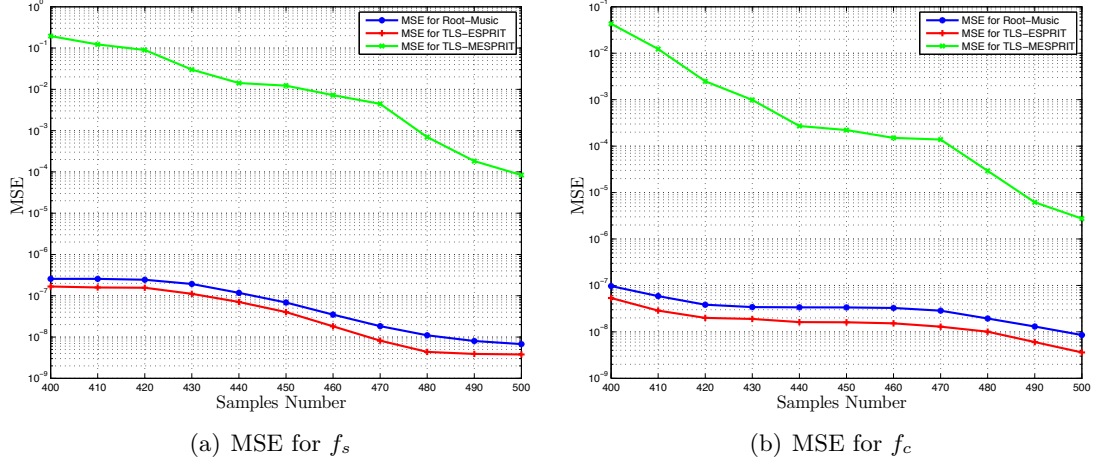


Figure 2.6: MSE for frequency estimation.

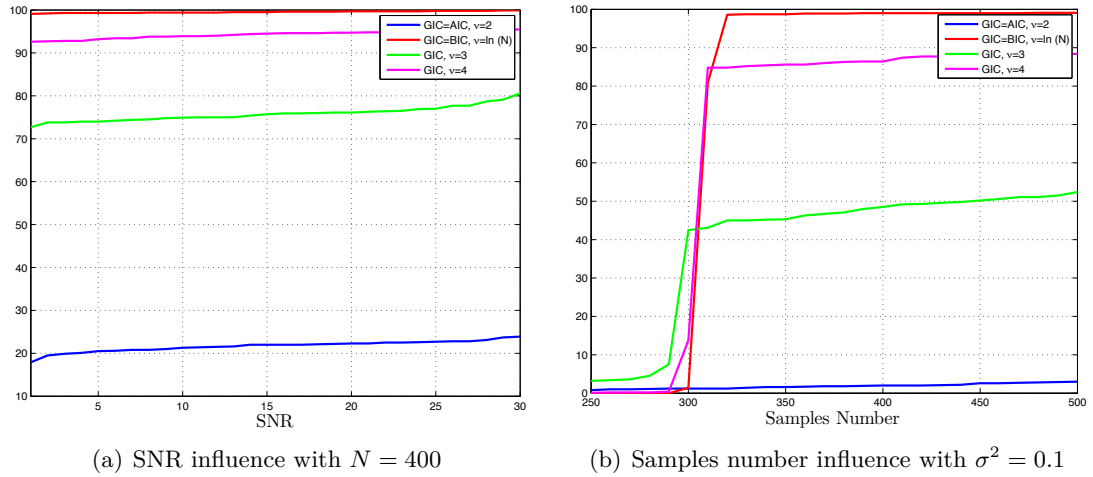


Figure 2.7: SNR and samples number influences on the model order selection based on eigenvalues of the covariance matrix.

2.6.2 Model Order Selection Performances

Figures 2.7 and 2.8 present the SNR and samples number influences on the model order selection. It can be seen from these figures that the model order detection probability increases when the samples number N and SNR increases. Results of these figure prove that the BIC is the best model order selection compared to others ITC.

2. STATOR CURRENT PARAMETERS ESTIMATION AND FAULT SEVERITY ANALYSIS

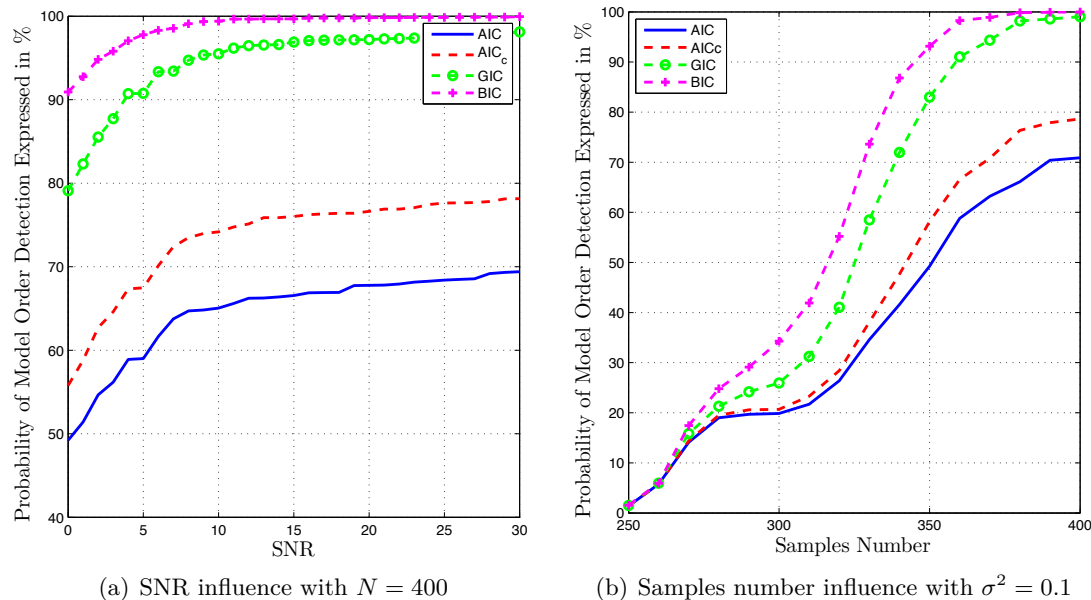


Figure 2.8: SNR and samples number influences on the model order selection based on penalized likelihood metric.

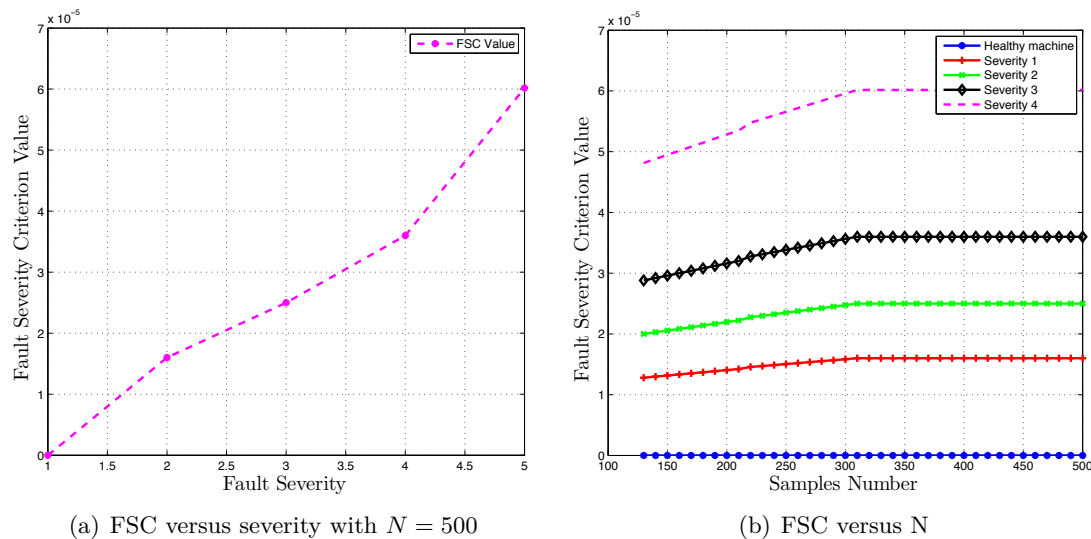


Figure 2.9: Severity and samples number influences in FSC value with $SNR = 30$.

2.6.3 Fault Severity Criterion Performances

Figure 2.9(a) presents the FSC value versus considered severities. According to this figure, the FSC value increases when the severity increases. Figure 2.9(b) depicts

the FSC value versus N with different severities. It can be seen that the FSC value increases when the samples number N increases. Then, the proposed FSC can measure the machine state and it is better as N increases.

2.7 Conclusion

This chapter has proposed an induction machine condition monitoring and fault detection architecture. Four steps are required: stator current acquisition, stator current model parameters estimation, FSC value computation, and detection techniques. Parameters estimation are divided into three main estimations parts: model order selection using the ITC, frequency estimation using subspace techniques, and amplitude and phases estimations using LSE. It have be shown that the BIC is more efficient than other ITC and the Modified-ESPRIT is the best frequency estimation technique for stator current under faulty conditions in stationnary environments. An another conclusion is that FSC can be used to measure the state and the severity of induction machines.

2. STATOR CURRENT PARAMETERS ESTIMATION AND FAULT SEVERITY ANALYSIS

Induction Machine Fault Detection based on the Gen- eralised Likelihood Ratio Test

Contents

3.1	Introduction	81
3.2	Statistical Decision Theory	81
3.2.1	Simple Binary Hypothesis Testing	81
3.2.2	Bayes Criterion	83
3.2.3	Minmax Criterion	88
3.2.4	Neyman-Pearson Criterion	89
3.2.5	Receiver Operating Characteristics	91
3.3	Composite Hypothesis Testing	93
3.3.1	BLRT Approach for Composite Hypothesis Testing	93
3.3.2	GLRT Approach for Composite Hypothesis Testing	95
3.4	Proposed Induction Machine Faults Detector	97
3.4.1	Problem Formulation	97
3.4.2	GLRT of the Stator Current Model	98
3.4.3	Performance of the Proposed Faults Detector	100
3.4.4	Proposed Induction Machine Faults Detection Architecture	103
3.5	Simulations Results	103
3.5.1	Simulations Parameters	103
3.5.2	ROC curves and Histogram	104
3.5.3	Influences of SNR , N , and P_{Fa}	105

3. INDUCTION MACHINE FAULT DETECTION BASED ON THE GENERALISED LIKELIHOOD RATIO TEST

3.6 Conclusion	105
---------------------------------	------------

3.1 Introduction

This chapter considers the problem of induction machine faults detection using the statistical decision theory. This problem is mainly referred to as hypothesis testing in the signal processing community. There are two possible hypotheses: \mathcal{H}_0 the machine is healthy (i.e. null hypothesis) and \mathcal{H}_1 the machine is faulty (i.e alternative hypothesis). The objective is then to determine which of these two hypotheses best describes experimental measurements (i.e binary detection problem). This detection problem can be found in many topics such as: communication, radar, and sonar. To address the problem of induction machine faults detection, a decision rule has been proposed. This decision rule is based on the Neyman-Pearson (NP) detector. The NP detector is based on the Generalized Likelihood Ratio Test (GLRT) approach for which the unknown parameters are replaced by their estimates. Specifically, four estimations are required, which are model order, frequency, phase and amplitude estimations. The model order is obtained using the BIC. TLS-ESPRIT is used to estimate frequencies. Then, phases and amplitudes are obtained using the LSE. The proposed approach performance is assessed using simulation data by plotting the Receiver Operating Characteristic (ROC) curves.

3.2 Statistical Decision Theory

This section presents the basic concepts of the statistical decision theory. We start with the simple binary hypothesis testing assuming that the statistical information under each hypothesis is known. We present three main decision rules: Bayes, minmax, and Neyman Pearson. We present also the way to analyze performances of a detector.

3.2.1 Simple Binary Hypothesis Testing

In the simple binary hypothesis testing problem, there are two hypotheses: \mathcal{H}_0 and \mathcal{H}_1 . \mathcal{H}_0 is referred to the null hypothesis and \mathcal{H}_1 is referred to the alternative hypothesis. The probability density function (PDF) under each assumed hypothesis is completely known. This hypothesis test problem is called a binary hypothesis test since the decision have be to made between two hypothesis. The objective then is to

3. INDUCTION MACHINE FAULT DETECTION BASED ON THE GENERALISED LIKELIHOOD RATIO TEST

Table 3.1: The four possible case of a binary hypothesis test.

		Decisions	
		Signal Present	Signal Absent
Inputs	Signal Present	Detection P_D	Miss Detection $P_M = 1 - P_D$
	Signal Absent	False Alarm P_{Fa}	Correct Rejection $P_R = 1 - P_{Fa}$

design a good decision rule $\phi(\mathbf{x})$:

$$\phi(\mathbf{x}) = \begin{cases} 0 & \text{decide } \mathcal{H}_0 \\ 1 & \text{decide } \mathcal{H}_1 \end{cases} \quad (3.1)$$

For example, in radar detection problem as well as in other applications, there are two hypothesis:

\mathcal{H}_0 : The signal is absent.

\mathcal{H}_1 : The signal is present.

For this hypothesis testing, there are four possible cases that can occur:

- Decide that \mathcal{H}_0 is true when \mathcal{H}_0 is true. It is a *correct rejection*.
- Decide that \mathcal{H}_1 is true when \mathcal{H}_1 is true. It is called *detection*.
- Decide that \mathcal{H}_1 is true when \mathcal{H}_0 is true. It is a *Type I error* called *false alarm*.
- Decide that \mathcal{H}_0 is true when \mathcal{H}_1 is true. It is a *Type II error* called *miss detection*.

For each case, a probability can be associated (see Tab.3.1). P_R , P_D , P_{Fa} , and P_M represent the *correct rejection* probability, the *detection* probability, the *false alarm* probability, and the *miss* probability, respectively. In statistics, P_{Fa} and P_D are termed the significance level and the power of the test, respectively. These probabilities can be determined from the conditional probabilities:

$$\begin{aligned} P_R &= P(\mathcal{H}_0 | \mathcal{H}_0) \\ P_D &= P(\mathcal{H}_1 | \mathcal{H}_1) \\ P_{Fa} &= P(\mathcal{H}_1 | \mathcal{H}_0) \\ P_M &= P(\mathcal{H}_0 | \mathcal{H}_1) \end{aligned} \quad (3.2)$$

where $P(\mathcal{H}_i | \mathcal{H}_j)$ is the conditional probability that indicates the probability of deciding \mathcal{H}_i when \mathcal{H}_j is true. According to the definition of the conditional probabilities, these probabilities can be expressed also as

$$\begin{aligned}
 P_R &= \int_{R_0} p(\mathbf{x} | \mathcal{H}_0) d\mathbf{x} \\
 P_D &= \int_{R_1} p(\mathbf{x} | \mathcal{H}_1) d\mathbf{x} \\
 P_{Fa} &= \int_{R_1} p(\mathbf{x} | \mathcal{H}_0) d\mathbf{x} \\
 P_M &= \int_{R_0} p(\mathbf{x} | \mathcal{H}_1) d\mathbf{x}
 \end{aligned} \tag{3.3}$$

where $p(\mathbf{x} | \mathcal{H}_i)$ is the PDF under \mathcal{H}_i and $R_i = \{\mathbf{x} : \text{decide } \mathcal{H}_i\}$ is the critical region that verifies:

$$\begin{aligned}
 R_0 \cup R_1 &= R \\
 R_0 \cap R_1 &= \emptyset
 \end{aligned} \tag{3.4}$$

where R_0 is the complement set of R_1 .

The correct decision probability P_C and the error probability P_E are given by

$$\begin{aligned}
 P_C &= P(\mathcal{H}_0; \mathcal{H}_0) + P(\mathcal{H}_1; \mathcal{H}_1) \\
 &= P(\mathcal{H}_0 | \mathcal{H}_0) P(\mathcal{H}_0) + P(\mathcal{H}_1 | \mathcal{H}_1) P(\mathcal{H}_1) \\
 P_E &= P(\mathcal{H}_1; \mathcal{H}_0) + P(\mathcal{H}_0; \mathcal{H}_1) \\
 &= P(\mathcal{H}_1 | \mathcal{H}_0) P(\mathcal{H}_0) + P(\mathcal{H}_0 | \mathcal{H}_1) P(\mathcal{H}_1)
 \end{aligned} \tag{3.5}$$

where $P(\mathcal{H}_i)$ is the prior probability of the respective hypothesis \mathcal{H}_i . Then, these probabilities can be expressed as

$$\begin{aligned}
 P_C &= (1 - P_{Fa}) P(\mathcal{H}_0) + P_D P(\mathcal{H}_1) \\
 P_E &= P_{Fa} P(\mathcal{H}_0) + P_M P(\mathcal{H}_1)
 \end{aligned} \tag{3.6}$$

It is not possible to reduce both error probabilities simultaneously [295]. The main objective then is to achieve a trade-off between the two considered errors. In binary hypothesis testing, there are three main decision rule: the Bayes', the mini-max, and the Neyman–Pearson Criteria.

3.2.2 Bayes Criterion

Bayes rule can be used to minimize the average cost or risk in a decision making, which depends on the prior probabilities of two hypotheses, cost assignments, and

3. INDUCTION MACHINE FAULT DETECTION BASED ON THE GENERALISED LIKELIHOOD RATIO TEST

conditional densities of the observations under the two hypotheses [331]. Considering the four decision possibilities, costs could be assigned to each decision in order to increase and decrease the effect of each decision in the Bayes decision rule. Costs are due to the fact that some actions are taken based on the decision made and consequences of one decision are different from consequences of another [332]. Let $C_{i,j}$ represents the cost of deciding that \mathcal{H}_i is true when \mathcal{H}_j holds. The Bayes risk called also the average cost $\mathcal{R}(\phi)$ is defined as

$$\begin{aligned}\mathcal{R}(\phi) &= \mathcal{R}(\phi | \mathcal{H}_0) P(\mathcal{H}_0) + \mathcal{R}(\phi | \mathcal{H}_1) P(\mathcal{H}_1) \\ &= \sum_{i=0}^1 \sum_{j=0}^1 C_{ij} P(\mathcal{H}_i | \mathcal{H}_j) P(\mathcal{H}_j)\end{aligned}\quad (3.7)$$

where $\mathcal{R}(\phi | \mathcal{H}_i)$ is the risk under \mathcal{H}_i , $P(\mathcal{H}_i | \mathcal{H}_j)$ is the conditional probability that indicates the probability of deciding \mathcal{H}_i when \mathcal{H}_j is true and $P(\mathcal{H}_j)$ is the prior probability of the respective hypothesis \mathcal{H}_j . Then, the Bayes risk is given by

$$\begin{aligned}\mathcal{R}(\phi) &= C_{00}P(\mathcal{H}_0) \int_{R_0} p(\mathbf{x} | \mathcal{H}_0) d\mathbf{x} + C_{01}P(\mathcal{H}_1) \int_{R_0} p(\mathbf{x} | \mathcal{H}_1) d\mathbf{x} \\ &\quad + C_{10}P(\mathcal{H}_0) \int_{R_1} p(\mathbf{x} | \mathcal{H}_0) d\mathbf{x} + C_{11}P(\mathcal{H}_1) \int_{R_1} p(\mathbf{x} | \mathcal{H}_1) d\mathbf{x}\end{aligned}\quad (3.8)$$

Since $\int_{R_0} p(\mathbf{x} | \mathcal{H}_i) d\mathbf{x} = 1 - \int_{R_1} p(\mathbf{x} | \mathcal{H}_i) d\mathbf{x}$, the Bayes risk becomes

$$\begin{aligned}\mathcal{R}(\phi) &= C_{00}P(\mathcal{H}_0) + C_{01}P(\mathcal{H}_1) \\ &\quad + \int_{R_1} [(C_{10}P(\mathcal{H}_0) - C_{00}P(\mathcal{H}_0)) p(\mathbf{x} | \mathcal{H}_0)] d\mathbf{x} \\ &\quad + \int_{R_1} [(C_{11}P(\mathcal{H}_1) - C_{01}P(\mathcal{H}_1)) p(\mathbf{x} | \mathcal{H}_1)] d\mathbf{x}\end{aligned}\quad (3.9)$$

It can be observed that the quantity $C_{00}P(\mathcal{H}_0) + C_{01}P(\mathcal{H}_1)$ is constant, independent of how we assign points in the observation space, and that the only variable quantity is the region of integration R_1 . Terms $[(C_{10}P(\mathcal{H}_0) - C_{00}P(\mathcal{H}_0)) p(\mathbf{x} | \mathcal{H}_0)]$ and $[(C_{11}P(\mathcal{H}_1) - C_{01}P(\mathcal{H}_1)) p(\mathbf{x} | \mathcal{H}_1)]$ are both positive. Consequently, we include \mathbf{x} in

R_1 only if the integrand is negative. Then, the decision rule becomes

$$\begin{array}{c} \mathcal{H}_1 \\ \succ \\ [(C_{01}P(\mathcal{H}_1) - C_{11}P(\mathcal{H}_1))p(\mathbf{x} | \mathcal{H}_1)] \\ \prec \\ \mathcal{H}_0 \end{array} \quad \begin{array}{c} \succ \\ \\ \prec \end{array} \quad [(C_{10}P(\mathcal{H}_0) - C_{00}P(\mathcal{H}_0))p(\mathbf{x} | \mathcal{H}_0)] \quad (3.10)$$

Under the reasonable assumption that the cost of a wrong decision is higher than the cost of a correct decision (i.e. $C_{10} \succ C_{00}$ and $C_{01} \succ C_{11}$), the detector that minimizes the Bayes risk is

$$\begin{array}{c} \mathcal{H}_1 \\ \frac{p(\mathbf{x} | \mathcal{H}_1)}{p(\mathbf{x} | \mathcal{H}_0)} \succ \gamma = \frac{(C_{10} - C_{00})P(\mathcal{H}_0)}{(C_{01} - C_{11})P(\mathcal{H}_1)} \\ \prec \\ \mathcal{H}_0 \end{array} \quad (3.11)$$

The ratio of $p(\mathbf{x} | \mathcal{H}_1)$ over $p(\mathbf{x} | \mathcal{H}_0)$ is called the likelihood ratio

$$\Lambda(\mathbf{x}) = \frac{p(\mathbf{x} | \mathcal{H}_1)}{p(\mathbf{x} | \mathcal{H}_0)} \quad (3.12)$$

When $\frac{C_{01}-C_{11}}{C_{10}-C_{00}} = 1$, the Bayes rule becomes minimizing the probability of error or maximum a posteriori (MAP). In this case, the likelihood ratio test (LRT) becomes

$$\begin{array}{c} \mathcal{H}_1 \\ \succ \\ \Lambda(\mathbf{x}) \succ \gamma = \frac{P(\mathcal{H}_0)}{P(\mathcal{H}_1)} \\ \prec \\ \mathcal{H}_0 \end{array} \quad (3.13)$$

Considering the case when the prior probabilities are not available, a decision rule based on likelihood functions can be developed

$$\begin{array}{l} \mathcal{H}_0 : p(\mathbf{x} | \mathcal{H}_0) \succ p(\mathbf{x} | \mathcal{H}_1) \\ \mathcal{H}_1 : p(\mathbf{x} | \mathcal{H}_0) \prec p(\mathbf{x} | \mathcal{H}_1) \end{array} \quad (3.14)$$

It is called maximum likelihood (ML) rule

$$\begin{array}{c} \mathcal{H}_1 \\ \succ \\ \Lambda(\mathbf{x}) \succ \gamma = 1 \\ \prec \\ \mathcal{H}_0 \end{array} \quad (3.15)$$

Note that the ML decision rule can be considered as a special case of the MAP decision rule when $P(\mathcal{H}_0) = P(\mathcal{H}_1)$. However, the required prior probabilities of the hypotheses

3. INDUCTION MACHINE FAULT DETECTION BASED ON THE GENERALISED LIKELIHOOD RATIO TEST

and cost assignments may not be necessarily available to implement these decision rules.

To illustrate the application of Bayes criterion, we consider the classical example of the signal detection problem:

$$\begin{aligned} \mathcal{H}_0 : x[n] &= b[n] & n = 0, 1, \dots, N-1 \\ \mathcal{H}_1 : x[n] &= s[n] + b[n] & n = 0, 1, \dots, N-1 \end{aligned} \quad (3.16)$$

where $s[n]$ is assumed known and $b[n]$ is a White Gaussian Noise (WGN) with variance σ^2 . It is a problem of detecting a known deterministic signal in WGN. The likelihoods are

$$\begin{aligned} p(\mathbf{x} | \mathcal{H}_1) &= \prod_{n=0}^{N-1} \frac{1}{\sqrt{2\pi\sigma^2}} \exp\left[-\frac{1}{2\sigma^2} (x[n] - s[n])^2\right] \\ p(\mathbf{x} | \mathcal{H}_0) &= \prod_{n=0}^{N-1} \frac{1}{\sqrt{2\pi\sigma^2}} \exp\left[-\frac{1}{2\sigma^2} x^2[n]\right] \end{aligned} \quad (3.17)$$

The LRT is easily obtained as

$$\Lambda(x) = \exp\left[-\frac{1}{2\sigma^2} \sum_{n=0}^{N-1} \left[(x[n] - s[n])^2 - x^2[n]\right]\right] \quad (3.18)$$

Taking the logarithm, the Bayes test is

$$\ln \Lambda(x) = \frac{1}{\sigma^2} \sum_{n=0}^{N-1} x[n] s[n] - \frac{1}{2\sigma^2} \sum_{n=0}^{N-1} s^2[n] \underset{\mathcal{H}_0}{\succ} \underset{\mathcal{H}_1}{\prec} \ln \gamma \quad (3.19)$$

An example of detecting a known deterministic signal in WGN is the DC level

$$\begin{aligned} \mathcal{H}_0 : x[n] &= b[n] & n = 0, 1, \dots, N-1 \\ \mathcal{H}_1 : x[n] &= m + b[n] & n = 0, 1, \dots, N-1 \end{aligned} \quad (3.20)$$

where $m > 0$ is known and $b[n]$ is a WGN with variance σ^2 . This example corresponds to detection of noisy amplitude. The considered hypotheses can be written also as

$$\begin{aligned} \mathcal{H}_0 : x[n] &\sim \mathcal{N}(0, \sigma^2) & n = 0, 1, \dots, N-1 \\ \mathcal{H}_1 : x[n] &\sim \mathcal{N}(m, \sigma^2) & n = 0, 1, \dots, N-1 \end{aligned} \quad (3.21)$$

Then the Bayes test becomes:

$$\ln \Lambda(x) = \frac{m}{\sigma^2} \sum_{n=0}^{N-1} x[n] - \frac{Nm^2}{2\sigma^2} \underset{\mathcal{H}_0}{\overset{\mathcal{H}_1}{\gamma}} \ln(\gamma) \quad (3.22)$$

This test can be expressed in term of the sample mean $\bar{x} = \frac{1}{N} \sum_{n=0}^{N-1} x[n]$

$$\frac{1}{N} \sum_{n=0}^{N-1} x[n] \underset{\mathcal{H}_0}{\overset{\mathcal{H}_1}{\gamma}} \gamma' = \frac{\sigma^2}{Nm} \ln(\gamma) + \frac{m}{2} \quad (3.23)$$

To determine performance of the detector, the distribution of the decision statistic $T(x) = \frac{1}{N} \sum_{n=0}^{N-1} x[n]$ needs to be known. It can be demonstrated that

$$\begin{aligned} \mathcal{H}_0 : E(T(x); \mathcal{H}_0) &= 0 \quad \text{and} \quad \text{var}(T(x); \mathcal{H}_0) = \frac{\sigma^2}{N} \\ \mathcal{H}_1 : E(T(x); \mathcal{H}_1) &= m \quad \text{and} \quad \text{var}(T(x); \mathcal{H}_1) = \frac{\sigma^2}{N} \end{aligned} \quad (3.24)$$

Then the statistic test $T(x)$ is Gaussian under each hypothesis

$$\begin{cases} \mathcal{N}\left(0, \frac{\sigma^2}{N}\right) & \text{under } \mathcal{H}_0 \\ \mathcal{N}\left(m, \frac{\sigma^2}{N}\right) & \text{under } \mathcal{H}_1 \end{cases} \quad (3.25)$$

Figure 3.1 illustrates PDFs under \mathcal{H}_0 and \mathcal{H}_1 probabilities. False alarm and detection probabilities can be formulated as

$$\begin{aligned} P_{Fa} &= \int_{\sigma'}^{+\infty} p(\mathbf{x} | \mathcal{H}_0) d\mathbf{x} \\ &= Q\left(\frac{\gamma'}{\sqrt{\frac{\sigma^2}{N}}}\right) \\ P_D &= \int_{\sigma'}^{+\infty} p(\mathbf{x} | \mathcal{H}_1) d\mathbf{x} \\ &= Q\left(\frac{\gamma' - m}{\sqrt{\frac{\sigma^2}{N}}}\right) \end{aligned} \quad (3.26)$$

where $Q(x) = \int_x^{\infty} \frac{1}{\sqrt{2\pi}} \exp\left(-\frac{t^2}{2}\right) dt$ is the complementary cumulative distribution

3. INDUCTION MACHINE FAULT DETECTION BASED ON THE GENERALISED LIKELIHOOD RATIO TEST

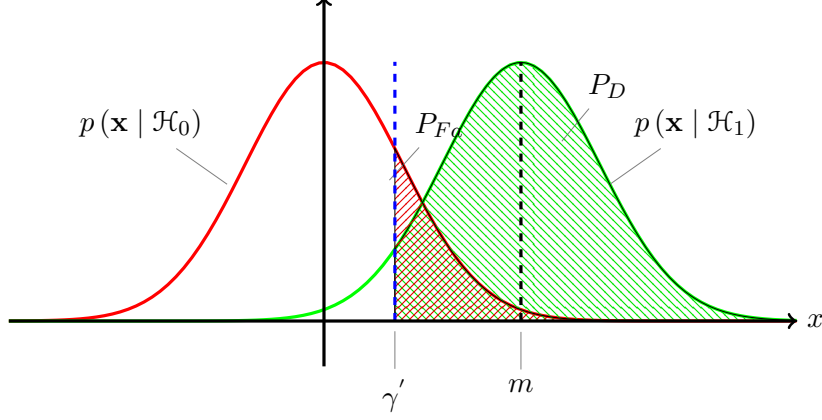


Figure 3.1: Probability density functions under \mathcal{H}_0 and \mathcal{H}_1 .

function.

3.2.3 Minmax Criterion

When a priori probabilities are not known and the cost information is available, a criterion called minmax can be used. It consists to select a value of $P(\mathcal{H}_1)$ for which the risk is maximum, and then minimize that risk function [333]. Minmax decision rule minimizes the maximum Bayes risk by using the Bayes decision rule corresponding to the least favorable prior probability assignment $P(\mathcal{H}_1)$. In fact, it is a variant of Bayes rule which prior probabilities are assumed unknown and the cost structure is assumed known.

Since $P(\mathcal{H}_1) = 1 - P(\mathcal{H}_0)$, We can express the Bayes' risk as

$$\mathcal{R}(\phi) = C_{00}(1 - P_{Fa}) + C_{10}P_{Fa} + P(\mathcal{H}_1)[(C_{11} - C_{00}) + (C_{01} - C_{11})P_M - (C_{10} - C_{00})P_{Fa}] \quad (3.27)$$

A fixed value P_1^* of $P(\mathcal{H}_1)$, the optimal threshold is given by

$$\gamma^* = \frac{(1 - P^*(\mathcal{H}_1))(C_{10} - C_{00})}{P^*(\mathcal{H}_1)(C_{01} - C_{11})} \quad (3.28)$$

There are two extremes possible values of $P(\mathcal{H}_1)$:

- When $P(\mathcal{H}_1) = 0$, then the threshold is ∞ . In this case, the only possible decision is to decide \mathcal{H}_0 , and then $P_M = 1$, $P_{Fa} = 0$, $\mathcal{R}(\phi) = C_{00}$.

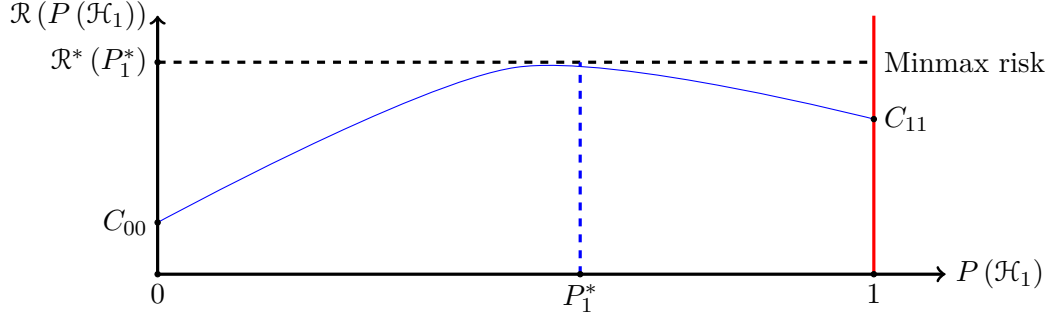


Figure 3.2: Risk \mathcal{R} versus $P(\mathcal{H}_1)$.

- When $P(\mathcal{H}_1) = 1$, then the threshold is 0. In this case, the only possible decision is to decide \mathcal{H}_1 and then $P_M = 0$, $P_{Fa} = 1$, $\mathcal{R}(\phi) = C_{11}$.

Figure 3.2 shows the Bayes risk as a function of $P(\mathcal{H}_1)$.

This rule consists to find P_1^* for which $\frac{\partial \mathcal{R}(P(\mathcal{H}_1))}{\partial P(\mathcal{H}_1)} = 0$. This problem can be formulated by the following called minmax equation:

$$(C_{11} - C_{00}) + (C_{01} - C_{11})P_M - (C_{10} - C_{00})P_{Fa} = 0 \quad (3.29)$$

If $(C_{00} = C_{11} = 0)$, the minmax equation is reduced to

$$C_{01}P_M = C_{10}P_{Fa} \quad (3.30)$$

If furthermore $(C_{01} = C_{10} = 1)$, the minmax equation is reduced to

$$P_M = P_{Fa} \quad (3.31)$$

3.2.4 Neyman-Pearson Criterion

Neyman-Pearson (NP) decision rule maximizes the detection probability P_D (minimizes the missed probability $P_M = 1 - P_D$) for a given constraint on the false alarm probability $P_{Fa} = \alpha$. This rule can be formulated as the following objective function

$$J = P_D + \lambda(P_{Fa} - \alpha) \quad (3.32)$$

3. INDUCTION MACHINE FAULT DETECTION BASED ON THE GENERALISED LIKELIHOOD RATIO TEST

where $\lambda < 0$ is the Lagrange multiplier. The question then is to choose those decision regions where P_D is maximum. Therefore, the objective function is written in term of R_1

$$\begin{aligned} J &= \int_{R_1} p(\mathbf{x}; \mathcal{H}_1) d\mathbf{x} + \lambda \left(\int_{R_1} p(\mathbf{x}; \mathcal{H}_0) d\mathbf{x} - \alpha \right) \\ &= \int_{R_1} [p(\mathbf{x}; \mathcal{H}_1) + \lambda p(\mathbf{x}; \mathcal{H}_0)] d\mathbf{x} - \lambda\alpha \end{aligned} \quad (3.33)$$

The term $\lambda\alpha$ is a fixed positive cost and the remainder term is an adjustable cost. To maximize J , we should include \mathbf{x} in R_1 if the integrand is positive for that value of \mathbf{x} or if

$$p(\mathbf{x}; \mathcal{H}_1) + \lambda p(\mathbf{x}; \mathcal{H}_0) > 0 \quad (3.34)$$

The NP decision rule decides \mathcal{H}_1 if

$$\frac{p(\mathbf{x}; \mathcal{H}_1)}{p(\mathbf{x}; \mathcal{H}_0)} > -\lambda = \gamma \quad (3.35)$$

Therefore, if PDFs under both hypotheses are available, the optimal detector is the LRT. The LRT decide \mathcal{H}_1 if

$$\Lambda(\mathbf{x}) > \gamma \quad (3.36)$$

where the threshold γ is found from

$$P_{Fa} = \int_{\{\mathbf{x}: \Lambda(\mathbf{x}) > \gamma\}} p(\mathbf{x}; \mathcal{H}_0) d\mathbf{x} \quad (3.37)$$

Then, the threshold determines the performance of the NP detector in terms of the two errors I and II. Note that when PDFs under both the hypotheses are completely known the NP detector is the uniformly most powerful (UMP) detector.

Consider the example (3.1), the NP threshold is

$$\gamma' = \sqrt{\frac{\sigma^2}{N}} Q^{-1}(\alpha) \quad (3.38)$$

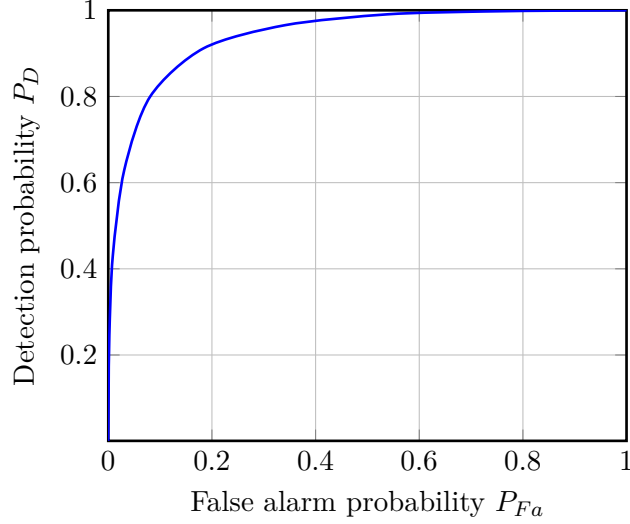


Figure 3.3: Example of ROC curve.

where $P_{Fa} = \alpha$ is the constraint. The detection probability is given by

$$\begin{aligned}
 P_D &= Q\left(\frac{\sqrt{\frac{\sigma^2}{N}}Q^{-1}(\alpha) - m}{\sqrt{\frac{\sigma^2}{N}}}\right) \\
 &= Q\left(Q^{-1}(\alpha) - \sqrt{\frac{Nm^2}{\sigma^2}}\right)
 \end{aligned} \tag{3.39}$$

3.2.5 Receiver Operating Characteristics

Receiver Operating Characteristics (ROC) is an alternative way to analyse performance of a detector in binary hypothesis testing. It is a two-dimensional graph of the detection probability versus the false alarm probability. This curve depends on the conditional PDF of the observed signal under each hypothesis and not on the assigned costs or the a priori probabilities. An example of ROC curve is illustrated in fig.3.3. The basic properties of a ROC curve are:

- The detection performance display of the ROC curve is reasonable when considering a typical P_D of better than 0.5 at ranges of P_{Fa} than 0.1 [333].
- The ROC curve is monotone increasing and concave (i.e the domain of the achievable pairs (P_D, P_{Fa}) is convex).

3. INDUCTION MACHINE FAULT DETECTION BASED ON THE GENERALISED LIKELIHOOD RATIO TEST

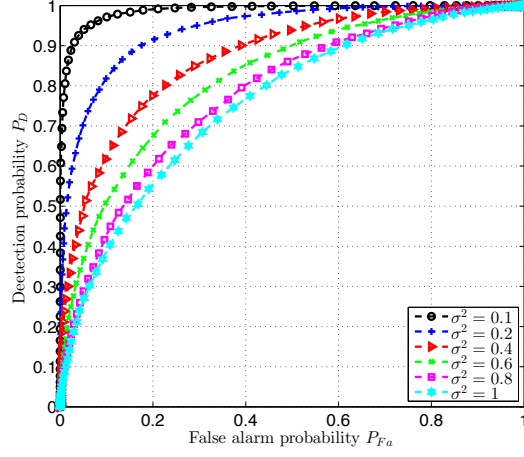


Figure 3.4: ROC curves with $m = 0.1$ and $N = 100$.

- The performance of a detector is always above the diagonal ($P_D = P_{Fa}$), because the diagonal is the same as guessing.
- The slope of a ROC curve, $\frac{\partial P_D}{\partial P_{Fa}}$, at a particular point is equal to the threshold value γ which is chosen to obtain the corresponding false alarm and detection probabilities at that point.
- In the Bayes criterion, the false alarm and detection probabilities are determined on the point of the ROC curve at which the tangent has a slope of the threshold γ [332].
- The threshold of minmax test is determined by the intersection between the ROC curve and the line:

$$(C_{11} - C_{00}) + (C_{01} - C_{11})(1 - P_D) - (C_{10} - C_{00})P_{Fa} = 0 \quad (3.40)$$

The detection performance then can be investigated using the detection and the false alarm probabilities:

$$\begin{aligned} P_{Fa} &= \int_{\gamma'}^{+\infty} p(\mathbf{x} | \mathcal{H}_0) d\mathbf{x} \\ P_D &= \int_{\gamma'}^{+\infty} p(\mathbf{x} | \mathcal{H}_1) d\mathbf{x} \end{aligned} \quad (3.41)$$

In the classical detection problem shown in 3.1, the NP detector performance increases if the noise variance σ^2 decreases (see Fig.3.4).

3.3 Composite Hypothesis Testing

In previous sections, we have developed the decision rules of simple binary hypothesis testing that parameters characterizing each hypothesis are known. The detector in this case corresponds to uniformly most powerful (UMP) detector. Now, we consider cases where these parameters may not be known. In fact, the likelihood functions associated to the two considered hypotheses depend on one or more unknown parameters. Then, the performance of the detector depends on the true value of PDFs parameters. This problem is called composite hypothesis testing that finds its applications in a variety of problem areas in signal processing community [334]. In general tests, There are two approaches to composite hypothesis testing: Bayesian approach and the Generalized likelihood ratio test (GLRT) approach. The Bayesian formulation, the unknown parameters are assumed to be random quantities. The GLRT formulation, the unknown parameters are first estimated and then used in the LRT. In this section, we study two main problems: non nuisance parameters (i.e. with known noise parameters) and nuisance parameters (i.e. with unknown noise parameters).

3.3.1 BLRT Approach for Composite Hypothesis Testing

Bayesian likelihood ratio test (BLRT) is a composite hypothesis testing approach that the unknown parameters are considered as realizations of random variables and are assigned a prior PDF. If the prior PDFs are denoted by $p(\Theta_0)$ and $p(\Theta_1)$, respect

$$\begin{aligned} p(\mathbf{x}; \mathcal{H}_0) &= \int p(\mathbf{x} | \Theta_0; \mathcal{H}_0) p(\Theta_0) d\Theta_0 \\ p(\mathbf{x}; \mathcal{H}_1) &= \int p(\mathbf{x} | \Theta_1; \mathcal{H}_1) p(\Theta_1) d\Theta_1 \end{aligned} \quad (3.42)$$

where $p(\mathbf{x} | \Theta_i; \mathcal{H}_i)$ is the conditional PDF of \mathbf{x} , conditioned on Θ_i , assuming \mathcal{H}_i is true. Forming the LRT, the optimal NP detector decides \mathcal{H}_1 if

$$\Lambda(\mathbf{x}) = \frac{\int p(\mathbf{x} | \Theta_1; \mathcal{H}_1) p(\Theta_1) d\Theta_1}{\int p(\mathbf{x} | \Theta_0; \mathcal{H}_0) p(\Theta_0) d\Theta_0} \succ \gamma \quad (3.43)$$

We consider the problem of unknown amplitude detection in WGN

$$\begin{aligned} \mathcal{H}_0 : x[n] &= b[n] \\ \mathcal{H}_1 : x[n] &= m + b[n] \end{aligned} \quad (3.44)$$

3. INDUCTION MACHINE FAULT DETECTION BASED ON THE GENERALISED LIKELIHOOD RATIO TEST

where m is unknown and $b[n]$ is a WGN with variance σ^2 . This detection problem becomes

$$\begin{aligned} \mathcal{H}_0 : m &= 0 \\ \mathcal{H}_1 : m &\neq 0 \end{aligned} \quad (3.45)$$

To apply the Bayesian approach, we assume $m \sim \mathcal{N}(0, \sigma_m^2)$ and m is independent of $b[n]$. The conditional PDFs under \mathcal{H}_0 and \mathcal{H}_1 are given by

$$p(\mathbf{x}; \mathcal{H}_0) = \frac{1}{(2\pi\sigma^2)^{\frac{N}{2}}} \exp\left[-\frac{1}{2\sigma^2} \sum_{n=0}^{N-1} x^2[n]\right] \quad (3.46a)$$

and

$$\begin{aligned} p(\mathbf{x}; \mathcal{H}_1) &= \int_{-\infty}^{+\infty} p(\mathbf{x} | m; \mathcal{H}_1) p(m) dm \\ &= \int_{-\infty}^{+\infty} \frac{1}{(2\pi\sigma^2)^{\frac{N}{2}}} \exp\left[-\frac{1}{2\sigma^2} \sum_{n=0}^{N-1} (x[n] - m)^2\right] \\ &\quad \times \frac{1}{\sqrt{2\pi\sigma_m^2}} \exp\left(-\frac{1}{2\sigma_m^2} m^2\right) dm \end{aligned} \quad (3.46b)$$

Then, the NP decide \mathcal{H}_1 if

$$\frac{p(\mathbf{x}; \mathcal{H}_0)}{p(\mathbf{x}; \mathcal{H}_1)} = \frac{\frac{1}{\sqrt{2\pi\sigma_m^2}} \int_{-\infty}^{+\infty} \exp\left(-\frac{1}{2}Q(m)\right) dm}{\exp\left(-\frac{1}{2\sigma^2} \sum_{n=0}^{N-1} x^2[n]\right)} \succ \gamma \quad (3.47)$$

where $Q(m) = \frac{1}{\sigma^2} \sum_{n=0}^{N-1} (x[n] - m)^2 + \frac{m^2}{\sigma_m^2}$. Simplifying the previous expression, this test decide \mathcal{H}_1 if

$$\frac{\sigma_{m|x}}{\sigma_m} \exp\left(\frac{N^2\sigma_{m|x}^2 \bar{x}^2}{2\sigma^4}\right) \succ \gamma \quad (3.48)$$

where $\frac{1}{\sigma_{m|x}^2} = \left(\frac{N}{\sigma^2} + \frac{1}{\sigma_m^2}\right)$. Taking the logarithm on both sides and simplifying expression, the test decide \mathcal{H}_1 if

$$\bar{x}^2 \succ \gamma' \quad (3.49)$$

where $\gamma' = \frac{2\sigma^2(\sigma^2 + \sigma_m^2)}{\sigma_m^2} \left(\ln \gamma + \frac{1}{2} \ln \left(1 + \frac{\sigma_m^2}{\sigma^2}\right)\right)$. In NP test, the false alarm probability is fixed at some desired value α . Since $\alpha = \int_{\gamma'}^{+\infty} \frac{1}{(2\pi\sigma^2)^{\frac{N}{2}}} \exp\left(\frac{1}{2\sigma^2} \bar{x}^2\right) dx$, it can be observed that exact knowledge of m is not important because it does not appear in the

decision rule.

Unfortunately, the BLRT discussed earlier suffers from several weaknesses:

- It requires a multidimensional integrations with dimension equal to the unknown parameters number. These integrals do not yield closed-form solution.
- The choice of prior PDFs is hard to justify in most applications.

On account of the above disadvantages, one can use an alternative hypothesis testing approach referred to as generalized likelihood ratio test (GLRT) and is presented in the following.

3.3.2 GLRT Approach for Composite Hypothesis Testing

Generalized likelihood-ratio test (GLRT) approach is a common approach to handle the composite hypothesis-testing problem. This strategy is based on the likelihood ratio that the unknown parameters are replaced by their ML estimates. It is an asymptotically UMP test among all the invariant statistical tests [335]. Therefore, the GLRT is defined as the ratio of the maximum value of the likelihood under \mathcal{H}_0 to the maximum under \mathcal{H}_1 . In this case, the optimal NP detector decides \mathcal{H}_1 if

$$\mathcal{L}_G(\mathbf{x}) = \frac{\max p(\mathbf{x} | \mathcal{H}_1, \Theta_1)}{\max p(\mathbf{x} | \mathcal{H}_0, \Theta_0)} \succ \gamma \quad (3.50)$$

Therefore, the GLRT decide \mathcal{H}_1 if

$$\mathcal{L}_G(\mathbf{x}) = \frac{p(\mathbf{x}; \hat{\Theta}_1)}{p(\mathbf{x}; \hat{\Theta}_0)} \succ \gamma \quad (3.51)$$

where $\hat{\Theta}_i$ are the MLE of the unknown parameters Θ_i under \mathcal{H}_i . The GLRT is often preferable to Bayesian approaches thanks to its ease of implementation and less restrictive assumptions. Furthermore, this approach does not require the specification of prior probability distributions for the unknown parameters [335].

Consider the previous example given in 3.45, then the GLRT decide \mathcal{H}_1 if

$$\mathcal{L}_G(\mathbf{x}) = \frac{p(\mathbf{x}; \hat{m}, \mathcal{H}_1)}{p(\mathbf{x}; \mathcal{H}_0)} \succ \gamma \quad (3.52)$$

3. INDUCTION MACHINE FAULT DETECTION BASED ON THE GENERALISED LIKELIHOOD RATIO TEST

Substituting for the MLE of m , the likelihood ratio becomes

$$\mathcal{L}_G(\mathbf{x}) = \frac{\frac{1}{(2\pi\sigma^2)^{\frac{N}{2}}} \exp\left[-\frac{1}{2\sigma^2} \sum_{n=0}^{N-1} (x[n] - \bar{x})^2\right]}{\frac{1}{(2\pi\sigma^2)^{\frac{N}{2}}} \exp\left[-\frac{1}{2\sigma^2} \sum_{n=0}^{N-1} x^2[n]\right]} \succ \gamma \quad (3.53)$$

where $\hat{m} = \bar{x}$. Simplifying the likelihood ratio and taking the logarithm, we can obtain

$$T(\mathbf{x}) = |\bar{x}| \succ \gamma' \quad (3.54)$$

where $\gamma' = \frac{2\sigma^2 \ln \gamma}{N}$. The asymptotic PDF of the modified GLRT statistic is given by

$$2 \ln(\mathcal{L}_G(\mathbf{x})) = \frac{N\bar{x}^2}{\sigma^2} \sim \begin{cases} \chi_1^2 & \text{under } \mathcal{H}_0 \\ \chi_1^2(\lambda) & \text{under } \mathcal{H}_1 \end{cases} \quad (3.55)$$

where $\lambda = \frac{Nm^2}{\sigma^2}$ is the noncentrality parameter. The exact detection performance is given by

$$P_{Fa} = 2Q\left(\sqrt{\gamma'}\right) \quad (3.56a)$$

and

$$P_D = Q\left(Q^{-1}\left(\frac{P_{Fa}}{2}\right) + \sqrt{\lambda}\right) + Q\left(Q^{-1}\left(\frac{P_{Fa}}{2}\right) - \sqrt{\lambda}\right) \quad (3.56b)$$

where P_{Fa} is the desired false alarm probability.

We consider now, when variances are unknown σ^2 . The GLRT decides \mathcal{H}_1 if

$$\mathcal{L}_G(\mathbf{x}) = \frac{p(\mathbf{x}; \hat{m}, \hat{\sigma}_1^2, \mathcal{H}_1)}{p(\mathbf{x}; \hat{\sigma}_0^2, \mathcal{H}_0)} \succ \gamma \quad (3.57)$$

Then, the GLRT becomes

$$\mathcal{L}_G(\mathbf{x}) = \left(\frac{\hat{\sigma}_0^2}{\hat{\sigma}_1^2}\right)^{\frac{N}{2}} \succ \gamma \quad (3.58)$$

where

$$\hat{\sigma}_0^2 = \sum_{n=0}^{N-1} x^2[n] \quad (3.59a)$$

3.4 Proposed Induction Machine Faults Detector

and

$$\begin{aligned}\hat{\sigma}_1^2 &= \sum_{n=0}^{N-1} (x[n] - \bar{x})^2 \\ &= \hat{\sigma}_0^2 - \bar{x}^2\end{aligned}\tag{3.59b}$$

Taking the logarithm, this test can be written also as

$$2 \ln (\mathcal{L}_G(\mathbf{x})) = N \left(1 + \frac{\bar{x}^2}{\hat{\sigma}_1^2} \right) \succ \ln \gamma\tag{3.60}$$

It can be seen that this test is equivalent to the following test statistic

$$T(\mathbf{x}) = \frac{\bar{x}^2}{\hat{\sigma}_1^2} \succ \gamma'\tag{3.61}$$

γ' is chosen independent of the true variance value σ^2 because the PDF of $T(\mathbf{x})$ under \mathcal{H}_0 does not depend on σ^2 . Therefore, the false alarm and the detection probabilities are the same as those given in (3.56).

3.4 Proposed Induction Machine Faults Detector

This section proposes an induction machine faults detector based on the optimal GLRT. It proposes also an faults detection flowchart to simplify the implementation of the proposed detector.

3.4.1 Problem Formulation

The induction machine faults detection can be formulated in terms of the binary hypotheses test:

\mathcal{H}_0 : The machine is healthy.

\mathcal{H}_1 : The machine is faulty.

To address this fault detection problem, a hypothesis test can be used to make a decision using a parametric stator current model. Then, the proposed fault detection strategy is composed of three steps, which are stator current model selection, model parameters estimation and decision making.

3. INDUCTION MACHINE FAULT DETECTION BASED ON THE GENERALISED LIKELIHOOD RATIO TEST

Fault detection using advanced statistical signal processing techniques require a general signal model. The induction machine stator current in presence of faults can be described by the following model:

$$\mathbf{x} = \mathbf{H}(\boldsymbol{\Omega})\boldsymbol{\theta} + \mathbf{b} \quad (3.62)$$

Parameters of stator current model are obtained using the BIC for model order and the TLS-ESPRIT for frequency estimation. Then, phases and amplitudes are obtained using the LSE.

From the detection theory viewpoint, induction machine fault detection is a binary hypothesis test. The main objective is to decide between the hypothesis \mathcal{H}_0 is referred to as the null hypothesis and \mathcal{H}_1 as the alternative one. The null hypothesis \mathcal{H}_0 corresponds to the case where the signal only contains harmonic components. Mathematically, this implies that the amplitude a_l are equal to 0 for all non-harmonic frequencies $f_l \neq kf_s$ ($k \in \mathbb{N}$) [336]. Therefore, using the matrix notation in (3.62), this hypothesis test can be described in a matrix form as follows:

$$\begin{aligned} \mathcal{H}_0 : \mathbf{A}\boldsymbol{\theta} &= \mathbf{0}_r \\ \mathcal{H}_1 : \mathbf{A}\boldsymbol{\theta} &\neq \mathbf{0}_r \end{aligned} \quad (3.63)$$

where $\mathbf{0}_r$ is a $(r \times 1)$ vector containing 0 and \mathbf{A} is an $(r \times p)$ matrix ($r \leq p = 2L$) of rank r that extracts the amplitude of the faulty components. This matrix is an $(p \times p)$ identity matrix from which rows corresponding to the fundamental frequency and all harmonic components are removed according to the algorithm defined in Algo. 7. The frequency evaluation is made by respecting the authorized variation given by the standard IEC 038 [301]. In this algorithm, the symbol $\lfloor \cdot \rfloor$ denotes the round function. Since the stator current model parameters are unknown, the faults detection problem is a composite hypothesis testing.

3.4.2 GLRT of the Stator Current Model

Regarding the stator current model, the unknown parameters are $L, \boldsymbol{\Omega}, \theta$, and σ^2 . If we assume that the model order L is correctly estimated and we consider $\Theta = \begin{bmatrix} \theta & \sigma^2 \end{bmatrix}$, two cases can be distinguished:

- The clairvoyant detector that requires a perfect knowledge of $\boldsymbol{\Omega}$.

3.4 Proposed Induction Machine Faults Detector

Algorithm 7 Computation \mathbf{A} matrix.

Require: N -data samples $x[n]$

- 1) Model Order Estimation.
- 2) Frequency Estimation.
- 3) Compute the matrix \mathbf{A} according to

$$\Delta f \leftarrow 10^{-2} f_s$$

for $k = 1$ **to** \hat{L} **do**

$$\text{Distance} = \left| \hat{f}_k - \left\lfloor \frac{\hat{f}_k}{f_s} \right\rfloor \times f_s \right|$$

if $\text{Distance} \leq \Delta f$ **then**

Append k and $(k + \hat{L})$ to the array Rows-to-Delete.

end if

end for

$$\mathbf{A} = \mathbf{I}_{2L}$$

Remove the rows of the matrix \mathbf{A} corresponding to elements of the array Rows-to-Delete.

- The blind detector that replaces $\mathbf{\Omega}$ with its subspace estimator $\hat{\mathbf{\Omega}}$.

Then, the retained detector is the blind detector. To simplify the notation, the matrix $\mathbf{H}(\hat{\mathbf{\Omega}})$ will be noted \mathbf{H} .

The GLRT of the considered stator current model decides \mathcal{H}_1 if

$$\mathcal{L}_G(\mathbf{x}) = \frac{p(\mathbf{x}; \hat{\boldsymbol{\theta}}_1, \hat{\sigma}_1^2)}{p(\mathbf{x}; \hat{\boldsymbol{\theta}}_0, \hat{\sigma}_0^2)} \succ \gamma \quad (3.64)$$

where

$$p(\mathbf{x}, \boldsymbol{\theta}_i, \sigma_i^2) = \frac{1}{(2\pi\sigma_i^2)^{\frac{N}{2}}} \times \exp\left(\frac{-1}{2\sigma_i^2} (\mathbf{x} - \mathbf{H}\boldsymbol{\theta}_i)^T (\mathbf{x} - \mathbf{H}\boldsymbol{\theta}_i)\right) \quad (3.65)$$

$\hat{\boldsymbol{\theta}}_i$ and $\hat{\sigma}_i^2$ are the MLEs of $\boldsymbol{\theta}_i$ and σ_i^2 under \mathcal{H}_i . Under \mathcal{H}_0 , $\hat{\boldsymbol{\theta}}_0$ the constrained MLE of $\boldsymbol{\theta}$ is given by [298]

$$\hat{\boldsymbol{\theta}}_0 = \hat{\boldsymbol{\theta}}_1 - \mathbf{d} = \hat{\boldsymbol{\theta}}_1 - (\mathbf{H}^T \mathbf{H})^{-1} \mathbf{A}^T \left[\mathbf{A} (\mathbf{H}^T \mathbf{H})^{-1} \mathbf{A}^T \right]^{-1} \mathbf{A} \hat{\boldsymbol{\theta}}_1 \quad (3.66)$$

where

- $\hat{\boldsymbol{\theta}}_1 = \hat{\boldsymbol{\theta}} = (\mathbf{H}^T \mathbf{H})^{-1} \mathbf{H}^T \mathbf{x}$ is the unconstrained MLE of $\boldsymbol{\theta}$.
- $\mathbf{d} = (\mathbf{H}^T \mathbf{H})^{-1} \mathbf{A}^T \left[\mathbf{A} (\mathbf{H}^T \mathbf{H})^{-1} \mathbf{A}^T \right]^{-1} \mathbf{A} \hat{\boldsymbol{\theta}}_1$ is a correcting term that enforces the constraint $\mathbf{A} \hat{\boldsymbol{\theta}}_0 = \mathbf{0}$.

3. INDUCTION MACHINE FAULT DETECTION BASED ON THE GENERALISED LIKELIHOOD RATIO TEST

$\hat{\sigma}_i^2$ is found by maximizing $p(\mathbf{x}, \hat{\boldsymbol{\theta}}_i, \sigma_i^2)$ over σ_i^2 , then

$$\hat{\sigma}_i^2 = \frac{1}{N} (\mathbf{x} - \mathbf{H}\hat{\boldsymbol{\theta}}_i)^T (\mathbf{x} - \mathbf{H}\hat{\boldsymbol{\theta}}_i) \quad (3.67)$$

Therefore

$$p(\mathbf{x}; \hat{\boldsymbol{\theta}}_i, \hat{\sigma}_i^2) = \frac{1}{(2\pi\hat{\sigma}_i^2)^{\frac{N}{2}}} \times \exp\left(-\frac{N}{2}\right) \quad (3.68)$$

Thus, the GLRT is

$$\mathcal{L}_G(\mathbf{x}) = \left(\frac{\hat{\sigma}_0^2}{\hat{\sigma}_1^2}\right)^{\frac{N}{2}} \quad (3.69)$$

Let $\mathcal{J}'(\mathbf{x}) = \mathcal{L}_G(\mathbf{x})^{\frac{2}{N}} - 1$ is a monotonically increasing function of $\mathcal{L}_G(\mathbf{x})$, then

$$\begin{aligned} \mathcal{J}'(\mathbf{x}) &= \frac{\hat{\sigma}_0^2 - \hat{\sigma}_1^2}{\hat{\sigma}_1^2} \\ &= \frac{(\mathbf{x} - \mathbf{H}\hat{\boldsymbol{\theta}}_0)^T (\mathbf{x} - \mathbf{H}\hat{\boldsymbol{\theta}}_0) - (\mathbf{x} - \mathbf{H}\hat{\boldsymbol{\theta}}_1)^T (\mathbf{x} - \mathbf{H}\hat{\boldsymbol{\theta}}_1)}{(\mathbf{x} - \mathbf{H}\hat{\boldsymbol{\theta}}_1)^T (\mathbf{x} - \mathbf{H}\hat{\boldsymbol{\theta}}_1)} \\ &= \frac{(\mathbf{A}\hat{\boldsymbol{\theta}}_1)^T \left[\mathbf{A} (\mathbf{H}^T \mathbf{H})^{-1} \mathbf{A}^T \right]^{-1} (\mathbf{A}\hat{\boldsymbol{\theta}}_1)}{\mathbf{x}^T (\mathbf{I} - \mathbf{H} (\mathbf{H}^T \mathbf{H})^{-1} \mathbf{H}^T) \mathbf{x}} \end{aligned} \quad (3.70)$$

3.4.3 Performance of the Proposed Faults Detector

To analyze performances of the proposed detector, distributions under the two hypothesis \mathcal{H}_0 and \mathcal{H}_1 are needed. To determine these distributions, we define $\mathcal{N}(\mathbf{x})$ and $\mathcal{D}(\mathbf{x})$ according to the following equivalent statistic:

$$\begin{aligned} \mathcal{J}'(\mathbf{x}) &= \frac{(\mathbf{A}\hat{\boldsymbol{\theta}}_1)^T \left[\mathbf{A} (\mathbf{H}^T \mathbf{H})^{-1} \mathbf{A}^T \right]^{-1} (\mathbf{A}\hat{\boldsymbol{\theta}}_1) / \sigma^2}{\mathbf{x}^T (\mathbf{I} - \mathbf{H} (\mathbf{H}^T \mathbf{H})^{-1} \mathbf{H}^T) \mathbf{x} / \sigma^2} \\ &= \frac{\mathcal{N}(\mathbf{x})}{\mathcal{D}(\mathbf{x})} \end{aligned} \quad (3.71)$$

and we search the corresponding PDFs.

3.4 Proposed Induction Machine Faults Detector

The denominator $\mathcal{D}(\mathbf{x})$ is given by

$$\begin{aligned}
 \mathcal{D}(\mathbf{x}) &= \frac{1}{\sigma^2} \mathbf{x}^T \left(\mathbf{I} - \mathbf{H} \left(\mathbf{H}^T \mathbf{H} \right)^{-1} \mathbf{H}^T \right) \mathbf{x} \\
 &= \frac{1}{\sigma^2} \mathbf{x}^T (\mathbf{I} - \mathbf{P}_{\mathbf{H}}) \mathbf{x} \\
 &= \frac{1}{\sigma^2} \mathbf{x}^T \mathbf{P}_{\mathbf{H}}^{\perp} \mathbf{x} \\
 &= \frac{1}{\sigma^2} \left\| \mathbf{P}_{\mathbf{H}}^{\perp} \mathbf{x} \right\|^2
 \end{aligned} \tag{3.72}$$

where $\mathbf{P}_{\mathbf{H}} = \mathbf{H} \left(\mathbf{H}^T \mathbf{H} \right)^{-1} \mathbf{H}^T$ is an orthogonal projection matrix onto the subspace of \mathbb{R}^N spanned by the columns of \mathbf{H} (the signal subspace) and $\mathbf{P}_{\mathbf{H}}^{\perp} = (\mathbf{I} - \mathbf{P}_{\mathbf{H}})$ is another orthogonal projection matrix onto the subspace of \mathbb{R}^N orthogonal to the subspace spanned by the range of \mathbf{H} (the noise subspace) and has rank $(N - p)$. Since $\mathbf{P}_{\mathbf{H}}^{\perp} \mathbf{H} = \mathbf{0}$, we have under \mathcal{H}_i

$$\begin{aligned}
 \mathcal{D}(\mathbf{x}) &= \frac{1}{\sigma^2} (\mathbf{H}\boldsymbol{\theta}_i + \mathbf{b})^T \mathbf{P}_{\mathbf{H}}^{\perp} (\mathbf{H}\boldsymbol{\theta}_i + \mathbf{b}) \\
 &= \frac{1}{\sigma^2} \mathbf{b}^T \mathbf{P}_{\mathbf{H}}^{\perp} \mathbf{b} \\
 &= \left(\frac{\mathbf{b}}{\sigma} \right)^T \mathbf{P}_{\mathbf{H}}^{\perp} \left(\frac{\mathbf{b}}{\sigma} \right)
 \end{aligned} \tag{3.73}$$

since $\left(\frac{\mathbf{b}}{\sigma} \right) \sim \mathcal{N}(\mathbf{0}, \mathbf{I})$, it can be shown that [295]

$$\mathcal{D}(\mathbf{x}) \sim \begin{cases} \chi_{N-p}^2 & \text{under } \mathcal{H}_0 \\ \chi_{N-p}^2 & \text{under } \mathcal{H}_1 \end{cases} \tag{3.74}$$

where χ_{N-p}^2 is the chi-squared PDF with $(N - p)$ degrees of freedom.

To find the PDF of the numerator $\mathcal{N}(\mathbf{x})$ we note that it is a function of $\hat{\boldsymbol{\theta}}_1$ only. Let

$$\mathcal{Z}_1(\mathbf{x}) = \alpha^T \hat{\boldsymbol{\theta}}_1 = \alpha^T \left(\mathbf{H}^T \mathbf{H} \right)^{-1} \mathbf{H}^T \mathbf{x} \tag{3.75a}$$

and

$$\mathcal{Z}_2(\mathbf{x}) = \mathbf{d}^T \mathbf{x} \tag{3.75b}$$

are linear forms in \mathbf{x} where $\mathbf{d} = \mathbf{H} \left(\mathbf{H}^T \mathbf{H} \right)^{-1} \alpha$ and α is an arbitrary $(p \times 1)$ vector. Therefore, $\mathcal{D}(\mathbf{x}) = \frac{1}{\sigma^2} \mathbf{x}^T \mathbf{P}_{\mathbf{H}}^{\perp} \mathbf{x}$ and $\mathcal{Z}_2(\mathbf{x})$ are independent under either hypothesis for all \mathbf{d} (because $\mathbf{P}_{\mathbf{H}}^{\perp} \mathbf{d} = \mathbf{0}$). Thus, $\mathcal{Z}_1(\mathbf{x})$ is independent of $\mathcal{D}(\mathbf{x})$ for all α . It can be

3. INDUCTION MACHINE FAULT DETECTION BASED ON THE GENERALISED LIKELIHOOD RATIO TEST

concluded that $\hat{\boldsymbol{\theta}}_1$ is independent of $\mathcal{D}(\mathbf{x})$ and hence $\mathcal{N}(\mathbf{x})$ is independent of $\mathcal{D}(\mathbf{x})$. As conclusion the numerator $\mathcal{N}(\mathbf{x})$ has the PDF [295]

$$\mathcal{N}(\mathbf{x}) \sim \begin{cases} \chi_r^2 & \text{under } \mathcal{H}_0 \\ \chi_r'^2(\lambda) & \text{under } \mathcal{H}_1 \end{cases} \quad (3.76)$$

where $\chi_r'^2(\lambda)$ is the noncentral chi-squared PDF with r degrees of freedom and the noncentrality parameter λ that is given by

$$\lambda = \frac{(\mathbf{A}\hat{\boldsymbol{\theta}}_1)^T \left[\mathbf{A} (\mathbf{H}^T \mathbf{H})^{-1} \mathbf{A}^T \right]^{-1} (\mathbf{A}\hat{\boldsymbol{\theta}}_1)}{\sigma^2} \quad (3.77)$$

Normalizing the numerator and the denominator by the corresponding degrees of freedom produces

$$\mathcal{J}(\mathbf{x}) = \frac{\mathcal{N}(\mathbf{x})/r}{\mathcal{D}(\mathbf{x})/(N-p)} \sim \begin{cases} F_{r,(N-p)} & \text{under } \mathcal{H}_0 \\ F_{r,(N-p)}'(\lambda) & \text{under } \mathcal{H}_1 \end{cases} \quad (3.78)$$

where $F_{r,N-p}$ denotes an F distribution with r numerator degrees of freedom and $N-p$ denominator degrees of freedom and $F_{r,N-p}'(\lambda)$ denotes a noncentral F distribution with r numerator degrees of freedom, $N-p$ denominator degrees of freedom and noncentrality parameters λ .

For a NP test, detector Performances are assessed through two criteria: the detection probability P_D that is the power of the detector and the false alarm probability P_{Fa} that is the level of the detector. These probabilities are functions of γ , which are given by

$$\begin{aligned} P_{Fa} &= Q_{F_{r,N-p}}(\gamma') \\ P_D &= Q_{F_{r,N-p}'(\lambda)}(\gamma') \end{aligned} \quad (3.79)$$

where $Q_{PDF}(x)$ is the complementary commutative distribution function for a PDF of random variable x .

Since the false alarm probability is independent of noise parameters, the proposed detector is called the constant-false alarm rate (CFAR) detector [337]. Finally, the

Table 3.2: Simulation parameters (L=5).

Amplitudes	a_0	a_1	a_2	a_3	a_4
Healthy machine	0	0	2	0	0
Severity 1	0.004	0.004	2	0.004	0.004
Severity 2	0.005	0.005	2	0.005	0.005
Severity 3	0.006	0.006	2	0.006	0.006
Severity 4	0.008	0.0091	2	0.007	0.0067

proposed CFAR detector decide \mathcal{H}_1 if

$$\mathcal{J}(\mathbf{x}) = \frac{N-p}{r} \frac{(\mathbf{A}\hat{\boldsymbol{\theta}}_1)^T \left[\mathbf{A} (\mathbf{H}^T \mathbf{H})^{-1} \mathbf{A}^T \right]^{-1} (\mathbf{A}\hat{\boldsymbol{\theta}}_1)}{\mathbf{x}^T (\mathbf{I} - \mathbf{H} (\mathbf{H}^T \mathbf{H})^{-1} \mathbf{H}^T) \mathbf{x}} \succ \gamma' \quad (3.80)$$

3.4.4 Proposed Induction Machine Faults Detection Architecture

To simplify the implementation of the proposed detector, a fault detection architecture is proposed in Fig.3.5). The proposed approach relies on five steps for decision making, which are: motor current acquisition, model parameters estimation, matrix \mathbf{A} computation, criterion computation, and threshold computation according to desired P_{Fa} .

3.5 Simulations Results

In this section, simulations results are presented to illustrate the performance of the proposed detector.

3.5.1 Simulations Parameters

Simulations have been performed to investigate the detection performance of the proposed GLRT detector. this detector is tested using synthetic signals modeled by (3 – 1) and the frequency structure given in (3 – 3) with $F_S = 1000Hz$, $f_s = 50$, $f_c = 5$, and $k = \{0, 1, 2\}$. Simulation parameters are given by Table 3.2. All simulation results are obtained using 1000 Monte Carlo Trials.

3. INDUCTION MACHINE FAULT DETECTION BASED ON THE GENERALISED LIKELIHOOD RATIO TEST

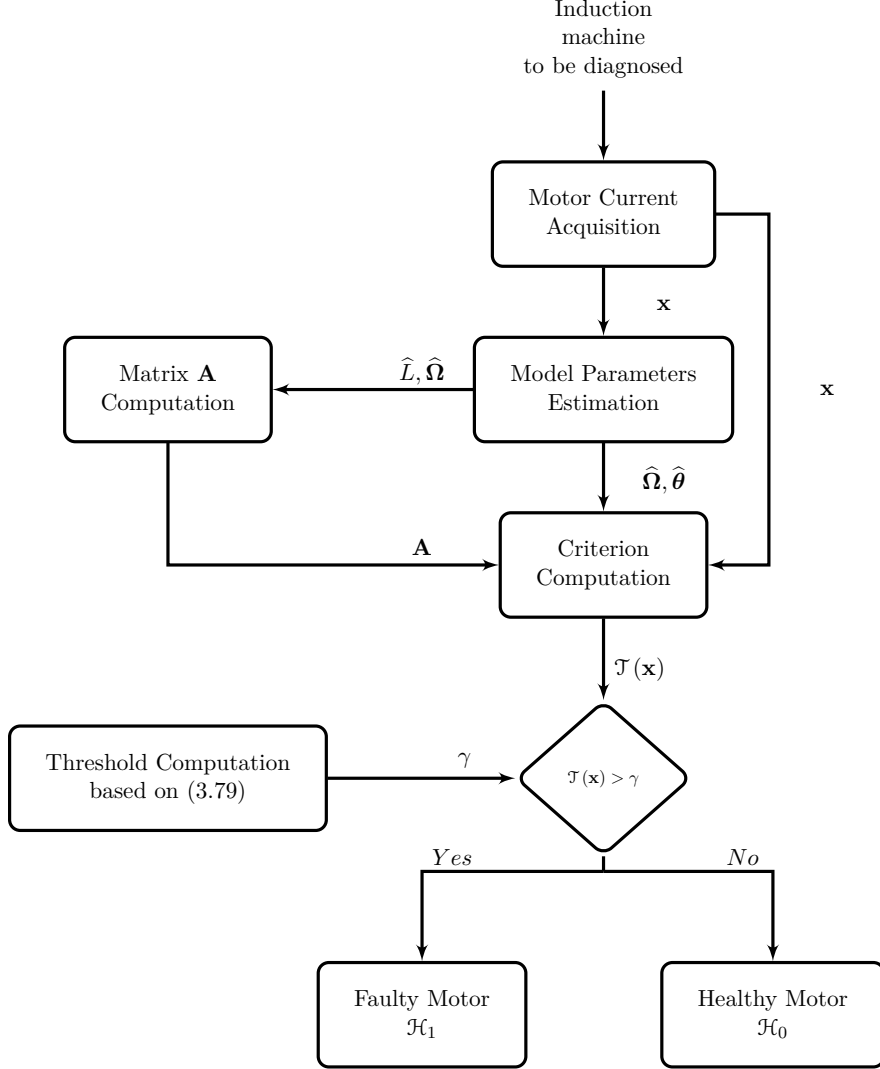


Figure 3.5: Proposed fault detection architecture of induction machines.

3.5.2 ROC curves and Histogram

Figure 3.6(b) shows the histogram of the GLRT under \mathcal{H}_0 (healthy machine) and \mathcal{H}_1 (faulty machine with severity 4) with a $SNR = 30dB$, $P_{Fa} = 10^{-3}$, and $N = 600$ samples. This figure shows that two PDFs under \mathcal{H}_0 and \mathcal{H}_1 are distinct. Consequently, the fault can be detected with high confidence by setting an appropriate threshold based on the desired P_{Fa} . Figure 3.6(a) depicts Receiver operation characteristics (ROC) curves for the considered fault severities with a $SNR = 30dB$, $P_{Fa} = 10^{-3}$,

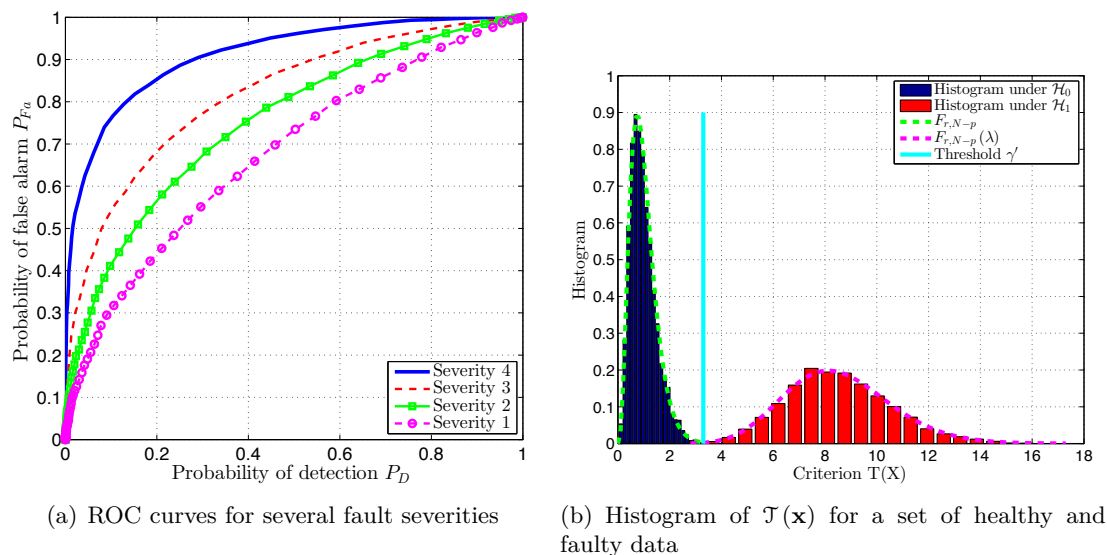


Figure 3.6: ROC curves and histogram of the estimated $\mathcal{J}(\mathbf{x})$.

and $N = 600$ samples. These curves are ways to measure performances of the proposed detector that represent the evolution of P_D versus P_{Fa} .

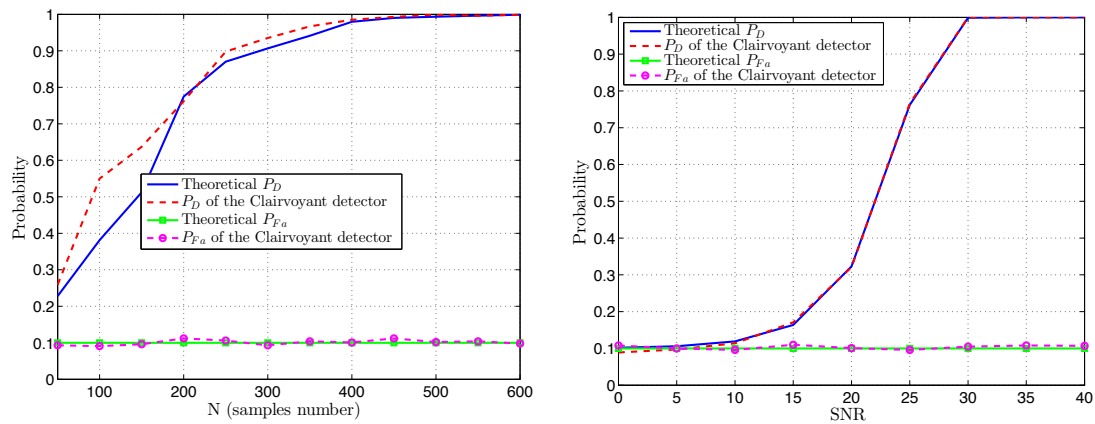
3.5.3 Influences of SNR , N , and P_{Fa}

Figures 3.7 and 3.8 demonstrate the robustness of the proposed detector under various values of SNR , N , and P_{Fa} . Figure 3.7(a) shows samples number influence on the detection and false alarm probabilities with $SNR = 30dB$ and $P_{Fa} = 10^{-3}$. Figure 3.7(b) depicts samples number influence on the P_D and P_{Fa} with $P_{Fa} = 10^{-3}$, and $N = 600$ samples. It can be concluded from these figures that the proposed approach gives better performance when N or SNR increase and it is able to provide good detection performance since $SNR \geq 25$ and $N \geq 400$ samples. This figure shows that the threshold increases when the P_{Fa} is decreased, which affects the detection ability of the proposed detector. In fact, the P_{Fa} must be chosen adequately in order to detect incipient faults.

3.6 Conclusion

This chapter has presented different parametric detection approaches of the statistical decision theory. There are three main decision rules of the binary hypothesis

3. INDUCTION MACHINE FAULT DETECTION BASED ON THE GENERALISED LIKELIHOOD RATIO TEST



(a) Evolution of P_D and P_{F_a} with respect to N . (b) Evolution of P_D and P_{F_a} with respect to SNR.

Figure 3.7: GLRT performance with respect to N and SNR

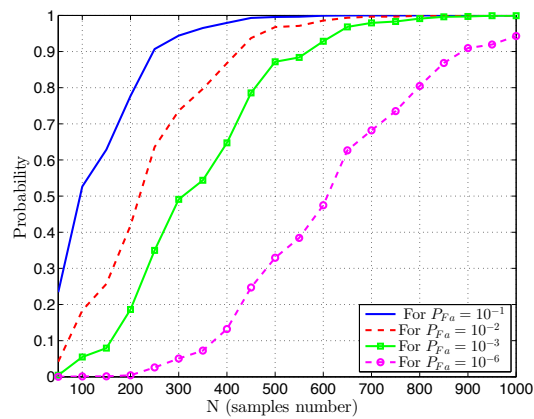


Figure 3.8: Evolution of P_D with respect to N for several desired fault alarm probability.

testing: Bayes, minmax, and NP decision rules. The Bayes criterion is based on the existence of a prior probability and costs of each possible decision. The Bayes risk can be minimized to design the threshold, which it is compared with LRT to obtain a decision. The MAP and the ML rule are the particular case of this criterion. The minmax is used when a priori probabilities are not available. In situations where we have no information about priori probabilities and costs assignments, the NP criterion can be applied to choose the threshold of the LRT. The NP criterion optimizes the detection probability given a fixed level of false alarm probability. The ROC curve, which is a plot of the probability of detection versus the probability of false alarm, was useful in analyzing the performance of detectors. This chapter has also studied the composite hypothesis testing when parameters characterizing a hypothesis may not be known, which is the case in many real-world applications. There are two approaches to composite hypothesis testing: the Bayesian approach and the GLRT approach. The Bayesian approach considers the unknown parameters as random variables. The GLRT approach replace the unknown parameters by their maximum likelihood estimates.

Induction machine faults detection problem has been formulated as a detection of deterministic signals with unknown parameters. The stator current has been modeled by multiple sinusoids with unknown parameters in a white Gaussian noise. BIC and TLS-ESPRIT has been used to estimate the model order and frequencies, respectively. The detection has been examined as a detection of the classical linear model with unknown variance (nuisance parameter). To address this problem, the GLRT has been proposed and the distribution of this test statistic has also been determined to analyze performances. A fault detection architecture has been proposed to simplify the implementation of the proposed detector. It has been shown that the GLRT performs correctly for N greater than 400 samples and $SNR \geq 25$ dB.

3. INDUCTION MACHINE FAULT DETECTION BASED ON THE GENERALISED LIKELIHOOD RATIO TEST

Experimental Validation

Contents

4.1	Introduction	110
4.2	Experimental Setup Description	110
4.2.1	Setup Description for Bearing Faults	111
4.2.2	Setup Description for Broken Rotor Bars	111
4.3	Experimental Results for Bearing Faults	111
4.3.1	Spectral Estimation Techniques	112
4.3.2	Demodulation Techniques	114
4.3.3	Fault Severity Analysis	117
4.3.4	GLRT-Based Faults Detection	119
4.4	Experimental Results for Broken Rotor Bars	120
4.4.1	Spectral Estimation Techniques	120
4.4.2	Demodulation Techniques	121
4.4.3	Fault Severity Detection	124
4.4.4	GLRT-Based Faults Detection	125
4.5	Conclusion	127

4. EXPERIMENTAL VALIDATION



Figure 4.1: Machinery fault simulator.

4.1 Introduction

This chapter describes the experimental setup that allows validating the previous proposed techniques for induction machine condition monitoring and fault detection. It presents the experimental results of two main considered faults: broken rotor bars and bearing faults. The efficiency of the proposed fault analysis and detection approaches is evaluated on experimental stator currents measurements. For feature extraction techniques, three main categories are considered: demodulation techniques, nonparametric and parametric techniques. Performances of fault severity criterion and faults detector are also evaluated in this chapter.

4.2 Experimental Setup Description

The proposed approaches for induction machine faults analysis are tested on experimental data for broken rotor bars and bearing faults. The experimental setup is shown by Fig. 4.1.

4.3 Experimental Results for Bearing Faults

Table 4.1: Bearing fault severity versus hole diameter.

Fault severity	1	2	3
Bearing hole diameter (inches)	0.007	0.014	0.02

4.2.1 Setup Description for Bearing Faults

A healthy machine and a faulty one with bearing fault types have been tested. These three-phase machines are 230/400 V, 0.75-kW, with pole pairs numbers equal to $p = 1$, and 2780 rpm rated speed. They have two 6204-2 ZR type bearings (single row and deep groove ball bearings) with the following parameters: outside diameter is 47 mm, inside diameter is 20 mm, and pitch diameter D is 31,85 mm. Bearings have 8 balls with an approximate diameter d of 12 mm and a contact angle of 0° (Fig. 1.3b). Bearing faults are obtained by drilling holes of several diameters in the inner raceway (faults ranging from 0.007 inches (0.178 mm) in diameter to 0.040 inches (1.016 mm) as it can be seen in Table 4.1). The stator currents acquisition is performed by a 24 bits acquisition card with 10 kHz sampling frequency. All experiments were done in steady state conditions. Machines under study are fed by a PWM inverter with a fundamental frequency equals to $f_s = 50$ Hz.

4.2.2 Setup Description for Broken Rotor Bars

A healthy machine and a faulty one with broken rotor bars have been tested. These three-phase machines are 230/400V and 5-kW. Broken rotor bars are obtained by drilling the bar of the squirrel cage. The stator currents acquisition is performed by a 24 bits acquisition card with 20 kHz sampling frequency. All the experiments were done in steady state conditions. The machines under study are fed by a PWM inverter with a fundamental frequency equals to $f_s = 50$ Hz.

4.3 Experimental Results for Bearing Faults

The first studied fault is the bearing fault. It is used to validate the proposed techniques based on the stator current measurements.

4. EXPERIMENTAL VALIDATION

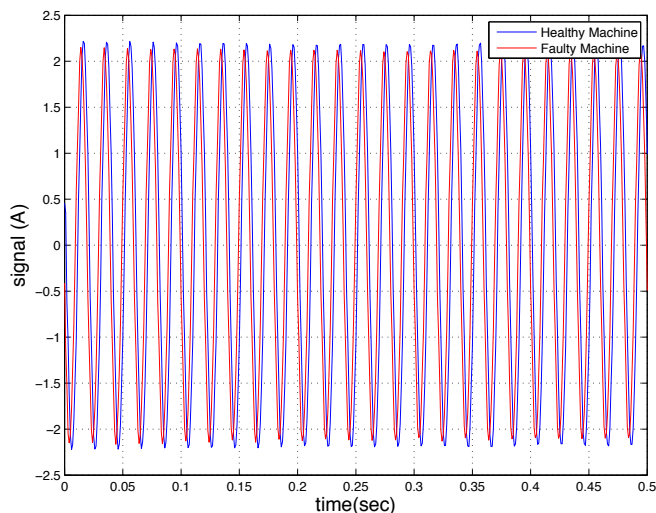


Figure 4.2: The stator current for healthy and faulty induction machines.

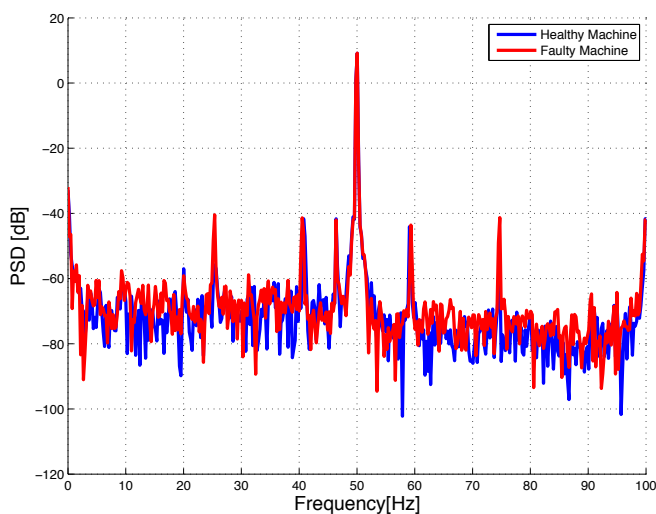


Figure 4.3: Spectral analysis by Welch periodogram using Hanning window ($N = 2000$) for a healthy and faulty induction machines with bearing faults.

4.3.1 Spectral Estimation Techniques

Figure 4.2 illustrates the stator current waveforms for healthy and faulty induction machines. According to this figure, stator currents are not exactly sinusoidal due to presence of space harmonics. Figure 4.3 shows the Welch periodograms using a sampling frequency $F_s = 1000\text{Hz}$, $N = 2000$ samples, and a Hanning window for healthy and faulty induction machines with bearing faults (severity4). This figure demonstrate

4.3 Experimental Results for Bearing Faults

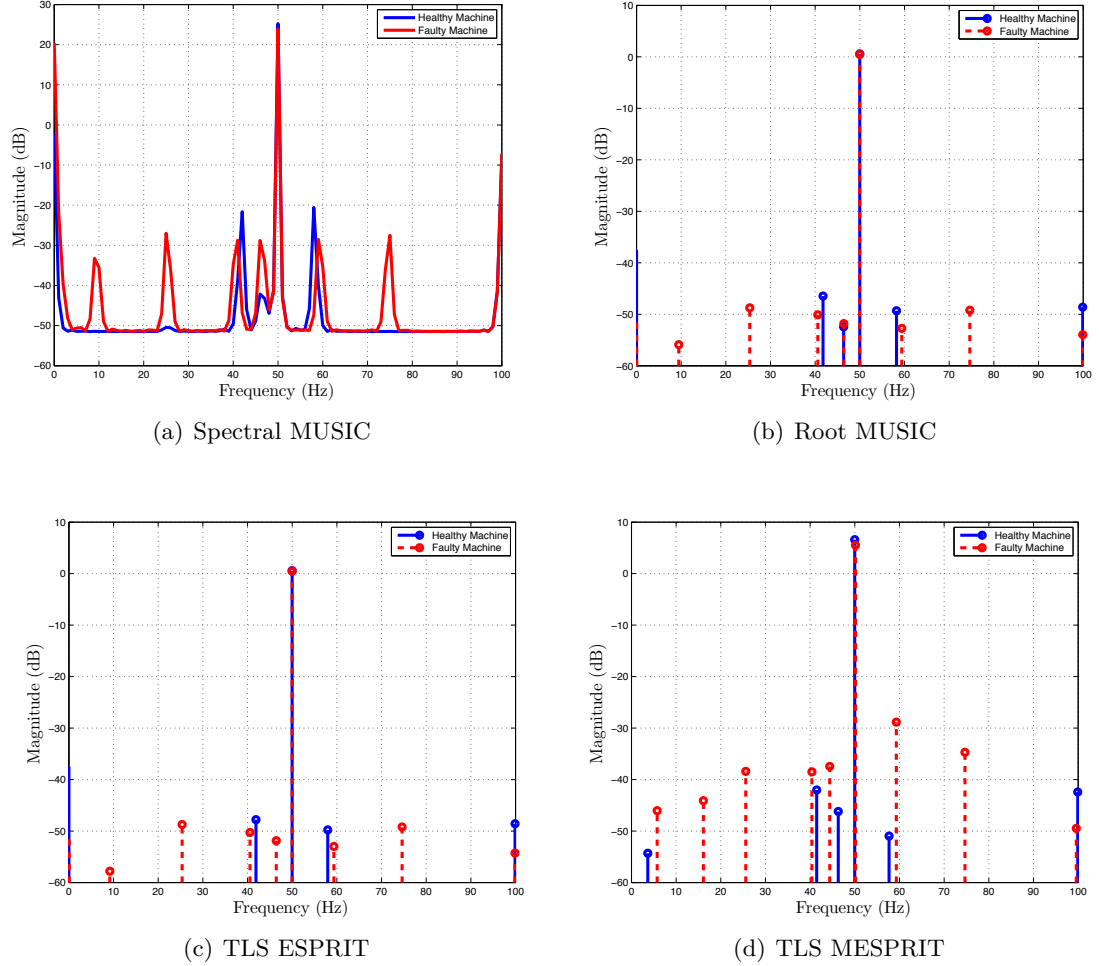


Figure 4.4: Stator current spectrum based on the subspace techniques and BIC criterion for a healthy and faulty induction machines with bearing faults (severity4).

that the FFT-based techniques does not allow to clearly distinguish frequencies. These techniques can be used to estimate the stator current power spectral density, but they suffer from a poor frequency resolution. Figure 4.4 shows the stator current spectrum using subspace techniques for healthy and faulty induction machines with bearing faults (severity4). The model order is obtained using the BIC criterion. It noticed that the spectral components caused by the specific faults appear in the spectrum for faulty induction machines in the neighborhood of the fundamental frequency. Furthermore, the stator current spectra contains also other frequencies due to manufacture imperfections such as natural level of eccentricities.

4. EXPERIMENTAL VALIDATION

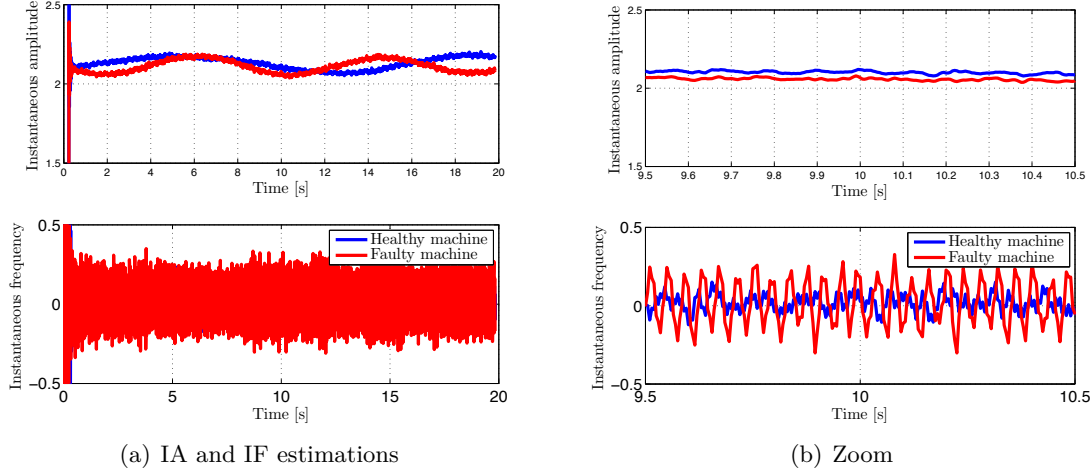


Figure 4.5: Synchronous demodulation for a healthy and faulty induction machines with bearing faults (severity4).

4.3.2 Demodulation Techniques

Figure 4.5 depicts the instantaneous amplitude (IA) and the instantaneous frequency (IF) using the synchronous demodulation (SD) for healthy and faulty machine with bearing faults (severity4). From this figure, it can be deduced that a frequency modulation occurs when a bearing fault exists. The amplitude modulation can be justified by the low-pass filtering stage which introduces a supplementary oscillations [5]. Figure 4.6 shows the IA and the IF based on the Hilbert transform (HT) for healthy and faulty machine with bearing faults (severity4). This technique also confirms the presence of the frequency modulation when the investigated fault is present. It can be noticed that this technique is well known approach to compute the analytical signal. According to this figure, the HT suffers from border effects which can lead to false interpretation results. Figure 4.7 presents the estimation of the IA and the IF using the Teager energy operator (TEO) for healthy and faulty machine with bearing faults (severity4). It can be seen from this figure that the bearing fault leads to the frequency modulation in the stator current. In fact, this technique estimates correctly the IA and the IF of the stator currents. Compared to classical demodulation techniques such as Hilbert transform, TEO has better time resolution. The main drawback of TOE is its sensitivity to noise.

IA and IF estimations using the Concordia transform (CT) approach are shown in

4.3 Experimental Results for Bearing Faults

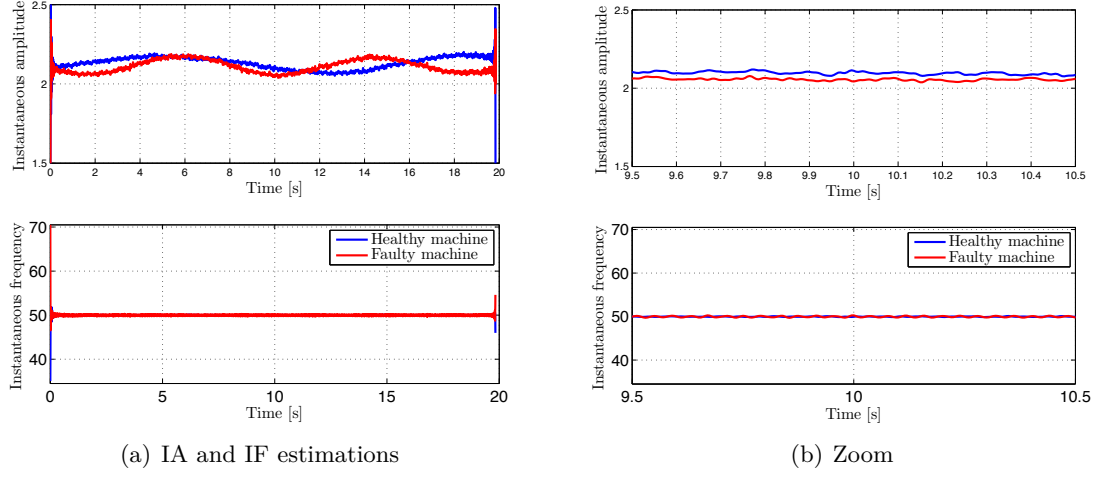


Figure 4.6: Hilbert transform-based demodulation for a healthy and faulty induction machines with bearing faults (severity4).

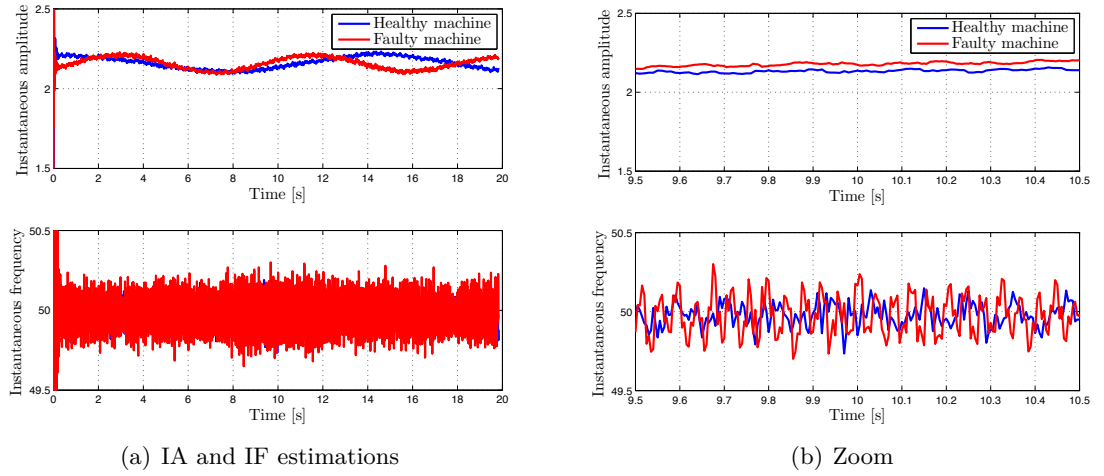


Figure 4.7: Teager energy operator-based demodulation for a healthy and faulty induction machines with bearing faults (severity4).

Fig.4.8 similarly to the previous techniques, the stator current is frequency modulated when the bearing fault is present. This technique performs correctly for balanced three-phase stator currents. In fact, the CT may lead to false interpretation results for unbalanced case. IA and IF estimations based on the Maximum Likelihood (ML) approach are depicted in Fig.4.9 According to this figure, the bearing fault lead to frequency modulation in the stator currents. Compared to CT technique, this technique

4. EXPERIMENTAL VALIDATION

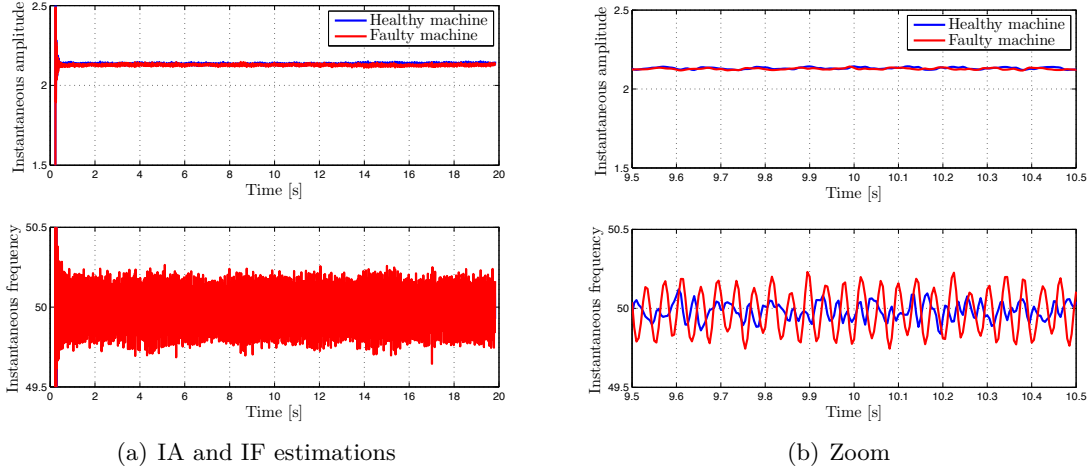


Figure 4.8: CT-based demodulation for a healthy and faulty induction machines with bearing faults (severity4).

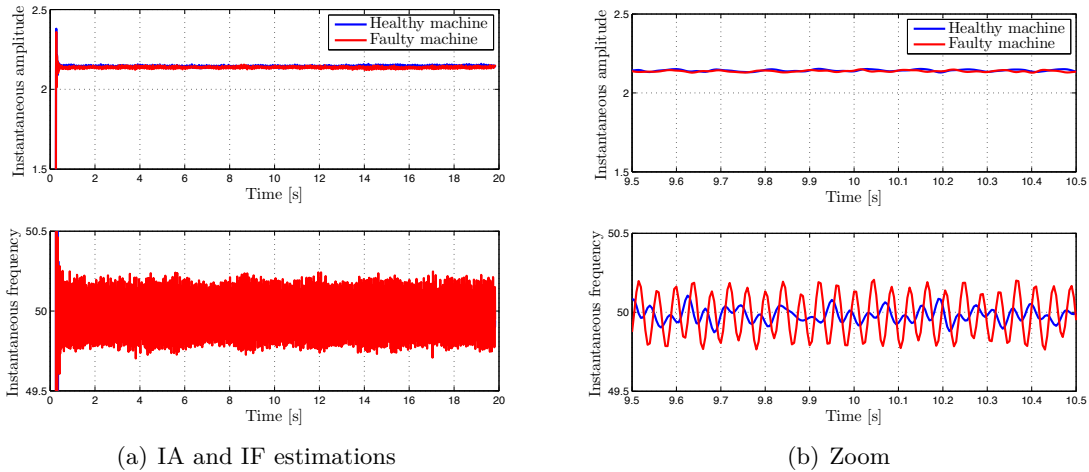


Figure 4.9: ML-based demodulation for a healthy and faulty induction machines with bearing faults (severity4).

performs also for unbalanced three-phase stator currents of amplitudes. In case of phase unbalanced systems, this technique is not appropriate technique. Figure 4.10 shows the IA and the IF using the principal component analysis (PCA) for healthy and faulty machine with bearing faults (severity4). Compared to the previous multidimensional demodulation techniques (CT and ML), the PCA also gives the better results in the case of the phase unbalanced systems.

4.3 Experimental Results for Bearing Faults

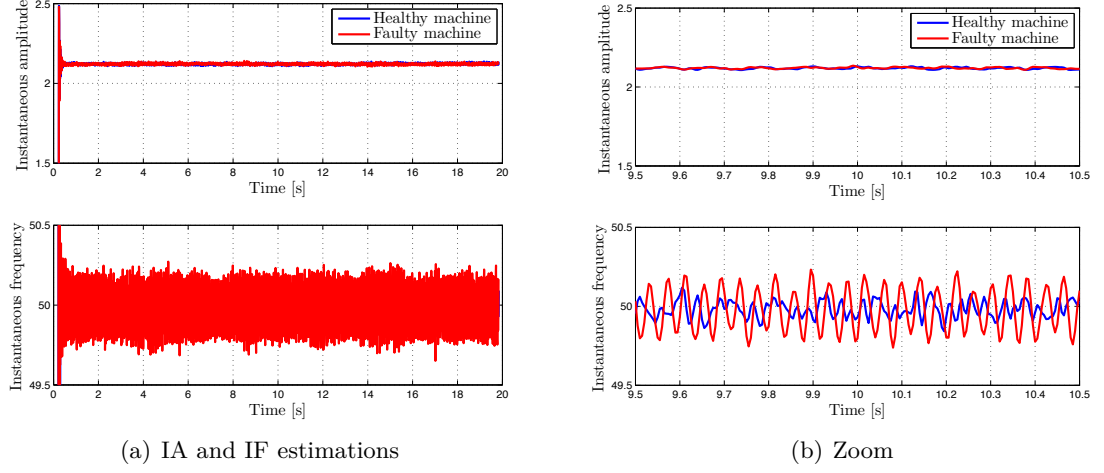


Figure 4.10: PCA-based demodulation for a healthy and faulty induction machines with bearing faults (severity4).

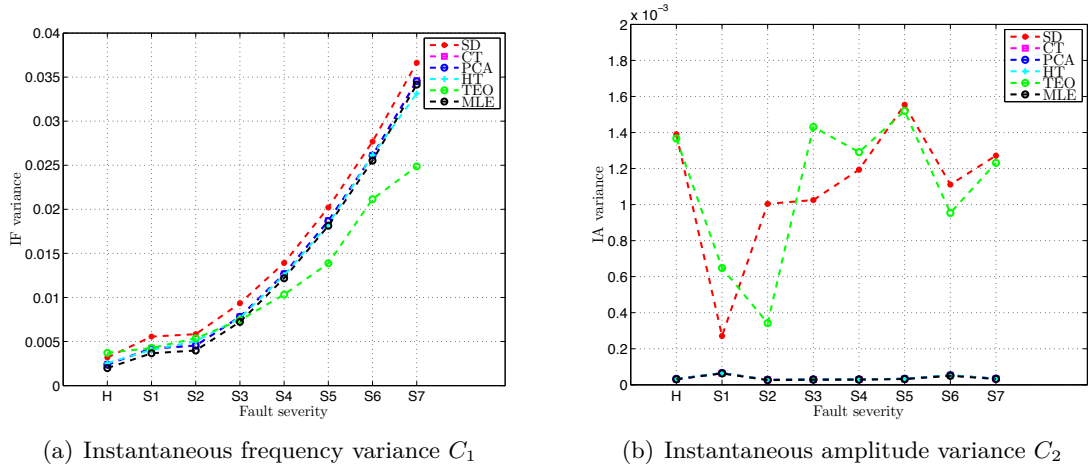


Figure 4.11: Fault severity criterion value versus bearing fault degrees using demodulation techniques.

4.3.3 Fault Severity Analysis

After demodulation stage of the stator currents, fault severity criteria can be assessed using the IF and the IA [5]. These criteria can be mathematically formulated as

$$\begin{cases} C_1 = \frac{1}{N} \sum_{n=0}^{N-1} (\hat{a}[n] - m(\hat{a}[n]))^2 \\ C_2 = \frac{1}{N} \sum_{n=0}^{N-1} (\hat{f}[n] - m(\hat{f}[n]))^2 \end{cases} \quad (4.1)$$

4. EXPERIMENTAL VALIDATION

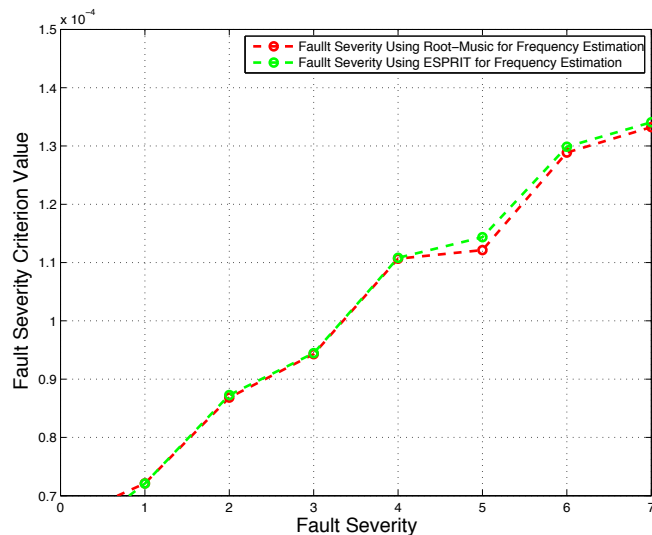


Figure 4.12: Fault severity criterion value versus bearing fault degrees of induction machines.

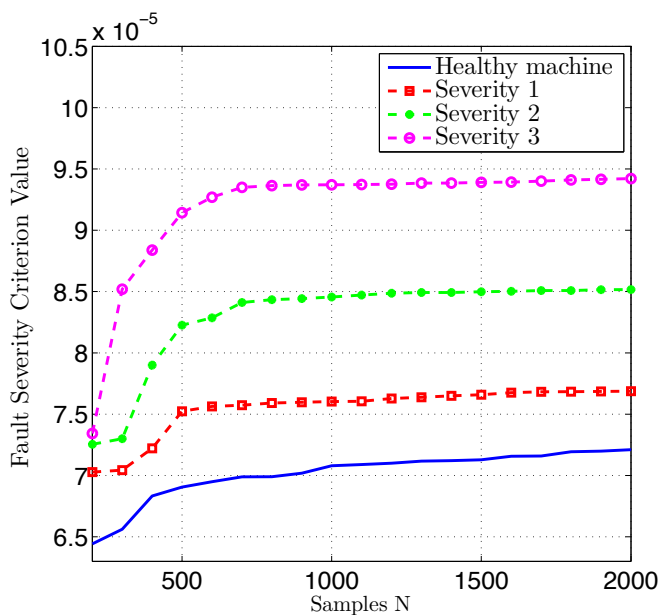


Figure 4.13: Fault severity criterion value versus N (samples number) for bearing faults using TLS ESPRIT, for healthy and faulty induction machines with bearing faults.

Figure 4.11 presents the fault severity criterion based on (4.1) for several bearing fault severities.

A fault severity criterion based on the amplitude evaluation of stator current fre-

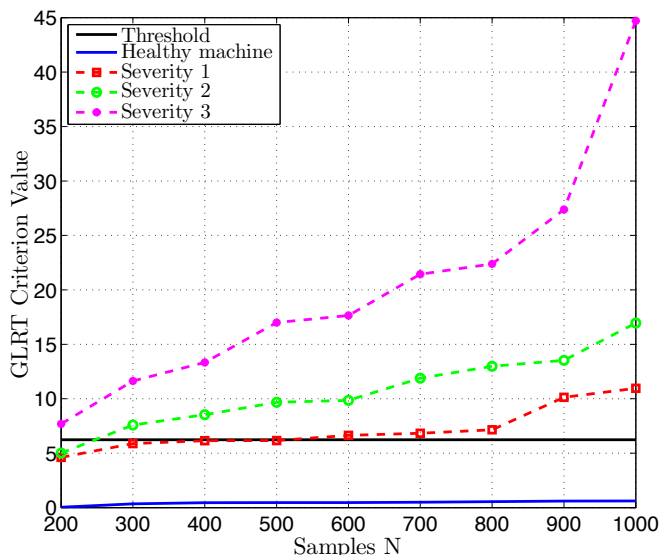


Figure 4.14: GLRT criterion with different N for a healthy machine and faulty induction machines with different considered severities of bearing faults ($P_{Fa} = 10^{-3}$).

quency components for different bearing fault degrees in induction machines is given by Fig. 4.12. According to this figure, FSC values based first on the estimation of fault frequency signature by TLS-ESPRIT or Root-MUSIC give almost the same results. Figure 4.13 shows the evolution of the FSC with respect to sample numbers. It can be shown that for low values of samples numbers the criterion increases. This is normal since we can assume that the estimation is not optimal. For N greater than 500 samples the criterion is constant for a given fault severity. It can be concluded that the proposed approach results are reliable for $N = 500$ samples.

4.3.4 GLRT-Based Faults Detection

Figure 4.14 shows the GLRT evolution with respect to samples number for healthy and faulty machines with different considered bearing faults severities. The major advantage of the proposed detector than the proposed fault severity criterion is its ability to automatically detect faults without comparison between a healthy machine and a faulty machine. According to fig.4.14, the GLRT value increases when the severity or the samples number increases. It is clear for a significant severity, the proposed detector is reliable even with small samples numbers. For lower severities, higher samples numbers are required for the GLRT. Then, it is preferable to choose $N \geq 400$ samples.

4. EXPERIMENTAL VALIDATION

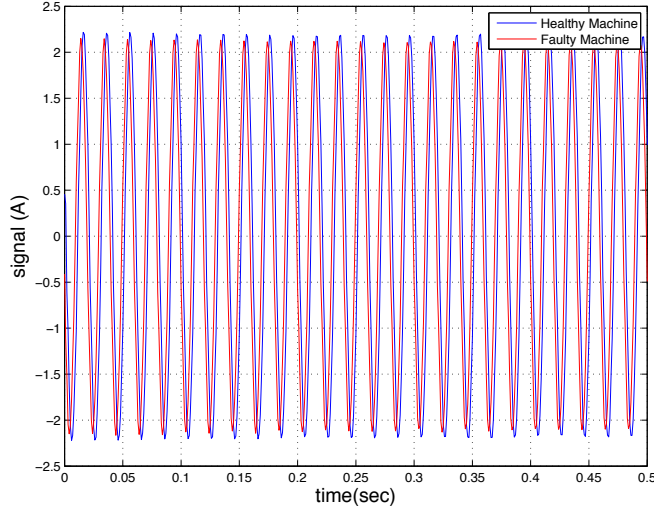


Figure 4.15: The stator current for healthy and faulty induction machines.

Therefore, the GLRT value can determine the fault severity and the machine state.

4.4 Experimental Results for Broken Rotor Bars

This section presents the experimental results for broken rotor bars detection. Stator currents have been used to reveal the presence of the fault using the proposed approaches.

4.4.1 Spectral Estimation Techniques

Figure 4.16 depicts the stator current waveforms for healthy and faulty induction machines. Figure 4.17 gives the Welch periodograms using a sampling frequency $F_s = 1000Hz$, $N = 4096$ samples, and a Hanning window for a healthy and faulty induction machines with broken rotor bar faults. This figure shows again that the FFT-based techniques suffer from a poor frequency resolution. Figure 4.18 shows the stator current spectrum by using subspace techniques for healthy and faulty induction machines with three broken rotor bars. The spectral components caused by the specific faults appear in the spectrum for the faulty induction machine. The appearance of new frequency components in the stator current spectrum is a signature of broken rotor bars. In addition, their amplitudes indicate the fault severity.

4.4 Experimental Results for Broken Rotor Bars

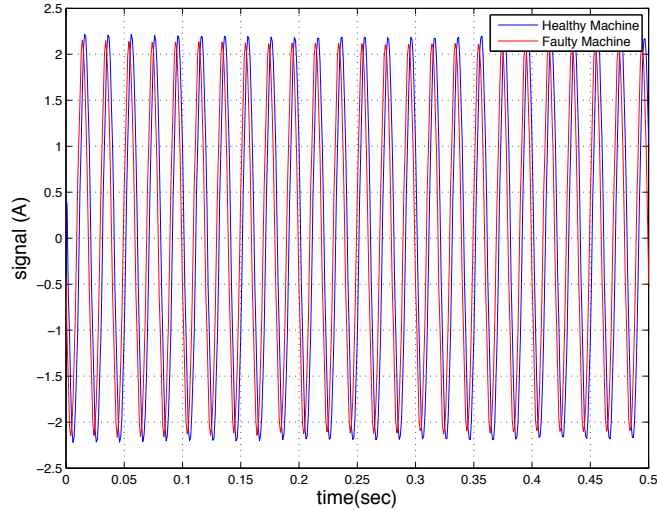


Figure 4.16: The stator current for healthy and faulty induction machines.

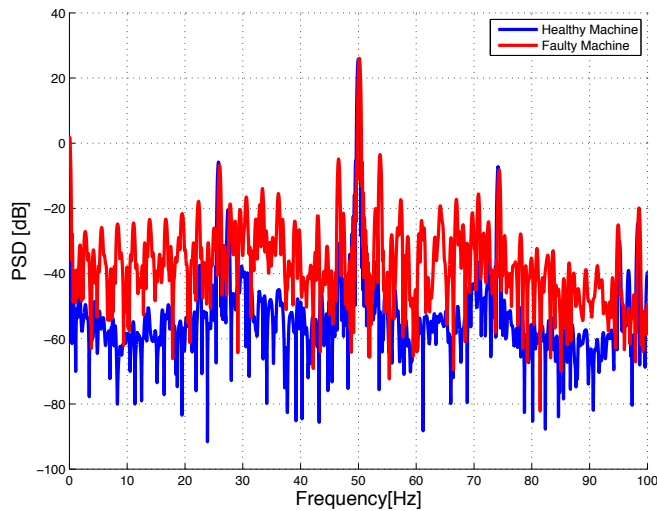


Figure 4.17: Spectral analysis by Welch periodogram using Hanning window ($N = 4096$) for a healthy and faulty induction machines with broken rotor bar faults.

4.4.2 Demodulation Techniques

Figure 4.19 depicts estimations of the IA and the IF using the SD approach for healthy and faulty machine with 3 broken rotor bars. According to this figure, it can be observed that frequency and amplitude modulations occur when rotor bars are broken. The main drawback of SD for broken rotor bars analysis is the low-pass filtering stage which is quite difficult and induce a long time before convergence. Estimations of the

4. EXPERIMENTAL VALIDATION

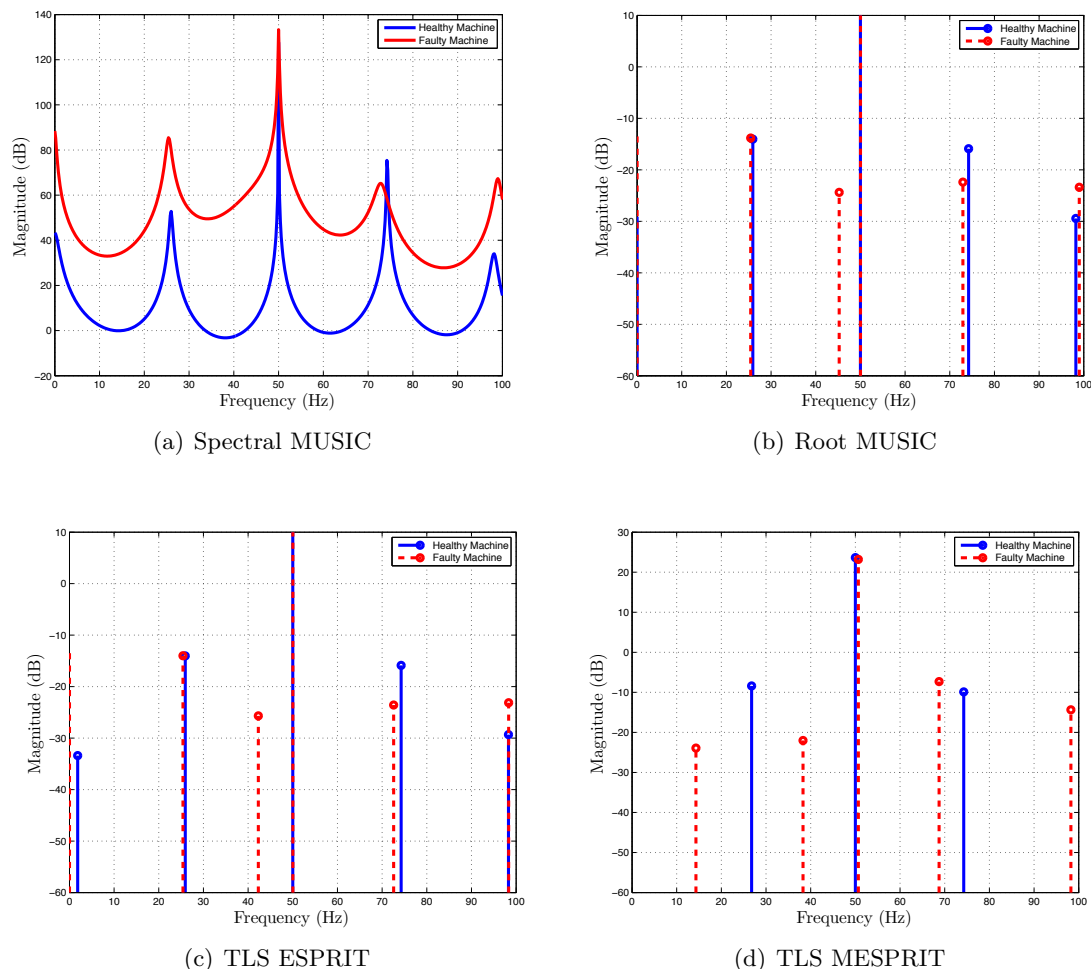


Figure 4.18: Stator current spectrum based on the subspace techniques and BIC criterion for a healthy and faulty induction machines with three broken rotor bars.

IA and the IF using the HT approach for healthy and faulty machine with 3 broken rotor bars are shown in Fig.4.20. As expected, amplitude and phase modulations are presented when broken rotor bars occur. It can be noticed that the HT approach suffers from border effects which can engender a poor interpretation of results. Figure 4.21 presents estimations of the IA and the IF using the TEO for healthy and faulty machine with 3 broken rotor bars. It can be seen from this figure that the broken rotor bars introduce both amplitude and frequency modulations of the stator currents. In fact, this technique estimates correctly the IA and the IF of the stator currents. The main drawback of TEO approach is its sensitivity to noise.

4.4 Experimental Results for Broken Rotor Bars

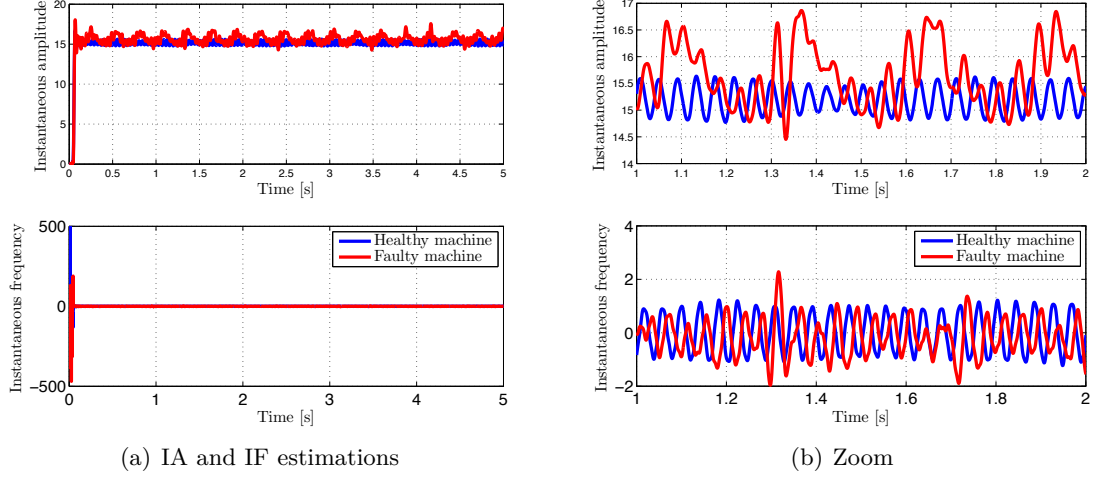


Figure 4.19: Synchronous demodulation for a healthy and faulty induction machines with three broken rotor bars.

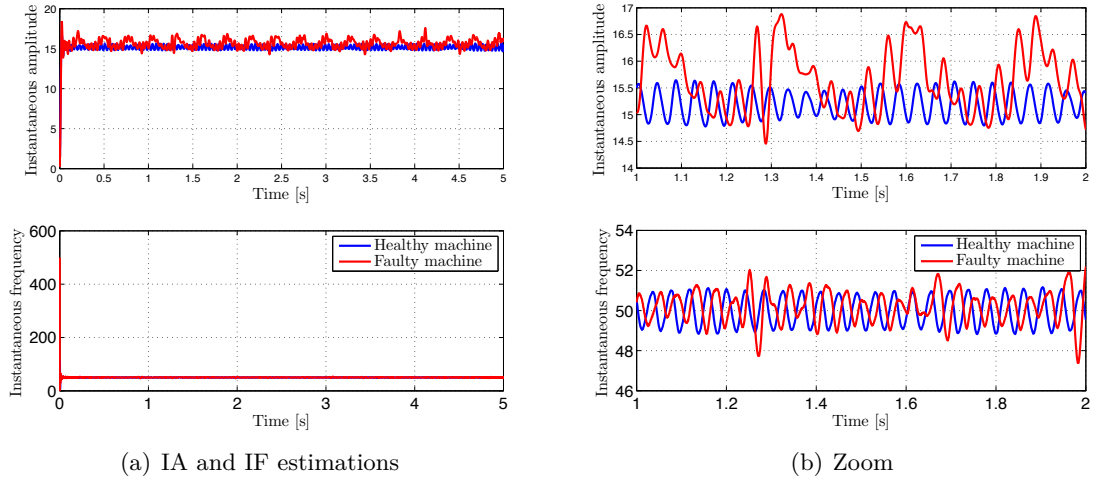


Figure 4.20: Hilbert transform-based demodulation for a healthy and faulty induction machines with three broken rotor bars.

Figures 4.22, 4.23, and 4.24 depict estimations of the IA and the IF using the multidimensional demodulation techniques (CT, ML, and PCA). Similarly to monodimensional techniques, these techniques confirm the presence of the both amplitude and frequency modulations when rotor bars are broken. According to these figures, PCA is the more suited technique in case of amplitude and phase unbalanced three phase stator currents. Unfortunately, performances of this technique depend on the stage of the

4. EXPERIMENTAL VALIDATION

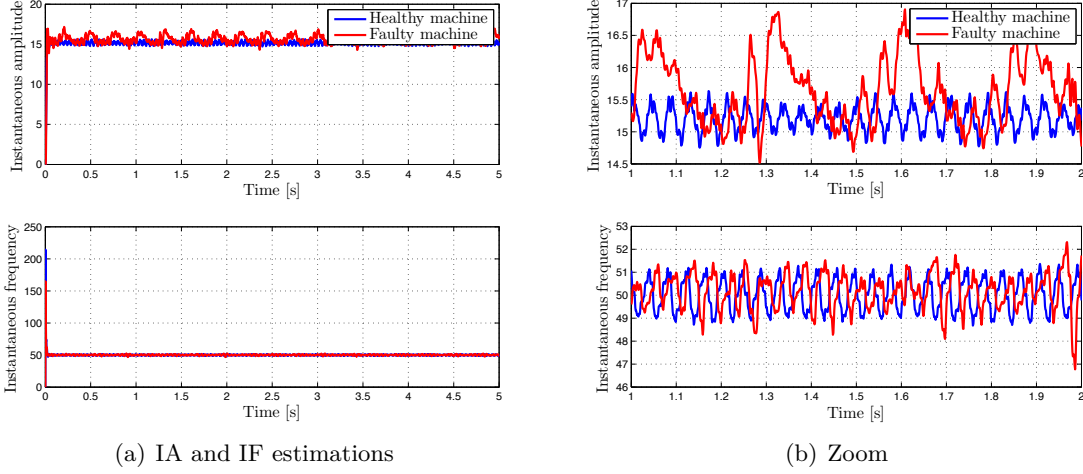


Figure 4.21: Teager energy operator-based demodulation for a healthy and faulty induction machines with three broken rotor bars.

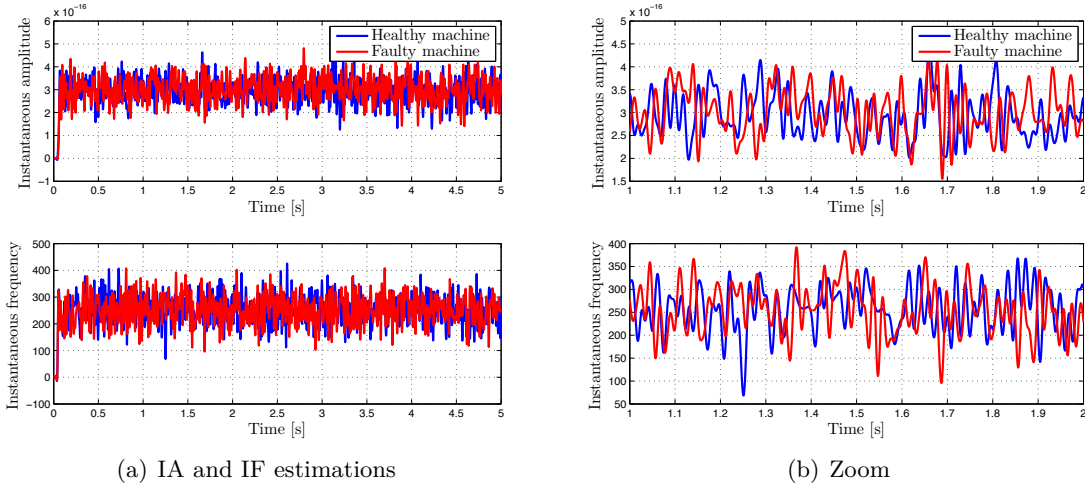


Figure 4.22: CT-based demodulation for a healthy and faulty induction machines with three broken rotor bars.

covariance matrix estimation and the separation of the signal and the noise subspaces.

4.4.3 Fault Severity Detection

Figure 4.25 gives the FSC value versus bearing fault degree. According to this figure, TLS-ESPRIT and Root-MUSIC give almost the same results. Figure 4.26 presents the FSC value versus samples number N using TLS ESPRIT, for healthy and faulty in-

4.4 Experimental Results for Broken Rotor Bars

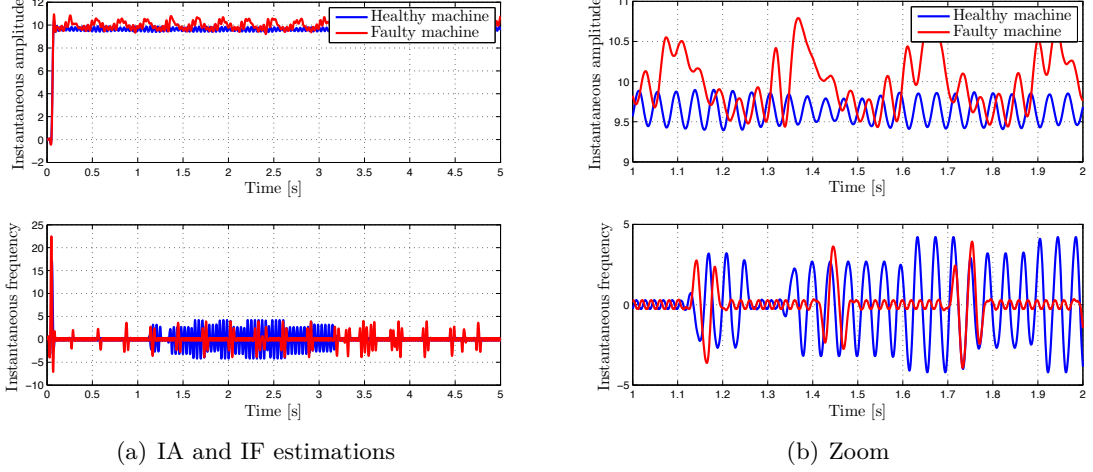


Figure 4.23: ML-based demodulation for a healthy and faulty induction machines with three broken rotor bars.

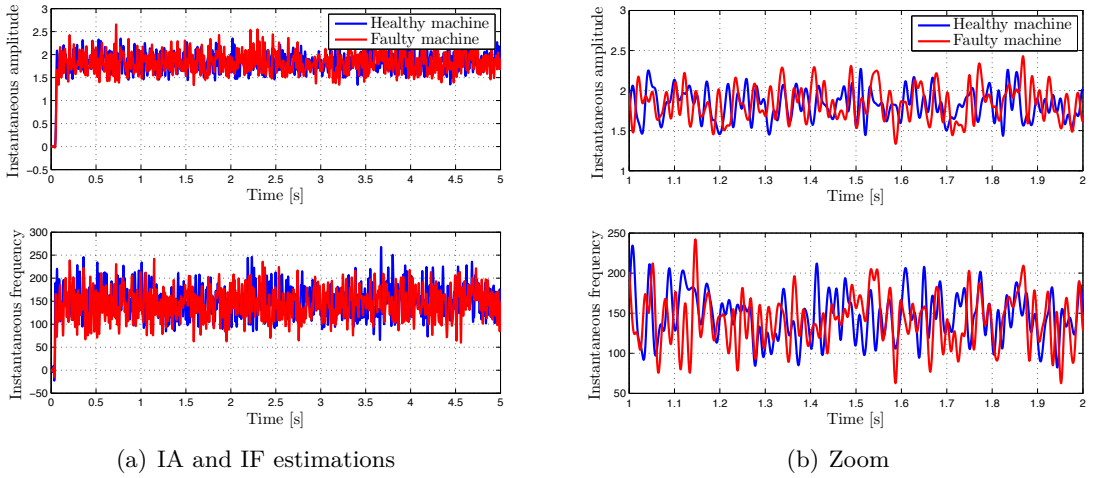


Figure 4.24: PCA-based demodulation for a healthy and faulty induction machines with three broken rotor bars.

duction machines with broken rotor bars. As for bearing faults, the FSC value increases with samples number and also with the broken rotor bars number (Fig 4.25).

4.4.4 GLRT-Based Faults Detection

Figure 4.27 gives the GLRT evolution with respect to sample numbers for healthy and faulty machines with 1, 2, and 3 broken rotor bars. It can be deduced that the

4. EXPERIMENTAL VALIDATION

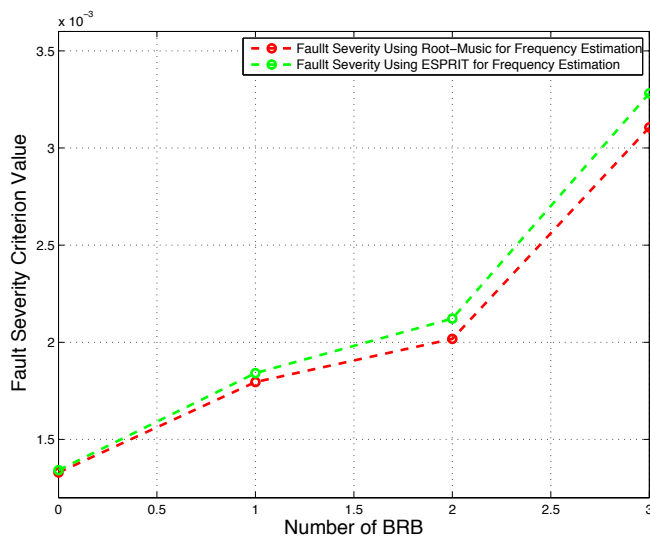


Figure 4.25: Fault severity criterion for different BRB fault degrees. In this figure, 0 corresponds to healthy induction machine and other values correspond to BRB number.

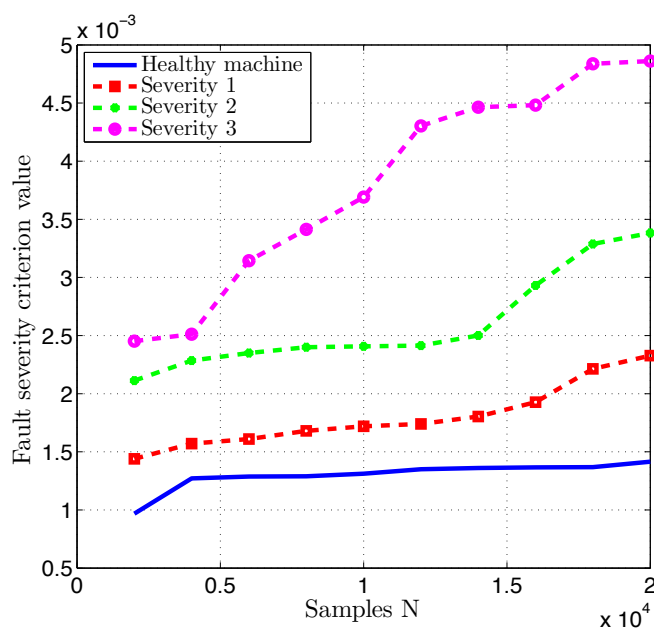


Figure 4.26: Fault severity criterion value for different N (samples number) for bearing faults using TLS ESPRIT, for healthy and faulty induction machines with broken rotor bars.

proposed detector performs correctly for increasing numbers of broken rotor bars or for increasing samples numbers. In fact, the proposed approach results are reliable for N

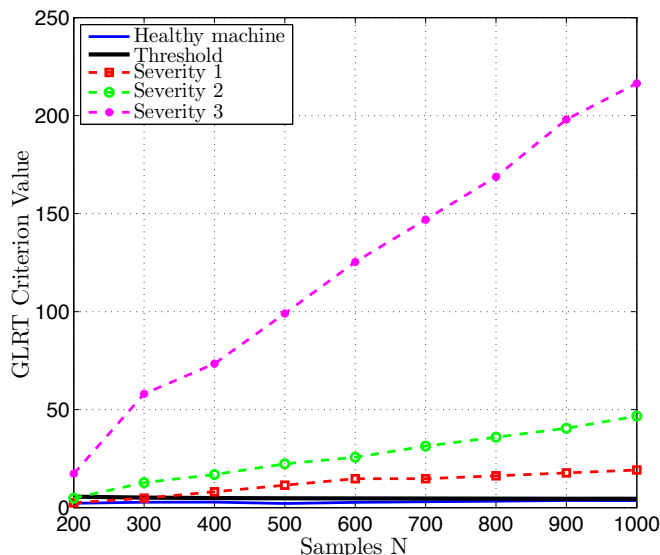


Figure 4.27: GLRT criterion with different N for a healthy machine and faulty induction machine with different considered severities of broken rotor bars ($P_{Fa} = 10^{-3}$).

greater than 400 samples. It can be concluded that the GLRT can detect broken rotor bars and its value can measure the fault severity.

4.5 Conclusion

This chapter has presented the experimental results for induction machine condition monitoring and fault detection. Two main faults have been investigated: broken rotor bars and bearing faults. The studied signal processing techniques to analyze these faults were: spectral estimation approaches, demodulation approaches, two fault severity criteria, and GLRT. The first severity criterion is based on the estimation of IA and IF. The second one is based on the evaluation of estimated amplitudes.

Based on the obtained results, it can be concluded that stator currents are not exactly sinusoidal due to the presence of space harmonics and faults. In fact, additional spectral components caused by these faults appear in the stator current spectra for faulty induction machines in the neighborhood of the fundamental frequency. Furthermore, other frequencies can appear in stator current spectra due to manufacturing imperfections such as the natural level of eccentricities. Compared to parametric-based techniques, periodogram and its extension do not allow to clearly distinguish frequencies. This

4. EXPERIMENTAL VALIDATION

poor frequency resolution is due to the fact that the main lobe increases as N decreases. Consequently, subspace techniques are efficient techniques to estimate PSD.

The IA and IF has been estimated using two main types of demodulation approaches: monodimensional and multidimensional approaches. Some conclusions can be deduced based on the achieved experimental results:

- When bearing faults are present, a frequency modulation can be observed in stator currents using demodulation approaches.
- When broken rotor bars appear, two modulations are present: amplitude and frequency modulations can be located in stator currents using demodulation approaches.
- For monodimensional demodulation techniques, it can be shown that: the HT suffers from border effects, the TEO is sensitive to noise, the SD is easy to implement but it requires a filtering stage tuning which is quite difficult.
- For multidimensional demodulation techniques, it can be shown that: the CT is valid only for balanced three-phase systems, the PCA performance depends on the covariance matrix estimation and its eigendecomposition, and the ML seems the suitable solution to analyze modulations of three-phase stator currents.

The major advantage of the proposed fault severity criteria is their abilities to measure and indicate the fault severity degree. Values of these criteria increase when the fault severity degree increase. For the second fault severity criterion, this increase is due to the fact that amplitudes of fault frequency components increase when severity increases.

Experimental results also show that the proposed GLRT detector is able to efficiently detect faults even for low signal acquisition duration and can track the fault severity. It seems that the proposed approaches can be easily implemented at a reasonable computational cost in real-world industry applications.

Conclusions and Recommendations for Future Research

Literature review of existing techniques of induction machines condition monitoring and faults detection was presented in the first chapter. This chapter has presented the advantages and the limitations of each described techniques. It has been concluded that the parametric techniques using the stator current are promising ones to analyze and detect faults under stationary conditions. Parametric estimation techniques were proposed in the second chapter to estimate stator current parameters. For frequency estimation, we have presented three main categories of subspace techniques: MUSIC, ESPRIT, and Modified-ESPRIT estimators. For model order selection, we have described two main types: estimator based on the covariance matrix estimation and estimator based the maximum likelihood estimate. A condition monitoring scheme has also been proposed to simplify the implementation of the criterion that allows to analyzing the fault severity in induction machines. Faults detector based on the GLRT was suggested in the third chapter. The proposed parametric techniques were successfully investigated in the fourth chapter. The achieved experimental results have demonstrated the effectiveness and the detection ability of the proposed techniques.

Some further works should study the stator current faulty model under non-stationary conditions. Stator current modeling under combined faults under stationary and non-stationary conditions is also needed. Some other recommendations can be proposed for continuing investigation in estimation and detection research fields for induction machine faults detection such as investigation of the proposed parametric techniques under different load conditions. It is important to investigate these techniques in non-stationary conditions. More experiments need to be carried out to further evaluate performances of the proposed methods in closed-loop control schemes for stationary conditions and non-stationary environments.

5. CONCLUSIONS AND RECOMMENDATIONS FOR FUTURE RESEARCH



References

- [1] <http://aboutelectrical.org/induction> Accessed: September 2016. ix, 8
- [2] G. Singh and S. A. S. Al Kazzaz, “Induction machine drive condition monitoring and diagnostic research—a survey,” *Electric Power Systems Research*, vol. 64, no. 2, pp. 145–158, August 2003. ix, 8, 9
- [3] R. Ahmad and S. Kamaruddin, “An overview of time-based and condition-based maintenance in industrial application,” *Computers & Industrial Engineering*, vol. 63, no. 1, pp. 135–149, February 2012. ix, 12, 13, 14, 15
- [4] T. Marwala, *Condition monitoring using computational intelligence methods: applications in mechanical and electrical systems*. Springer Science & Business Media, 2012. ix, 16
- [5] E. Elbouchikhi, V. Choqueuse, and M. Benbouzid, “Condition monitoring of induction motors based on stator currents demodulation,” *INTERNATIONAL REVIEW OF ELECTRICAL ENGINEERING-IREE*, vol. 10, no. 6, pp. 704–715, 2015. ix, 33, 34, 36, 114, 117
- [6] D. Vakman, “On the analytic signal, the teager-kaiser energy algorithm, and other methods for defining amplitude and frequency,” *IEEE Transactions on Signal Processing*, vol. 44, no. 4, pp. 791–797, 1996. ix, 35
- [7] I. Mohamed Shaluf and F.-R. Ahamadun, “Technological emergencies expert system (tees),” *Disaster Prevention and Management: An International Journal*, vol. 15, no. 3, pp. 414–424, 2006. ix, 41
- [8] P. Tavner, L. Ran, J. Penman, and H. Sedding, *Condition monitoring of rotating electrical machines*. IET, 2008, vol. 56. ix, 16, 19, 20, 30, 41, 43, 44

REFERENCES

- [9] S. Caldara, S. Nuccio, G. R. Galluzzo, and M. Trapanese, “A fuzzy diagnostic system: application to linear induction motor drives,” in *Instrumentation and Measurement Technology Conference, 1997. IMTC/97. Proceedings. Sensing, Processing, Networking., IEEE*, vol. 1. IEEE, 1997, pp. 257–262. ix, 42, 43
- [10] M. Świercz, “Signal processing methods for fault diagnostics in engineering systems,” in *Signal Processing Symposium (SPSymposium), 2015.* IEEE, 2015, pp. 1–6. 1
- [11] M. E. H. Benbouzid, “A review of induction motors signature analysis as a medium for faults detection,” *IEEE Transactions on Industrial Electronics*, vol. 47, no. 5, pp. 984–993, October 2000. 1, 16
- [12] S. Nandi, H. A. Toliyat, and X. Li, “Condition monitoring and fault diagnosis of electrical motors—a review,” *IEEE Transactions on Energy Conversion*, vol. 20, no. 4, pp. 719–729, December 2005. 9, 10
- [13] A. Siddique, G. Yadava, and B. Singh, “A review of stator fault monitoring techniques of induction motors,” *IEEE transactions on energy conversion*, vol. 20, no. 1, pp. 106–114, March 2005. 8, 16, 40
- [14] H. A. Toliyat, S. Nandi, S. Choi, and H. Meshgin-Kelk, *Electric Machines: Modeling, Condition Monitoring, and Fault Diagnosis.* CRC Press, October 2012. 1, 8
- [15] S. Karmakar, S. Chattopadhyay, M. Mitra, and S. Sengupta, *Induction Motor Fault Diagnosis: Approach through Current Signature Analysis.* Springer, 2016. 8, 10, 18
- [16] A. Gandhi, T. Corrigan, and L. Parsa, “Recent advances in modeling and online detection of stator interturn faults in electrical motors,” *IEEE Transactions on Industrial Electronics*, vol. 58, no. 5, pp. 1564–1575, 2011. 8
- [17] P. Zhang, Y. Du, T. G. Habetler, and B. Lu, “A survey of condition monitoring and protection methods for medium-voltage induction motors,” *IEEE Transactions on Industry Applications*, vol. 47, no. 1, pp. 34–46, January/ February 2011. 9, 16

-
- [18] S. Bindu and V. V. Thomas, “Diagnoses of internal faults of three phase squirrel cage induction motor — a review,” in *2014 International Conference on Advances in Energy Conversion Technologies (ICAECT)*. IEEE, January 2014, pp. 48–54. 9
- [19] G. Didier, E. Ternisien, O. Caspary, and H. Razik, “A new approach to detect broken rotor bars in induction machines by current spectrum analysis,” *Mechanical Systems and Signal Processing*, vol. 21, no. 2, pp. 1127–1142, 2007. 9
- [20] M. Blödt, P. Granjon, B. Raison, and G. Rostaing, “Models for bearing damage detection in induction motors using stator current monitoring,” *IEEE Transactions on Industrial Electronics*, vol. 55, no. 4, pp. 1813–1822, April 2008. 9, 10, 24, 38
- [21] J. Ilonen, J.-K. Kamarainen, T. Lindh, J. Ahola, H. Kalviainen, and J. Partanen, “Diagnosis tool for motor condition monitoring,” *IEEE Transactions on Industry Applications*, vol. 41, no. 4, pp. 963–971, July/August 2005. 10
- [22] D. Morinigo-Sotelo, L. A. García-Escudero, O. Duque-Perez, and M. Perez-Alonso, “Practical aspects of mixed-eccentricity detection in pwm voltage-source-inverter-fed induction motors,” *IEEE Transactions on Industrial Electronics*, vol. 57, no. 1, pp. 252–262, January 2010. 11
- [23] J. CusidóCusido, L. Romeral, J. A. Ortega, J. A. Rosero, and A. G. Espinosa, “Fault detection in induction machines using power spectral density in wavelet decomposition,” *IEEE Transactions on Industrial Electronics*, vol. 55, no. 2, pp. 633–643, 2008. 11
- [24] X. Gong, “Online nonintrusive condition monitoring and fault detection for wind turbines,” Ph.D. dissertation, University of Nebraska-Lincoln, December 2012. 11, 17, 18, 20
- [25] M. Rausand and A. Høyland, *System reliability theory: models, statistical methods, and applications*. John Wiley & Sons, 2004, vol. 396. 12
- [26] J. Ribrant, “Reliability performance and maintenance—a survey of failures in wind power systems,” Ph.D. dissertation, 2006. 12, 15

REFERENCES

- [27] P. J. Tavner and J. Penman, *Condition monitoring of electrical machines*. Research Studies Pre, 1987, vol. 1. 16
- [28] Y. D. Nyanteh, “Application of artificial intelligence to rotating machine condition monitoring,” 2013. 16
- [29] M. E. H. Benbouzid and G. B. Kliman, “What stator current processing-based technique to use for induction motor rotor faults diagnosis?” *IEEE Transactions on Energy Conversion*, vol. 18, no. 2, pp. 238–244, June 2003. 16
- [30] M. R. Mehrjou, N. Mariun, M. H. Marhaban, and N. Misron, “Rotor fault condition monitoring techniques for squirrel-cage induction machine—a review,” *Mechanical Systems and Signal Processing*, vol. 25, no. 8, pp. 2827–2848, 2011. 18, 19, 21
- [31] F. Filippetti, A. Bellini, and G.-A. Capolino, “Condition monitoring and diagnosis of rotor faults in induction machines: State of art and future perspectives,” in *2013 IEEE Workshop on Electrical Machines Design, Control and Diagnosis (WEMDCD)*, 2013.
- [32] S. Mortazavizadeh and S. Mousavi, “A review on condition monitoring and diagnostic techniques of rotating electrical machines,” *Physical Science International Journal*, vol. 4, no. 3, p. 310, 2014. 16
- [33] L. A. Toms and A. M. Toms, *Machinery Oil Analysis: Methods, Automation & benefits; a Guide for Maintenance Managers, Supervisors & Technicians*. STLE, Society of Tribologists and Lubrication Engineers, 2008. 17
- [34] S. Ebersbach, Z. Peng, and N. Kessissoglou, “The investigation of the condition and faults of a spur gearbox using vibration and wear debris analysis techniques,” *Wear*, vol. 260, no. 1, pp. 16–24, January 2006. 17
- [35] G. E. Newell, “Oil analysis cost-effective machine condition monitoring technique,” *Industrial Lubrication and Tribology*, vol. 51, no. 3, pp. 119–124, 1999. 17

-
- [36] Z. Peng and N. Kessissoglou, “An integrated approach to fault diagnosis of machinery using wear debris and vibration analysis,” *Wear*, vol. 255, no. 7, pp. 1221–1232, 2003. 17
- [37] T. Lindh *et al.*, “On the condition monitoring of induction machines,” Ph.D. dissertation, Lappeenranta University of Technology, December 2003. 17
- [38] W. R. Finley, M. M. Hodowanec, and W. G. Holter, “An analytical approach to solving motor vibration problems,” *IEEE Transactions on industry applications*, vol. 36, no. 5, pp. 1467–1480, September/October 2000. 17
- [39] W. R. Finley, M. Howdowanec, and W. G. Holter, “Diagnosing motor vibration problems,” in *Pulp and Paper Industry Technical Conference, 2000. Conference Record of 2000 Annual*. IEEE, 2000, pp. 165–180.
- [40] A. D. Nembhard, J. K. Sinha, A. J. Pinkerton, and K. Elbhah, “Combined vibration and thermal analysis for the condition monitoring of rotating machinery,” *Structural Health Monitoring*, vol. 13, no. 3, pp. 281–295, 2014. 17, 36
- [41] M. Janda, O. Vitek, and V. Hajek, *Induction Motors - Modelling and Control, Chapter 8 : Noise of Induction Machines*. INTECH Open Access Publisher, November 2012. 18
- [42] M. K. Nguyen, “Predicting electromagnetic noise in induction motors,” 2014. 18
- [43] P. Vijayraghavan and R. Krishnan, “Noise in electric machines: A review,” in *Industry Applications Conference, 1998. Thirty-Third IAS Annual Meeting. The 1998 IEEE*, vol. 1. IEEE, 1998, pp. 251–258. 18
- [44] A. Ellison and S. Yang, “Effects of rotor eccentricity on acoustic noise from induction machines,” in *Proceedings of the Institution of Electrical Engineers*, vol. 118, no. 1. IET, 1971, pp. 174–184. 18
- [45] A. Gaylard, A. Meyer, and C. Landy, “Acoustic evaluation of faults in electrical machines,” 1995. 18
- [46] S. Verma, “Noise and vibrations of electrical machines and drives; their production and means of reduction,” in *Power Electronics, Drives and Energy Systems*

REFERENCES

- for Industrial Growth, 1996.*, *Proceedings of the 1996 International Conference on*, vol. 2. IEEE, 1996, pp. 1031–1037. 18
- [47] W. Li and C. K. Mechefske, “Detection of induction motor faults: a comparison of stator current, vibration and acoustic methods,” *Journal of vibration and Control*, vol. 12, no. 2, pp. 165–188, 2006. 19, 21
- [48] S. Grubic, J. M. Aller, B. Lu, and T. G. Habetler, “A survey on testing and monitoring methods for stator insulation systems of low-voltage induction machines focusing on turn insulation problems,” *IEEE Transactions on Industrial Electronics*, vol. 55, no. 12, pp. 4127–4136, 2008. 19
- [49] M. Picazo-Rodenas, R. Royo, J. Antonino-Daviu, and J. Roger-Folch, “Use of infrared thermography for computation of heating curves and preliminary failure detection in induction motors,” in *International Conference on Electrical Machines (ICEM)*. IEEE, 2012, pp. 525–531. 20
- [50] P. Karvelis, G. Georgoulas, C. D. Stylios, I. P. Tsoumas, J. A. Antonino-Daviu, M. J. P. Ródenas, and V. Climente-Alarcón, “An automated thermographic image segmentation method for induction motor fault diagnosis,” in *IECON 2014-40th Annual Conference of the IEEE Industrial Electronics Society*. IEEE, 2014, pp. 3396–3402. 20
- [51] A. Garcia-Ramirez, L. Morales-Hernandez, R. Osornio-Rios, A. Garcia-Perez, and R. Romero-Troncoso, “Thermographic technique as a complement for mcsa in induction motor fault detection,” in *International Conference on Electrical Machines (ICEM)*. IEEE, 2014, pp. 1940–1945. 20
- [52] M. Blödt, “Condition monitoring of mechanical faults in variable speed induction motor drives. application of stator current time-frequency analysis and parameter estimation,” Ph.D. dissertation, 2006. 20, 23, 24
- [53] J. S. Hsu, “Monitoring of defects in induction motors through air-gap torque observation,” *IEEE Transactions on Industry Applications*, vol. 31, no. 5, pp. 1016–1021, 1995. 20, 21

-
- [54] R. Wieser, M. Schagginger, C. Kral, and F. Pirker, “The integration of machine fault detection into an indirect field oriented induction machine drive control scheme—the vienna monitoring method,” in *Industry Applications Conference, 1998. Thirty-Third IAS Annual Meeting. The 1998 IEEE*, vol. 1. IEEE, 1998, pp. 278–285. 20
- [55] R. Wieser, C. Kral, F. Pirker, and M. Schagginger, “On-line rotor cage monitoring of inverter-fed induction machines by means of an improved method,” *IEEE Transactions on Power Electronics*, vol. 14, no. 5, pp. 858–865, 1999. 20
- [56] C. Kral, F. Pirker, and G. Pascoli, “Detection of rotor faults in squirrel-cage induction machines at standstill for batch tests by means of the vienna monitoring method,” *IEEE Transactions on Industry Applications*, vol. 38, no. 3, pp. 618–624, 2002. 20
- [57] —, “Model-based detection of rotor faults without rotor position sensor—the sensorless vienna monitoring method,” *IEEE transactions on industry applications*, vol. 41, no. 3, pp. 784–789, 2005. 20
- [58] S. H. Kia, H. Henao, and G.-A. Capolino, “Torsional vibration assessment using induction machine electromagnetic torque estimation,” *IEEE Transactions on Industrial Electronics*, vol. 57, no. 1, pp. 209–219, 2010. 21
- [59] M. M. Stopa and B. de Jesus Cardoso Filho, “Load torque signature analysis: an alternative to mcsa to detect faults in motor driven loads,” in *Energy Conversion Congress and Exposition (ECCE), 2012 IEEE*. IEEE, 2012, pp. 4029–4036.
- [60] K. N. Gyftakis, D. V. Spyropoulos, J. C. Kappatou, and E. D. Mitronikas, “A novel approach for broken bar fault diagnosis in induction motors through torque monitoring,” *IEEE Transactions on Energy Conversion*, vol. 28, no. 2, pp. 267–277, June 2013. 21, 23
- [61] A. M. Da Silva, R. J. Povinelli, and N. A. Demerdash, “Rotor bar fault monitoring method based on analysis of air-gap torques of induction motors,” *IEEE Transactions on Industrial Informatics*, vol. 9, no. 4, pp. 2274–2283, November 2013. 21

REFERENCES

- [62] X. Gong and W. Qiao, "Current-based mechanical fault detection for direct-drive wind turbines via synchronous sampling and impulse detection," *IEEE Transactions on Industrial Electronics*, vol. 62, no. 3, pp. 1693–1702, March 2015. 21
- [63] F. Immovilli, A. Bellini, R. Rubini, and C. Tassoni, "Diagnosis of bearing faults in induction machines by vibration or current signals: A critical comparison," *IEEE Transactions on Industry Applications*, vol. 46, no. 4, pp. 1350–1359, May 2010. 21
- [64] L. Frosini and E. Bassi, "Stator current and motor efficiency as indicators for different types of bearing faults in induction motors," *IEEE Transactions on Industrial Electronics*, vol. 57, no. 1, pp. 244–251, January 2010.
- [65] V. Choqueuse, M. E. H. Benbouzid, Y. Amirat, and S. Turri, "Diagnosis of three-phase electrical machines using multidimensional demodulation techniques," *IEEE Transactions on Industrial Electronics*, vol. 59, no. 4, pp. 2014–2023, April 2012. 21, 33, 36
- [66] L. Frosini and E. Bassi, "Stator current and motor efficiency as indicators for different types of bearing faults in induction motors," *IEEE Transactions on Industrial electronics*, vol. 57, no. 1, pp. 244–251, January 2010. 21
- [67] T. Omar, N. Lahcène, I. Rachid, and F. Maurice, "Modeling of the induction machine for the diagnosis of rotor defects. part i. an approach of magnetically coupled multiple circuits," in *Proceedings of the 2005 IEEE IECON*. Sheraton Capital Center Raleigh, NC, USA: IEEE, November 2005, pp. 8–pp. 22
- [68] J. Faiz, B. M. Ebrahimi, and M. B. B. Sharifian, "Time stepping finite element analysis of broken bars fault in a three-phase squirrel-cage induction motor," *Progress In Electromagnetics Research*, vol. 68, pp. 53–70, 2007. 22
- [69] A. Singh, B. Grant, R. DeFour, C. Sharma, and S. Bahadoorsingh, "A review of induction motor fault modeling," *Electric Power Systems Research*, vol. 133, pp. 191–197, April 2016. 22, 25
- [70] A. Tenhunen, T. P. Holopainen, and A. Arkkio, "Effects of saturation on the forces in induction motors with whirling cage rotor," *IEEE Transactions on Magnetics*, vol. 40, no. 2, pp. 766–769, 2004. 22

-
- [71] A. Tenhunen, "Calculation of eccentricity harmonics of the air-gap flux density in induction machines by impulse method," *IEEE Transactions on Magnetics*, vol. 41, no. 5, pp. 1904–1907, 2005.
- [72] N. Bianchi, *Electrical machine analysis using finite elements*. CRC press, 2005.
- [73] B. Vaseghi, N. Takorabet, and F. Meibody-Tabar, "Transient finite element analysis of induction machines with stator winding turn fault," *Progress In Electromagnetics Research*, vol. 95, pp. 1–18, 2009. 22
- [74] B. Saied and A. J. Ali, "Fault prediction of deep bar cage rotor induction motor based on fem," *Progress In Electromagnetics Research B*, vol. 53, pp. 291–314, 2013. 22, 23
- [75] S. R. H. Hoole, *Finite elements, electromagnetics and design*. Elsevier, 1995. 22, 23, 24
- [76] J. Faiz and M. Ojaghi, "Unified winding function approach for dynamic simulation of different kinds of eccentricity faults in cage induction machines," *IET electric power applications*, vol. 3, no. 5, pp. 461–470, August 2009. 23
- [77] C. Rojas, M. Melero, M. Cabanas, J. Cano, G. Orcajo, and F. Pedrayes, "Finite element model for the study of inter-turn short circuits in induction motors," in *Diagnostics for Electric Machines, Power Electronics and Drives, 2007. SDEMPED 2007. IEEE International Symposium on*. IEEE, 2007, pp. 415–419. 23
- [78] L. Abdesselam, M. Ammar, and C. Guy, "Analysis of inter-turn short circuit in slots by finite element model," in *Environment and Electrical Engineering (EEEIC), 2011 10th International Conference on*. IEEE, 2011, pp. 1–4.
- [79] W. Zaabi, Y. Bensalem, and H. Trabelsi, "Fault analysis of induction machine using finite element method (fem)," in *Sciences and Techniques of Automatic Control and Computer Engineering (STA), 2014 15th International Conference on*. IEEE, 2014, pp. 388–393. 23
- [80] A. Bentounsi and A. Nicolas, "On line diagnosis of defaults on squirrel cage motors using fem," *IEEE Transactions on magnetics*, vol. 34, no. 5, pp. 3511–3514, 1998.

REFERENCES

- [81] R. Fiser and S. Ferkolj, "Application of a finite element method to predict damaged induction motor performance," *IEEE Transactions on Magnetics*, vol. 37, no. 5, pp. 3635–3639, 2001.
- [82] J. Faiz, B. M. Ebrahimi, and M. B. B. Sharifian, "Time stepping finite element analysis of broken bars fault in a three-phase squirrel-cage induction motor," *Progress In Electromagnetics Research*, vol. 68, pp. 53–70, 2007.
- [83] X. Ying, "Characteristic performance analysis of squirrel cage induction motor with broken bars," *IEEE Transactions on Magnetics*, vol. 45, no. 2, pp. 759–766, 2009.
- [84] —, "Performance evaluation and thermal fields analysis of induction motor with broken rotor bars located at different relative positions," *IEEE Transactions on Magnetics*, vol. 46, no. 5, pp. 1243–1250, 2010.
- [85] B. M. Ebrahimi, J. Faiz, S. Lotfi-Fard, and P. Pillay, "Novel indices for broken rotor bars fault diagnosis in induction motors using wavelet transform," *Mechanical Systems and Signal Processing*, vol. 30, pp. 131–145, 2012. 23
- [86] C. Schlensok and G. Henneberger, "Comparison of static, dynamic, and static-dynamic eccentricity in induction machines with squirrel-cage rotors using 2d-transient fem," *COMPEL-The international journal for computation and mathematics in electrical and electronic engineering*, vol. 23, no. 4, pp. 1070–1079, 2004. 23
- [87] J. Faiz, B. M. Ebrahimi, B. Akin, and H. A. Toliyat, "Finite-element transient analysis of induction motors under mixed eccentricity fault," *IEEE transactions on magnetics*, vol. 44, no. 1, pp. 66–74, 2008.
- [88] M.-J. Kim, B.-K. Kim, J.-W. Moon, Y.-H. Cho, D.-H. Hwang, and D.-S. Kang, "Analysis of inverter-fed squirrel-cage induction motor during eccentric rotor motion using fem," *IEEE Transactions on Magnetics*, vol. 44, no. 6, pp. 1538–1541, 2008.
- [89] P. V. Jover Rodríguez, A. Belahcen, A. Arkkio, A. Laiho, and J. A. Antonino-Daviu, "Air-gap force distribution and vibration pattern of induction motors

- under dynamic eccentricity,” *Electrical Engineering (Archiv fur Elektrotechnik)*, vol. 90, no. 3, pp. 209–218, 2008.
- [90] J. Martinez, A. Belahcen, J. Detoni, and A. Arkkio, “A 2d fem analysis of electromechanical signatures in induction motors under dynamic eccentricity,” *International Journal of Numerical Modelling: Electronic Networks, Devices and Fields*, vol. 27, no. 3, pp. 555–571, 2014. 23
- [91] J. Faiz, B. M. Ebrahimi, H. Toliyat, and W. Abu-Elhaija, “Mixed-fault diagnosis in induction motors considering varying load and broken bars location,” *Energy Conversion and Management*, vol. 51, no. 7, pp. 1432–1441, 2010. 23
- [92] N. R. Tavana and V. Dinavahi, “Real-time nonlinear magnetic equivalent circuit model of induction machine on fpga for hardware-in-the-loop simulation,” *IEEE Transactions on Energy Conversion*, vol. 31, no. 2, pp. 520–530, 2016. 23
- [93] K. Hameyer and R. Belmans, “Numerical modelling and design of electrical machines and drives,” 1998. 23
- [94] J. Faiz, M. Ghasemi-Bijan, and B. Ebrahimi, “An improved magnetic equivalent circuit method for evaluation of different inductances of a squirrel-cage induction motor in healthy and faulty conditions,” *Electromagnetics*, vol. 34, no. 5, pp. 363–379, 2014. 23
- [95] G. Y. Sizov, C.-C. Yeh, and N. A. Demerdash, “Magnetic equivalent circuit modeling of induction machines under stator and rotor fault conditions,” in *Electric Machines and Drives Conference, 2009. IEMDC’09. IEEE International*. IEEE, 2009, pp. 119–124. 23
- [96] R. Roshanfekar and A. Jalilian, “Analysis of rotor and stator winding inter-turn faults in wim using simulated mec model and experimental results,” *Electric Power Systems Research*, vol. 119, pp. 418–424, 2015. 23
- [97] A. Mahyob, M. O. Elmoctar, P. Reghem, and G. Barakat, “Induction machine modelling using permeance network method for dynamic simulation of air-gap eccentricity,” in *Power Electronics and Applications, 2007 European Conference on*. IEEE, 2007, pp. 1–9. 23

REFERENCES

- [98] B. Heller and V. Hamata, *Harmonic field effects in induction machines*. Elsevier Science & Technology, 1977. 23
- [99] S. Yang, *Low-noise electrical motors*. Oxford University Press, USA, 1981, vol. 13.
- [100] L. T.-P. Timár-P and P. Tímár, *Noise and vibration of electrical machines*. North Holland, 1989, vol. 34. 23
- [101] M. Blödt, M. Chabert, J. Regnier, and J. Faucher, “Mechanical load fault detection in induction motors by stator current time-frequency analysis,” *IEEE Transactions on Industry Applications*, vol. 42, no. 6, pp. 1454–1463, November/December 2006. 24
- [102] M. Blödt, J. Regnier, and J. Faucher, “Distinguishing load torque oscillations and eccentricity faults in induction motors using stator current wigner distributions,” *IEEE Transactions on Industry Applications*, vol. 45, no. 6, pp. 1991–2000, 2009. 24, 38
- [103] M. Ojaghi and J. Faiz, “Extension to multiple coupled circuit modeling of induction machines to include variable degrees of saturation effects,” *IEEE Transactions on Magnetics*, vol. 44, no. 11, pp. 4053–4056, 2008. 24
- [104] X. Luo, Y. Liao, H. A. Toliyat, A. El-Antably, and T. A. Lipo, “Multiple coupled circuit modeling of induction machines,” *IEEE Transactions on Industry Applications*, vol. 31, no. 2, pp. 311–318, 1995. 25
- [105] H. A. Toliyat and T. A. Lipo, “Transient analysis of cage induction machines under stator, rotor bar and end ring faults,” *IEEE Transactions on Energy Conversion*, vol. 10, no. 2, pp. 241–247, 1995. 25
- [106] J. Milimonfared, H. M. Kelk, A. Der Minassians, S. Nandi, and H. Toliyat, “A novel approach for broken rotor bar detection in cage induction motors,” in *Industry Applications Conference*, vol. 1. IEEE, 1998, pp. 286–290.
- [107] J. Milimonfared, H. M. Kelk, S. Nandi, A. Minassians, and H. A. Toliyat, “A novel approach for broken-rotor-bar detection in cage induction motors,” *IEEE Transactions on Industry Applications*, vol. 35, no. 5, pp. 1000–1006, 1999.

-
- [108] B. Liang, B. S. Payne, A. D. Ball, and S. D. Iwnicki, "Simulation and fault detection of three-phase induction motors," *Mathematics and computers in simulation*, vol. 61, no. 1, pp. 1–15, 2002. 25
- [109] T. Omar, N. Lahcène, I. Rachid, and F. Maurice, "Modeling of the induction machine for the diagnosis of rotor defects. part i. an approach of magnetically coupled multiple circuits," in *Proceedings of the 2005 IEEE IECON*. IEEE, 2005, pp. 8–pp.
- [110] —, "Modeling of the induction machine for the diagnosis of rotor defects. part. ii. simulation and experimental results," in *Proceedings of the 2005 IEEE IECON*. IEEE, 2005, pp. 8–pp.
- [111] J.-H. Jung and B.-H. Kwon, "Corrosion model of a rotor-bar-under-fault progress in induction motors," *IEEE Transactions on Industrial Electronics*, vol. 53, no. 6, pp. 1829–1841, December 2006.
- [112] G. Houdouin, G. Barakat, B. Dakyo, and E. Destobbeleer, "A winding function theory based global method for the simulation of faulty induction machines," in *IEEE International Electric Machines and Drives Conference (IEMDC)*, vol. 1. IEEE, 2003, pp. 297–303.
- [113] F. Pedrayes, C. Rojas, M. Cabanas, M. Melero, G. Orcajo, and J. Cano, "Application of a dynamic model based on a network of magnetically coupled reluctances to rotor fault diagnosis in induction motors," in *Diagnostics for Electric Machines, Power Electronics and Drives, 2007. SDEMPED 2007. IEEE International Symposium on*. IEEE, 2007, pp. 241–246.
- [114] S. Chen, "Induction machine broken rotor bar diagnostics using prony analysis," Ph.D. dissertation, University of Adelaide, 2008. 31
- [115] S. Chen and R. Živanović, "Modelling and simulation of stator and rotor fault conditions in induction machines for testing fault diagnostic techniques," *European Transactions on Electrical Power*, vol. 20, no. 5, pp. 611–629, 2010. 25
- [116] G. Bossio, C. De Angelo, C. Pezzani, J. Bossio, and G. Garcia, "Evaluation of harmonic current sidebands for broken bar diagnosis in induction motors,"

REFERENCES

- in *IEEE International Symposium on Diagnostics for Electric Machines, Power Electronics and Drives (SDEMPED)*. IEEE, 2009, pp. 1–6.
- [117] M. S. R. Krishna and K. S. Ravi, “Fault diagnosis of induction motor using motor current signature analysis,” in *Circuits, Power and Computing Technologies (ICCPCT), 2013 International Conference on*. IEEE, 2013, pp. 180–186. 25
- [118] G. M. Joksimovic and J. Penman, “The detection of inter-turn short circuits in the stator windings of operating motors,” *IEEE Transactions on Industrial Electronics*, vol. 47, no. 5, pp. 1078–1084, 2000.
- [119] V. Devanneaux, B. Dagues, J. Faucher, and G. Barakat, “An accurate model of squirrel cage induction machines under stator faults,” *Mathematics and computers in simulation*, vol. 63, no. 3, pp. 377–391, 2003.
- [120] M. Arkan, D. Kostic-Perovic, and P. Unsworth, “Modelling and simulation of induction motors with inter-turn faults for diagnostics,” *Electric Power Systems Research*, vol. 75, no. 1, pp. 57–66, 2005.
- [121] M. Sahraoui, A. Ghoggal, S. E. Zouzou, A. Aboubou, and H. Razik, “Modelling and detection of inter-turn short circuits in stator windings of induction motor,” in *IECON 2006-32nd Annual Conference on IEEE Industrial Electronics*. IEEE, 2006, pp. 4981–4986.
- [122] M. Bouzid and G. Champenois, “An efficient, simplified multiple-coupled circuit model of the induction motor aimed to simulate different types of stator faults,” *Mathematics and computers in simulation*, vol. 90, pp. 98–115, 2013. 25
- [123] H. A. Toliyat, M. S. Arefeen, and A. G. Parlos, “A method for dynamic simulation of air-gap eccentricity in induction machines,” *IEEE Transactions on Industry Applications*, vol. 32, no. 4, pp. 910–918, 1996. 25
- [124] G. M. Joksimovic, M. D. Durovic, J. Penman, and N. Arthur, “Dynamic simulation of dynamic eccentricity in induction machines-winding function approach,” *IEEE Transactions on Energy Conversion*, vol. 15, no. 2, pp. 143–148, 2000.

-
- [125] C. Mishra, A. Routray, and S. Mukhopadhyay, "Experimental validation of coupled circuit model and simulation of eccentric squirrel cage induction motor," in *Industrial Technology, 2006. ICIT 2006. IEEE International Conference on*. IEEE, 2006, pp. 2348–2353.
- [126] J. Faiz and M. Ojaghi, "Unified winding function approach for dynamic simulation of different kinds of eccentricity faults in cage induction machines," *IET electric power applications*, vol. 3, no. 5, pp. 461–470, 2009. 25
- [127] A. Purvee and G. Banerjee, "Dynamic simulation and experimental results of bearing faults of squirrel cage induction motor," in *Condition Monitoring and Diagnosis (CMD), 2012 International Conference on*. IEEE, 2012, pp. 718–722. 25
- [128] R. Lee, P. Pillay, and R. Harley, "D, q reference frames for the simulation of induction motors," *Electric power systems research*, vol. 8, no. 1, pp. 15–26, 1984. 25
- [129] P. Pillay and V. Levin, "Mathematical models for induction machines," in *Industry Applications Conference, 1995. Thirtieth IAS Annual Meeting, IAS'95., Conference Record of the 1995 IEEE*, vol. 1. IEEE, 1995, pp. 606–616. 25
- [130] A. R. Munoz and T. A. Lipo, "Complex vector model of the squirrel-cage induction machine including instantaneous rotor bar currents," *IEEE Transactions on industry applications*, vol. 35, no. 6, pp. 1332–1340, 1999. 25
- [131] S. Hamdani, O. Touhami, and R. Ibtouen, "Generalized two axes model of a squirrel-cage induction motor for rotor fault diagnosis," *Serbian journal of electrical engineering*, vol. 5, no. 1, pp. 155–170, 2008. 25
- [132] C. Cunha, F. B. R. Soares, P. Oliveira *et al.*, "A new method to simulate induction machines with rotor asymmetries," in *IECON 02 [Industrial Electronics Society, IEEE 2002 28th Annual Conference of the]*, vol. 1. IEEE, 2002, pp. 72–76.
- [133] L. M. R. Baccarini, B. R. de Menezes, and W. M. Caminhas, "Fault induction dynamic model, suitable for computer simulation: Simulation results and experimental validation," *Mechanical Systems and Signal Processing*, vol. 24, no. 1, pp. 300–311, 2010. 25

REFERENCES

- [134] C. M. Cunha, R. O. Lyra *et al.*, “Simulation and analysis of induction machines with rotor asymmetries,” *IEEE Transactions on Industry Applications*, vol. 41, no. 1, pp. 18–24, 2005. 25
- [135] M. Jannati, N. Idris, and Z. Salam, “A new method for modeling and vector control of unbalanced induction motors,” in *2012 IEEE Energy Conversion Congress and Exposition (ECCE)*. IEEE, 2012, pp. 3625–3632. 25
- [136] Y. Trachi, E. Elbouchikhi, V. Choqueuse, and M. E. H. Benbouzid, “Stator current analysis by subspace methods for fault detection in induction machines,” in *Proceedings of the 2015 IEEE IECON*, Yokohama, Japon, November 2012, pp. 1–6. 26, 31, 33, 55
- [137] M. E. H. Benbouzid, M. Vieira, and C. Theys, “Induction motors’ faults detection and localization using stator current advanced signal processing techniques,” *IEEE Transactions on Power Electronics*, vol. 14, no. 1, pp. 14–22, January 1999. 32
- [138] Y.-H. Kim, Y.-W. Youn, D.-H. Hwang, J.-H. Sun, and D.-S. Kang, “High-resolution parameter estimation method to identify broken rotor bar faults in induction motors,” *IEEE Transactions on Industrial Electronics*, vol. 60, no. 9, pp. 4103–4117, September 2013. 32, 33, 47
- [139] F. Cupertino, E. De Vanna, L. Salvatore, and S. Stasi, “Analysis techniques for detection of im broken rotor bars after supply disconnection,” *IEEE Transactions on Industry Applications*, vol. 40, no. 2, pp. 526–533, March/April 2004.
- [140] M. Sahraoui, A. J. M. Cardoso, and A. Ghoggal, “The use of a modified prony method to track the broken rotor bar characteristic frequencies and amplitudes in three-phase induction motors,” *IEEE Transactions on Industry Applications*, vol. 51, no. 3, pp. 2136–2147, May/June 2015.
- [141] E. Elbouchikhi, V. Choqueuse, M. E. H. Benbouzid, and J.-F. Charpentier, “Induction machine fault detection enhancement using a stator current high resolution spectrum,” in *Proceedings of the 2012 IEEE IECON*, Montreal, Canada, October 2012, pp. 3913–3918. 32, 70

-
- [142] B. Xu, L. Sun, L. Xu, and G. Xu, "Improvement of the Hilbert method via ESPRIT for detecting rotor fault in induction motors at low slip," *IEEE Transactions on Energy Conversion*, vol. 28, no. 1, pp. 225–233, March 2013. 39
- [143] —, "An ESPRIT-SAA-based detection method for broken rotor bar fault in induction motors," *IEEE Transactions on Energy Conversion*, vol. 27, no. 3, pp. 654–660, September 2012. 39
- [144] A. Garcia-Perez, R. de Jesus Romero-Troncoso, E. Cabal-Yepez, and R. A. Osornio-Rios, "The application of high-resolution spectral analysis for identifying multiple combined faults in induction motors," *IEEE Transactions on Industrial Electronics*, vol. 58, no. 5, pp. 2002–2010, May 2011. 31, 32, 55
- [145] E. Elbouchikhi, V. Choqueuse, and M. E. H. Benbouzid, "A parametric spectral estimator for faults detection in induction machines," in *Proceedings of the 2013 IEEE IECON*, Montreal, Canada, November 2013, pp. 7358–7363. 31, 54
- [146] —, "Induction machine faults detection using stator current parametric spectral estimation," *Mechanical Systems and Signal Processing*, vol. 52, pp. 447–464, June 2014. 31, 54
- [147] V. Choqueuse, A. Belouchrani, M. E. H. Benbouzid *et al.*, "Estimation of amplitude, phase and unbalance parameters in three-phase systems: analytical solutions, efficient implementation and performance analysis," *IEEE Transactions on Signal Processing*, vol. 62, no. 16, pp. 4064–4076, 2014. 31
- [148] E. Elbouchikhi, V. Choqueuse, and M. Benbouzid, "Induction machine bearing faults detection based on a multi-dimensional music algorithm and maximum likelihood estimation," *ISA transactions*, 2016. 31
- [149] J. Cusido, L. Romeral, J. Ortega, J. Rosero, A. G. Espinosa *et al.*, "Fault detection in induction machines using power spectral density in wavelet decomposition," *IEEE Transactions on Industrial Electronics*, vol. 55, no. 2, pp. 633–643, February 2008. 26
- [150] B. Ayhan, H. J. Trussell, M.-Y. Chow, and M.-H. Song, "On the use of a lower sampling rate for broken rotor bar detection with dtft and ar-based spectrum

REFERENCES

- methods,” *IEEE Transactions on Industrial Electronics*, vol. 55, no. 3, pp. 1421–1434, March 2008.
- [151] E. Elbouchikhi, V. Choqueuse, M. E. H. Benbouzid, and J. F. Charpentier, “Induction machine bearing failures detection using stator current frequency spectral subtraction,” in *2012 IEEE International Symposium on Industrial Electronics (ISIE)*. IEEE, 2012, pp. 1228–1233.
- [152] E. Elbouchikhi, V. Choqueuse, and M. E. H. Benbouzid, “On parametric spectral estimation for induction machine faults detection in stationary and non-stationary environments,” Ph.D. dissertation, University of Brest, November 2013. 37
- [153] E. Elbouchikhi, V. Choqueuse, Y. Trachi, and M. Benbouzid, “Induction machine bearing faults detection based on hilbert-huang transform,” in *Proceedings of the 2015 IEEE ISIE*, Rio de Janeiro, Brazil, June 2015, pp. 843–848. 26, 39
- [154] M. K. Steven *et al.*, *Modern spectral estimation: theory and application*. Signal Processing Series, 1988. 26, 30
- [155] S. M. Kay and S. L. Marple, “Spectrum analysis—a modern perspective,” *Proceedings of the IEEE*, vol. 69, no. 11, pp. 1380–1419, 1981. 26, 27
- [156] P. Stoica and R. L. Moses, *Introduction to spectral analysis*. Prentice hall Upper Saddle River, 1997, vol. 1. 29, 30
- [157] J. G. Proakis and D. G. Manolakis, *Digital signal processing: principles, algorithms and applications*. Prentice-Hall, Inc, 1996, vol. 11. 29
- [158] P. Stoica and R. L. Moses, *Spectral Analysis of Signals*. Pearson/Prentice Hall Upper Saddle River, NJ, March 2005. 30, 53, 54, 57
- [159] G. Gelle, M. Colas, and G. Delaunay, “Higher order statistics for detection and classification of faulty fanbelts using acoustical analysis,” in *Higher-Order Statistics, 1997., Proceedings of the IEEE Signal Processing Workshop on*. IEEE, 1997, pp. 43–46. 30
- [160] I. Howard, “Higher-order spectral techniques for machine vibration condition monitoring,” *Proceedings of the Institution of Mechanical Engineers, Part G: Journal of Aerospace Engineering*, vol. 211, no. 4, pp. 211–219, 1997.

-
- [161] N. Arthur and J. Penman, "Inverter fed induction machine condition monitoring using the bispectrum," in *Higher-Order Statistics, 1997., Proceedings of the IEEE Signal Processing Workshop on.* IEEE, 1997, pp. 67–71.
- [162] N. Arthur, J. Penman, A. McLean, and A. Parsons, "Induction machine condition monitoring with higher order spectra. i. fundamentals and fixed frequency operation," in *Industrial Electronics Society, 1998. IECON'98. Proceedings of the 24th Annual Conference of the IEEE*, vol. 3. IEEE, 1998, pp. 1889–1894.
- [163] N. Arthur and J. Penman, "Condition monitoring with non-linear signal processing," in *Non-Linear Signal and Image Processing (Ref. No. 1998/284), IEE Colloquium on.* IET, 1998, pp. 4–1.
- [164] —, "Induction machine condition monitoring with higher order spectra," *IEEE Transactions on Industrial Electronics*, vol. 47, no. 5, pp. 1031–1041, 2000. 30
- [165] —, "Induction machine condition monitoring with higher order spectra," *IEEE Transactions on Industrial Electronics*, vol. 47, no. 5, pp. 1031–1041, 2000.
- [166] A. Naid, F. S. Gu, Y. M. Shao, S. Al-Arbi, and A. Ball, "Bispectrum analysis of motor current signals for fault diagnosis of reciprocating compressors," in *Key Engineering Materials*, vol. 413. Trans Tech Publ, 2009, pp. 505–511.
- [167] F. Gu, Y. Shao, N. Hu, B. Fazenda, and A. Ball, "Motor current signal analysis using a modified bispectrum for machine fault diagnosis," in *ICCAS-SICE, 2009.* IEEE, 2009, pp. 4890–4895.
- [168] J. Tretrong, J. K. Sinha, F. Gu, and A. Ball, "Bispectrum of stator phase current for fault detection of induction motor," *ISA transactions*, vol. 48, no. 3, pp. 378–382, April 2009.
- [169] L. Saidi, H. Henao, F. Fnaiech, G.-A. Capolino, and G. Cirrincione, "Application of higher order spectral analysis for rotor broken bar detection in induction machines," in *Diagnostics for Electric Machines, Power Electronics & Drives (SDEMPED), 2011 IEEE International Symposium on.* IEEE, 2011, pp. 31–38.

REFERENCES

- [170] F. Gu, Y. Shao, N. Hu, A. Naid, and A. Ball, “Electrical motor current signal analysis using a modified bispectrum for fault diagnosis of downstream mechanical equipment,” *Mechanical Systems and Signal Processing*, vol. 25, no. 1, pp. 360–372, 2011.
- [171] L. Saidi, F. Fnaiech, H. Henao, G. Capolino, and G. Cirrincione, “Diagnosis of broken-bars fault in induction machines using higher order spectral analysis,” *ISA transactions*, vol. 52, no. 1, pp. 140–148, 2013.
- [172] J. K. Sinha and K. Elbhah, “A future possibility of vibration based condition monitoring of rotating machines,” *Mechanical Systems and Signal Processing*, vol. 34, no. 1, pp. 231–240, 2013.
- [173] K. Elbhah and J. K. Sinha, “Vibration-based condition monitoring of rotating machines using a machine composite spectrum,” *Journal of Sound and Vibration*, vol. 332, no. 11, pp. 2831–2845, 2013.
- [174] L. Saidi, J. B. Ali, and F. Fnaiech, “Bi-spectrum based-emd applied to the non-stationary vibration signals for bearing faults diagnosis,” *ISA transactions*, vol. 53, no. 5, pp. 1650–1660, 2014. 36
- [175] A. Alwodai, “Motor fault diagnosis using higher order statistical analysis of motor power supply parameters,” Ph.D. dissertation, University of Huddersfield, 2015.
- [176] Y. Wang, J. Xiang, R. Markert, and M. Liang, “Spectral kurtosis for fault detection, diagnosis and prognostics of rotating machines: A review with applications,” *Mechanical Systems and Signal Processing*, vol. 66, pp. 679–698, 2016. 30
- [177] C. L. Nikias and J. M. Mendel, “Signal processing with higher-order spectra,” *IEEE signal processing magazine*, vol. 10, no. 3, pp. 10–37, 1993. 30
- [178] M. Sahraoui, A. J. M. Cardoso, K. Yahia, and A. Ghoggal, “The use of the modified prony’s method for rotor speed estimation in squirrel-cage induction motors,” *IEEE Transactions on Industry Applications*, vol. 52, no. 3, pp. 2194–2202, 2016. 31

-
- [179] D. Potts and M. Tasche, "Parameter estimation for exponential sums by approximate prony method," *Signal Processing*, vol. 90, no. 5, pp. 1631–1642, 2010. 31
- [180] E. Elbouchikhi, V. Choqueuse, and M. Benbouzid, "Induction machine diagnosis using stator current advanced signal processing," *International Journal on Energy Conversion*, vol. 3, no. 3, pp. 76–87, 2015. 31, 37, 55
- [181] C. W. Therrien, *Discrete random signals and statistical signal processing*. Prentice Hall PTR, 1992. 32
- [182] F. Cong, J. Chen, G. Dong, and F. Zhao, "Short-time matrix series based singular value decomposition for rolling bearing fault diagnosis," *Mechanical Systems and Signal Processing*, vol. 34, no. 1, pp. 218–230, 2013. 32
- [183] H. Jiang, J. Chen, G. Dong, T. Liu, and G. Chen, "Study on hankel matrix-based svd and its application in rolling element bearing fault diagnosis," *Mechanical Systems and Signal Processing*, vol. 52, pp. 338–359, 2015. 32
- [184] S. H. Kia, H. Henao, and G.-A. Capolino, "A high-resolution frequency estimation method for three-phase induction machine fault detection," *IEEE Transactions on Industrial Electronics*, vol. 54, no. 4, pp. 2305–2314, August 2007. 32
- [185] E. Radoi and A. Quinquis, "A new method for estimating the number of harmonic components in noise with application in high resolution radar," *EURASIP Journal on Advances in Signal Processing*, vol. 2004, no. 8, pp. 1–12, 2004. 32
- [186] M. Wax and T. Kailath, "Detection of signals by information theoretic criteria," *IEEE Transactions on Acoustics, Speech and Signal Processing*, vol. 33, no. 2, pp. 387–392, April 1985. 33, 67
- [187] M. M. Begovic, P. M. Djuric, S. Dunlap, and A. G. Phadke, "Frequency tracking in power networks in the presence of harmonics," *IEEE Transactions on Power Delivery*, vol. 8, no. 2, pp. 480–486, 1993. 33, 34
- [188] P. Maragos, J. F. Kaiser, and T. F. Quatieri, "On amplitude and frequency demodulation using energy operators," *IEEE Transactions on signal processing*, vol. 41, no. 4, pp. 1532–1550, 1993.

REFERENCES

- [189] —, “Energy separation in signal modulations with application to speech analysis,” *IEEE transactions on signal processing*, vol. 41, no. 10, pp. 3024–3051, 1993. 34
- [190] M. Akke, “Frequency estimation by demodulation of two complex signals,” *IEEE Transactions on Power Delivery*, vol. 12, no. 1, pp. 157–163, 1997. 34
- [191] I. Jaksch, “Faults diagnosis of three-phase induction motors using envelope analysis,” in *Diagnostics for Electric Machines, Power Electronics and Drives, 2003. SDEMPED 2003. 4th IEEE International Symposium on*. IEEE, 2003, pp. 289–293. 34
- [192] I. Jaksch and J. Bazant, “Demodulation methods for exact induction motor rotor fault diagnostic,” in *Diagnostics for Electric Machines, Power Electronics and Drives, 2005. SDEMPED 2005. 5th IEEE International Symposium on*. IEEE, 2005, pp. 1–5.
- [193] I. Jaksch and P. Fuchs, “Rotor cage faults detection in induction motors by motor current demodulation analysis,” in *Diagnostics for Electric Machines, Power Electronics and Drives, 2007. SDEMPED 2007. IEEE International Symposium on*. IEEE, 2007, pp. 247–252.
- [194] M. Pineda-Sanchez, M. Riera-Guasp, J. A. Antonino-Daviu, J. Roger-Folch, J. Perez-Cruz, and R. Puche-Panadero, “Instantaneous frequency of the left side-band harmonic during the start-up transient: A new method for diagnosis of broken bars,” *IEEE Transactions on Industrial Electronics*, vol. 56, no. 11, pp. 4557–4570, 2009. 34
- [195] R. Puche-Panadero, M. Pineda-Sanchez, M. Riera-Guasp, J. Roger-Folch, E. Hurtado-Perez, and J. Perez-Cruz, “Improved resolution of the mcsa method via hilbert transform, enabling the diagnosis of rotor asymmetries at very low slip,” *IEEE Transactions on Energy Conversion*, vol. 24, no. 1, pp. 52–59, 2009. 34
- [196] R. Puche-Panadero, J. Pons-Llinares, J. Roger-Folch, and M. Pineda-Sanchez, “Diagnosis of eccentricity based on the hilbert transform of the startup transient current,” in *Diagnostics for Electric Machines, Power Electronics and Drives*,

-
2009. *SDEMPED 2009. IEEE International Symposium on*. IEEE, 2009, pp. 1–6. 34
- [197] I. Jaksch and P. Fuchs, “Demodulation analysis for exact rotor faults detection under changing parameters,” in *Diagnostics for Electric Machines, Power Electronics and Drives, 2009. SDEMPED 2009. IEEE International Symposium on*. IEEE, 2009, pp. 1–7. 36
- [198] B. Trajin, M. Chabert, J. Regnier, and J. Faucher, “Hilbert versus concordia transform for three-phase machine stator current time-frequency monitoring,” *Mechanical Systems and Signal Processing*, vol. 23, no. 8, pp. 2648–2657, 2009. 34, 36, 37
- [199] E. Elbouchikhi, V. Choqueuse, M. Benbouzid, J. A. Antonino-Daviu *et al.*, “Stator current demodulation for induction machine rotor faults diagnosis,” in *2014 First International Conference on Green Energy ICGE 2014*. IEEE, 2014, pp. 176–181. 33
- [200] H. Li, L. Fu, and Y. Zhang, “Bearing faults diagnosis based on teager energy operator demodulation technique,” in *2009 International Conference on Measuring Technology and Mechatronics Automation*, vol. 1. IEEE, 2009, pp. 594–597. 34
- [201] M. Pineda-Sanchez, R. Puche-Panadero, M. Riera-Guasp, J. Perez-Cruz, J. Roger-Folch, J. Pons-Llinares, V. Climente-Alarcon, and J. A. Antonino-Daviu, “Application of the teager-kaiser energy operator to the fault diagnosis of induction motors,” *IEEE Transactions on energy conversion*, vol. 28, no. 4, pp. 1036–1044, 2013. 34
- [202] Y. Amirat, V. Choqueuse, and M. Benbouzid, “Condition monitoring of wind turbines based on amplitude demodulation,” in *2010 IEEE Energy Conversion Congress and Exposition*. IEEE, 2010, pp. 2417–2421. 34, 36
- [203] Y. Amirat, V. Choqueuse, M. Benbouzid, and S. Turri, “Hilbert transform-based bearing failure detection in dfig-based wind turbines,” *International Review of Electrical Engineering*, vol. 6, no. 3, pp. 1249–1256, 2011. 34

REFERENCES

- [204] H. Nejjari and M. E. H. Benbouzid, "Monitoring and diagnosis of induction motors electrical faults using a current park's vector pattern learning approach," *IEEE Transactions on Industry Applications*, vol. 36, no. 3, pp. 730–735, 2000. 36, 44
- [205] A. Alkaya and İ. Eker, "Variance sensitive adaptive threshold-based pca method for fault detection with experimental application," *ISA transactions*, vol. 50, no. 2, pp. 287–302, 2011. 36
- [206] V. Choqueuse, M. E. H. Benbouzid, Y. Amirat, and S. Turri, "Diagnosis of three-phase electrical machines using multidimensional demodulation techniques," *IEEE Transactions on Industrial Electronics*, vol. 59, no. 4, pp. 2014–2023, 2012. 36
- [207] Y. Amirat, V. Choqueuse, and M. Benbouzid, "Wind turbine bearing failure detection using generator stator current homopolar component ensemble empirical mode decomposition," in *IECON 2012-38th Annual Conference on IEEE Industrial Electronics Society*. IEEE, 2012, pp. 3937–3942. 36
- [208] Y. Lei, J. Lin, Z. He, and M. J. Zuo, "A review on empirical mode decomposition in fault diagnosis of rotating machinery," *Mechanical Systems and Signal Processing*, vol. 35, no. 1, pp. 108–126, 2013.
- [209] W. Caesarendra, P. B. Kosasih, A. K. Tieu, C. A. S. Moodie, and B.-K. Choi, "Condition monitoring of naturally damaged slow speed slewing bearing based on ensemble empirical mode decomposition," *Journal of Mechanical Science and Technology*, vol. 27, no. 8, pp. 2253–2262, 2013.
- [210] Y. Amirat, V. Choqueuse, and M. Benbouzid, "Eemd-based wind turbine bearing failure detection using the generator stator current homopolar component," *Mechanical Systems and Signal Processing*, vol. 41, no. 1, pp. 667–678, 2013.
- [211] J. Faiz, V. Ghorbanian, and B. M. Ebrahimi, "Emd-based analysis of industrial induction motors with broken rotor bars for identification of operating point at different supply modes," *IEEE Transactions on Industrial Informatics*, vol. 10, no. 2, pp. 957–966, 2014.

-
- [212] D. Camarena-Martinez, M. Valtierra-Rodriguez, A. Garcia-Perez, R. A. Osornio-Rios, and R. d. J. Romero-Troncoso, "Empirical mode decomposition and neural networks on fpga for fault diagnosis in induction motors," *The Scientific World Journal*, vol. 2014, 2014. 44
- [213] J. Faiz, V. Ghorbanian, and B. M. Ebrahimi, "Emd-based analysis of industrial induction motors with broken rotor bars for identification of operating point at different supply modes," *IEEE Transactions on Industrial Informatics*, vol. 10, no. 2, pp. 957–966, 2014.
- [214] J. B. Ali, N. Fnaiech, L. Saidi, B. Chebel-Morello, and F. Fnaiech, "Application of empirical mode decomposition and artificial neural network for automatic bearing fault diagnosis based on vibration signals," *Applied Acoustics*, vol. 89, pp. 16–27, 2015. 36, 44
- [215] N. E. Huang, Z. Shen, S. R. Long, M. C. Wu, H. H. Shih, Q. Zheng, N.-C. Yen, C. C. Tung, and H. H. Liu, "The empirical mode decomposition and the hilbert spectrum for nonlinear and non-stationary time series analysis," vol. 454, no. 1971, pp. 903–995, 1998. 38
- [216] V. Fernandez-Cavero, D. Morinigo-Sotelo, O. Duque-Perez, and J. Pons-Llinares, "Fault detection in inverter-fed induction motors in transient regime: State of the art," in *Diagnostics for Electrical Machines, Power Electronics and Drives (SDEMPED), 2015 IEEE 10th International Symposium on*. IEEE, 2015, pp. 205–211. 38
- [217] E. El Ahmar, V. Choqueuse, M. Benbouzid, Y. Amirat, J. El Assad, R. Karam, and S. Farah, "Advanced signal processing techniques for fault detection and diagnosis in a wind turbine induction generator drive train: A comparative study," in *IEEE Energy Conversion Congress and Exposition (ECCE), 2010*, 2010, pp. 3576–3581. 38
- [218] E. ElBouchikhi, V. Choqueuse, M. Benbouzid, J.-F. Charpentier, and G. Barakat, "A comparative study of time-frequency representations for fault detection in wind turbine," in *IECON 2011-37th Annual Conference on IEEE Industrial Electronics Society*. IEEE, 2011, pp. 3584–3589.

REFERENCES

- [219] J. Pons-Llinares, J. A. Antonino-Daviu, M. Riera-Guasp, M. Pineda-Sanchez, and V. Climente-Alarcon, "Induction motor diagnosis based on a transient current analytic wavelet transform via frequency b-splines," *IEEE Transactions on Industrial Electronics*, vol. 58, no. 5, pp. 1530–1544, 2011.
- [220] K. S. Gaeid and H. W. Ping, "Wavelet fault diagnosis and tolerant of induction motor: A review," *International Journal of Physical Sciences*, vol. 6, no. 3, pp. 358–376, 2011.
- [221] V. Climente-Alarcon, J. Antonino-Daviu, M. Riera-Guasp, R. Puche-Panadero, and L. Escobar, "Application of the wigner–ville distribution for the detection of rotor asymmetries and eccentricity through high-order harmonics," *Electric Power Systems Research*, vol. 91, pp. 28–36, 2012.
- [222] J. Antonino-Daviu, S. Aviyente, E. G. Strangas, and M. Riera-Guasp, "Scale invariant feature extraction algorithm for the automatic diagnosis of rotor asymmetries in induction motors," *IEEE Transactions on Industrial Informatics*, vol. 9, no. 1, pp. 100–108, 2013.
- [223] E. Cabal-Yepez, A. G. Garcia-Ramirez, R. J. Romero-Troncoso, A. Garcia-Perez, and R. A. Osornio-Rios, "Reconfigurable monitoring system for time-frequency analysis on industrial equipment through stft and dwt," *IEEE Transactions on Industrial Informatics*, vol. 9, no. 2, pp. 760–771, 2013. 38
- [224] E. Elbouchikhi, V. Choqueuse, and M. E. H. Benbouzid, "Non-stationary spectral estimation for wind turbine induction generator faults detection," in *Industrial Electronics Society, IECON 2013-39th Annual Conference of the IEEE*. IEEE, 2013, pp. 7376–7381. 38
- [225] F. B. Batista, P. C. M. Lamim Filho, R. Pederiva, and V. A. D. Silva, "An empirical demodulation for electrical fault detection in induction motors," *IEEE Transactions on Instrumentation and Measurement*, vol. 65, no. 3, pp. 559–569, 2016. 39
- [226] R. Romero-Troncoso, A. Garcia-Perez, D. Morinigo-Sotelo, O. Duque-Perez, R. Osornio-Rios, and M. Ibarra-Manzano, "Rotor unbalance and broken rotor bar detection in inverter-fed induction motors at start-up and steady-state regimes

- by high-resolution spectral analysis,” *Electric Power Systems Research*, vol. 133, pp. 142–148, April 2016. 39
- [227] A. Garcia-Perez, R. J. Romero-Troncoso, E. Cabal-Yepez, R. Osornio-Rios, J. de Jesus Rangel-Magdaleno, H. Miranda *et al.*, “Startup current analysis of incipient broken rotor bar in induction motors using high-resolution spectral analysis,” in *Proceedings of the 2011 IEEE ISIE*, Bologna, Italy, September 2011, pp. 657–663. 39
- [228] R. Romero-Troncoso, D. Morinigo-Sotelo, O. Duque-Perez, P. Gardel-Sotomayor, R. Osornio-Rios, and A. Garcia-Perez, “Early broken rotor bar detection techniques in vsd-fed induction motors at steady-state,” in *IEEE International Symposium on Diagnostics for Electric Machines, Power Electronics and Drives (SDEMPED)*. IEEE, August 2013, pp. 105–113. 39
- [229] R. Romero-Troncoso, D. Morinigo-Sotelo, O. Duque-Perez, R. Osornio-Rios, M. Ibarra-Manzano, and A. Garcia-Perez, “Broken rotor bar detection in vsd-fed induction motors at startup by high-resolution spectral analysis,” in *International Conference on Electrical Machines (ICEM)*. IEEE, September 2014, pp. 1848–1854. 39
- [230] M. S. Ballal, Z. J. Khan, H. M. Suryawanshi, and R. L. Sonolikar, “Adaptive neural fuzzy inference system for the detection of inter-turn insulation and bearing wear faults in induction motor,” *IEEE Transactions on Industrial Electronics*, vol. 54, no. 1, pp. 250–258, 2007. 40
- [231] P. R. Cohen and E. A. Feigenbaum, *The handbook of artificial intelligence*. Butterworth-Heinemann, 2014, vol. 3. 40
- [232] F. Filippetti, G. Franceschini, C. Tassoni, and P. Vas, “Recent developments of induction motor drives fault diagnosis using ai techniques,” *IEEE transactions on industrial electronics*, vol. 47, no. 5, pp. 994–1004, October 2000. 40
- [233] A. Siddique, G. Yadava, and B. Singh, “Applications of artificial intelligence techniques for induction machine stator fault diagnostics: review,” in *IEEE International Symposium on Diagnostics for Electric Machines, Power Electronics and Drives (SDEMPED)*. IEEE, August 2003, pp. 29–34.

REFERENCES

- [234] M. A. Awadallah and M. M. Morcos, "Application of ai tools in fault diagnosis of electrical machines and drives-an overview," *IEEE Transactions on energy conversion*, vol. 18, no. 2, pp. 245–251, 2003. 40
- [235] A. Kandel, *Fuzzy expert systems*. CRC press, 1991. 40
- [236] X. Wen, "A hybrid intelligent technique for induction motor condition monitoring," Ph.D. dissertation, University of Portsmouth, 2011. 40
- [237] C. Angeli, "Diagnostic expert systems: From expert's knowledge to real-time systems," *Advanced knowledge based systems: Model, applications & research*, vol. 1, pp. 50–73, 2010. 40
- [238] S. M. M. Soe and M. P. P. Zaw, "Design and implementation of rule-based expert system for fault management," *World Academy of Science, Engineering and Technology*, vol. 48, pp. 34–39, 2008. 40
- [239] L. E. Widman and K. A. Loparo, "Artificial intelligence, simulation, and modeling," *Interfaces*, vol. 20, no. 2, pp. 48–66, 1990. 41
- [240] E. Turban and L. E. Frenzel, *Expert systems and applied artificial intelligence*. Prentice Hall Professional Technical Reference, 1992. 41
- [241] F. Filippetti, M. Martelli, G. Franceschini, and C. Tassoni, "Development of expert system knowledge base to on-line diagnosis of rotor electrical faults of induction motors," in *Industry Applications Society Annual Meeting, 1992., Conference Record of the 1992 IEEE*. IEEE, 1992, pp. 92–99. 41
- [242] D. Leith, N. Deans, and L. Stewart, "Condition monitoring of electrical machines using real-time expert system," in *Proc. 1988 Int. Conf. Electrical Machines*, vol. 3, 1988, pp. 297–302. 41
- [243] J. M. Mendel, "Fuzzy logic systems for engineering: a tutorial," *Proceedings of the IEEE*, vol. 83, no. 3, pp. 345–377, 1995. 41, 42
- [244] N. K. Kasabov, *Foundations of neural networks, fuzzy systems, and knowledge engineering*. Marcel Alencar, 1996. 42, 43

-
- [245] A. Pouliezios and G. S. Stavrakakis, *Real time fault monitoring of industrial processes*. Springer Science & Business Media, 2013, vol. 12. 42
- [246] M. Benbouzid and H. Nejjari, “A simple fuzzy logic approach for induction motors stator condition monitoring,” in *Electric Machines and Drives Conference, 2001. IEMDC 2001. IEEE International*. IEEE, 2001, pp. 634–639. 42
- [247] F. Zidani, M. E. H. Benbouzid, D. Diallo, and M. S. Naït-Saïd, “Induction motor stator faults diagnosis by a current concordia pattern-based fuzzy decision system,” *IEEE Transactions on Energy Conversion*, vol. 18, no. 4, pp. 469–475, December 2003.
- [248] M. Zeraoulia, A. Mamoune, H. Mangel, and M. Benbouzid, “A simple fuzzy logic approach for induction motors stator condition monitoring,” *J. Electrical Systems*, vol. 1, no. 1, pp. 15–25, 2005.
- [249] F. Zidani, D. Diallo, M. E. H. Benbouzid, and R. Naït-Saïd, “A fuzzy-based approach for the diagnosis of fault modes in a voltage-fed pwm inverter induction motor drive,” *IEEE Transactions on Industrial Electronics*, vol. 55, no. 2, pp. 586–593, February 2008.
- [250] M. F. D’Angelo, R. M. Palhares, R. H. Takahashi, and R. H. Loschi, “Fuzzy/bayesian change point detection approach to incipient fault detection,” *IET control theory & applications*, vol. 5, no. 4, pp. 539–551, March 2011.
- [251] R. J. Romero-Troncoso, R. Saucedo-Gallaga, E. Cabal-Yepez, A. Garcia-Perez, R. A. Osornio-Rios, R. Alvarez-Salas, H. Miranda-Vidales, and N. Huber, “Fpga-based online detection of multiple combined faults in induction motors through information entropy and fuzzy inference,” *IEEE Transactions on Industrial Electronics*, vol. 58, no. 11, pp. 5263–5270, 2011.
- [252] J. Zhang, W. Ma, J. Lin, L. Ma, and X. Jia, “Fault diagnosis approach for rotating machinery based on dynamic model and computational intelligence,” *Measurement*, vol. 59, pp. 73–87, 2015. 42
- [253] S. Ebersbach, “Artificial intelligent system for integrated wear debris and vibration analysis in machine condition monitoring,” Ph.D. dissertation, James Cook University, 2007. 42

REFERENCES

- [254] M. Berthold and D. J. Hand, *Intelligent data analysis: an introduction*. Springer Science & Business Media, 2003. 42
- [255] T. Munakata, *Fundamentals of the new artificial intelligence*. Springer, 1998, vol. 2. 43
- [256] Q.-j. Zhang and K. C. Gupta, *Neural networks for RF and microwave design (Book+ Neuromodeler Disk)*. Artech House, Inc., 2000. 43
- [257] Q.-J. Zhang, K. C. Gupta, and V. K. Devabhaktuni, “Artificial neural networks for rf and microwave design—from theory to practice,” *IEEE transactions on microwave theory and techniques*, vol. 51, no. 4, pp. 1339–1350, April 2003. 43
- [258] T. Ince, S. Kiranyaz, L. Eren, M. Askar, and M. Gabbouj, “Real-time motor fault detection by 1d convolutional neural networks,” *IEEE Transactions on Industrial Electronics*, to appear in 2017. 44
- [259] H. Nejari and M. Benbouzid, “Induction motor interturn short-circuit and bearing wear detection using artificial neural networks,” *Int. J. Electromotion*, vol. 5, no. 1, pp. 15–20, 1998. 44
- [260] G. Salles, F. Filippetti, C. Tassoni, G. Crelet, and G. Franceschini, “Monitoring of induction motor load by neural network techniques,” *IEEE Transactions on power electronics*, vol. 15, no. 4, pp. 762–768, July 2000.
- [261] K. Kim and A. G. Parlos, “Induction motor fault diagnosis based on neuropredictors and wavelet signal processing,” *IEEE/ASME Transactions on Mechatronics*, vol. 7, no. 2, pp. 201–219, June 2002.
- [262] H. C. Cho, J. Knowles, M. S. Fadali, and K. S. Lee, “Fault detection and isolation of induction motors using recurrent neural networks and dynamic bayesian modeling,” *IEEE Transactions on Control Systems Technology*, vol. 18, no. 2, pp. 430–437, 2010.
- [263] H. Su and K. T. Chong, “Induction machine condition monitoring using neural network modeling,” *IEEE Transactions on Industrial Electronics*, vol. 54, no. 1, pp. 241–249, 2007.

-
- [264] V. N. Ghate and S. V. Dudul, "Cascade neural-network-based fault classifier for three-phase induction motor," *IEEE Transactions on Industrial Electronics*, vol. 58, no. 5, pp. 1555–1563, May 2011.
- [265] J. Zarei, "Induction motors bearing fault detection using pattern recognition techniques," *Expert systems with Applications*, vol. 39, no. 1, pp. 68–73, 2012.
- [266] M. D. Prieto, G. Cirrincione, A. G. Espinosa, J. A. Ortega, and H. Henao, "Bearing fault detection by a novel condition-monitoring scheme based on statistical-time features and neural networks," *IEEE Transactions on Industrial Electronics*, vol. 60, no. 8, pp. 3398–3407, August 2013.
- [267] J. Zarei, M. A. Tajeddini, and H. R. Karimi, "Vibration analysis for bearing fault detection and classification using an intelligent filter," *Mechatronics*, vol. 24, no. 2, pp. 151–157, 2014.
- [268] W. Li, Z. Zhu, F. Jiang, G. Zhou, and G. Chen, "Fault diagnosis of rotating machinery with a novel statistical feature extraction and evaluation method," *Mechanical Systems and Signal Processing*, vol. 50, pp. 414–426, 2015.
- [269] G. H. Bazan, P. R. Scalassara, W. Endo, A. Goedtel, W. F. Godoy, and R. H. C. Palácios, "Stator fault analysis of three-phase induction motors using information measures and artificial neural networks," *Electric Power Systems Research*, vol. 143, pp. 347–356, 2017. 44
- [270] C. Bishop, *Pattern Recognition and Machine Learning (Information Science and Statistics)*, 1st edn. 2006. corr. 2nd printing edn. Springer, New York, 2007. 44
- [271] S. Abe, *Support vector machines for pattern classification*. Springer, 2005, vol. 2. 44
- [272] B. Samanta, "Gear fault detection using artificial neural networks and support vector machines with genetic algorithms," *Mechanical Systems and Signal Processing*, vol. 18, no. 3, pp. 625–644, 2004. 44
- [273] M. Barakat, D. Lefebvre, M. Khalil, O. Mustapha, and F. Druaux, "Bsp-bdt classification technique: Application to rolling elements bearing," in *2010 Conference on Control and Fault-Tolerant Systems (SysTol)*. IEEE, 2010, pp. 654–659.

REFERENCES

- [274] L. M. R. Baccarini, V. V. R. e Silva, B. R. De Menezes, and W. M. Caminhas, “Svm practical industrial application for mechanical faults diagnostic,” *Expert Systems with Applications*, vol. 38, no. 6, pp. 6980–6984, 2011.
- [275] D. Matic, F. Kulić, M. Pineda-Sánchez, and I. Kamenko, “Support vector machine classifier for diagnosis in electrical machines: Application to broken bar,” *Expert Systems with Applications*, vol. 39, no. 10, pp. 8681–8689, 2012.
- [276] S. B. Salem, K. Bacha, and A. Chaari, “Support vector machine based decision for mechanical fault condition monitoring in induction motor using an advanced hilbert-park transform,” *ISA transactions*, vol. 51, no. 5, pp. 566–572, June 2012. 44
- [277] H. Keskes, A. Braham, and Z. Lachiri, “Broken rotor bar diagnosis in induction machines through stationary wavelet packet transform and multiclass wavelet svm,” *Electric Power Systems Research*, vol. 97, pp. 151–157, 2013.
- [278] J. Seshadrinath, B. Singh, and B. K. Panigrahi, “Incipient turn fault detection and condition monitoring of induction machine using analytical wavelet transform,” *IEEE Transactions on Industry Applications*, vol. 50, no. 3, pp. 2235–2242, May/June 2014.
- [279] X. Zhang, Y. Liang, J. Zhou *et al.*, “A novel bearing fault diagnosis model integrated permutation entropy, ensemble empirical mode decomposition and optimized svm,” *Measurement*, vol. 69, pp. 164–179, 2015.
- [280] H. Keskes and A. Braham, “Recursive undecimated wavelet packet transform and dag svm for induction motor diagnosis,” *IEEE Transactions on Industrial Informatics*, vol. 11, no. 5, pp. 1059–1066, October 2015. 44
- [281] D. Whitley, “A genetic algorithm tutorial,” *Statistics and computing*, vol. 4, no. 2, pp. 65–85, 1994. 44
- [282] V. Martínez-Martínez, F. J. Gomez-Gil, J. Gomez-Gil, and R. Ruiz-Gonzalez, “An artificial neural network based expert system fitted with genetic algorithms for detecting the status of several rotary components in agro-industrial machines using a single vibration signal,” *Expert Systems with Applications*, vol. 42, no. 17, pp. 6433–6441, 2015. 45

-
- [283] N. Soni and T. Kumar, "Study of various mutation operators in genetic algorithms," *IJCSIT) International Journal of Computer Science and Information Technologies*, vol. 5, no. 3, pp. 4519–4521, 2014. 45
- [284] H. Razik, M. B. de Rossiter Correa, and E. R. C. Da Silva, "A novel monitoring of load level and broken bar fault severity applied to squirrel-cage induction motors using a genetic algorithm," *IEEE Transactions on Industrial Electronics*, vol. 56, no. 11, pp. 4615–4626, November 2009. 46
- [285] A. Raie and V. Rashtchi, "Using a genetic algorithm for detection and magnitude determination of turn faults in an induction motor," *Electrical Engineering (Archiv fur Elektrotechnik)*, vol. 84, no. 5, pp. 275–279, 2002. 46
- [286] Z. Wang, Y. Liu, and P. J. Griffin, "A combined ann and expert system tool for transformer fault diagnosis," *IEEE Transactions on Power Delivery*, vol. 13, no. 4, pp. 1224–1229, 1998. 46
- [287] C. E. Lin, J.-M. Ling, and C.-L. Huang, "An expert system for transformer fault diagnosis using dissolved gas analysis," *IEEE Transactions on Power Delivery*, vol. 8, no. 1, pp. 231–238, 1993.
- [288] M. Shukri, M. Khalid, R. Yusuf, and M. Shafawi, "Induction machine diagnostic using adaptive neuro fuzzy inferencing system," in *Knowledge-Based Intelligent Information and Engineering Systems*. Springer, 2004, pp. 380–387.
- [289] B.-S. Yang, M.-S. Oh, A. C. C. Tan *et al.*, "Fault diagnosis of induction motor based on decision trees and adaptive neuro-fuzzy inference," *Expert Systems with Applications*, vol. 36, no. 2, pp. 1840–1849, 2009.
- [290] V. T. Tran and B.-S. Yang, "Machine fault diagnosis and condition prognosis using classification and regression trees and neuro-fuzzy inference systems," *Control and Cybernetics*, vol. 39, no. 1, pp. 25–54, 2010.
- [291] L. Zhang, G. Xiong, H. Liu, H. Zou, and W. Guo, "Bearing fault diagnosis using multi-scale entropy and adaptive neuro-fuzzy inference," *Expert Systems with Applications*, vol. 37, no. 8, pp. 6077–6085, 2010.

REFERENCES

- [292] S. G. Vijay, S. Kumar, P. P. Srinivasa, S. Sriram, and R. B. Rao, “Evaluation of effectiveness of wavelet based denoising schemes using ann and svm for bearing condition classification,” *Computational intelligence and neuroscience*, vol. 2012, p. 16, 2012.
- [293] Y. Li, M. Xu, H. Zhao, and W. Huang, “Hierarchical fuzzy entropy and improved support vector machine based binary tree approach for rolling bearing fault diagnosis,” *Mechanism and Machine Theory*, vol. 98, pp. 114–132, 2016. 46
- [294] S. Z. Gürbüz, “Radar detection and identification of human signatures using moving platforms,” Ph.D. dissertation, Georgia Institute of Technology, December 2009. 46
- [295] S. M. Kay, *Fundamentals of statistical signal processing, Volume II: Detection theory*. Prentice Hall Upper Saddle River, NJ, USA:, January 1998. 46, 83, 101, 102
- [296] S. Choi, B. Akin, M. M. Rahimian, and H. A. Toliyat, “Implementation of a fault-diagnosis algorithm for induction machines based on advanced digital-signal-processing techniques,” *IEEE Transactions on Industrial Electronics*, vol. 58, no. 3, pp. 937–948, March 2011. 47
- [297] Y. Selén, “Model selection and sparse modeling,” Ph.D. dissertation, Department of Information Technology, Uppsala University, October 2007. 51, 53
- [298] S. M. Kay, *Fundamentals of Statistical Processing, Volume I: Estimation Theory*. Upper Saddle River, Prentice Hall, Signal Processing, April 1993. 51, 53, 54, 99
- [299] P. Stoica and P. Babu, “The gaussian data assumption leads to the largest Cramér-Rao bound [lecture notes],” *IEEE Signal Processing Magazine*, vol. 28, no. 3, pp. 132–133, May 2011. 51
- [300] M. Rosenblatt, “A central limit theorem and a strong mixing condition,” *Proceedings of the National Academy of Sciences of the United States of America*, vol. 42, no. 1, p. 43, 1956. 52
- [301] “International Electrotechnical Commission IEC 038, Standard Voltages,” in *International Electrotechnical Commission*, 1999. 53, 70, 98

-
- [302] E. Elbouchikhi, V. Choqueuse, and M. E. H. Benbouzid, “Current frequency spectral subtraction and its contribution to induction machines’ bearings condition monitoring,” *IEEE Transactions on Energy Conversion*, vol. 28, no. 1, pp. 135–144, December 2013. 53
- [303] P. Stoica, “List of references on spectral line analysis,” *Signal Processing*, vol. 31, no. 3, pp. 329–340, September 1993. 53, 55
- [304] S. Kay and S. Saha, “Mean likelihood frequency estimation,” *IEEE Transactions on Signal Processing*, vol. 48, no. 7, pp. 1937–1946, July 2000. 54
- [305] J. K. Nielsen, “Some new results on the estimation of sinusoids in noise,” Ph.D. dissertation, Ph. d. thesis, Aalborg University, Denmark, 2012. 56
- [306] F. Castanié, *Digital spectral analysis: parametric, non-parametric and advanced methods*. John Wiley & Sons, 2013. 56
- [307] Y. Hua, A. Gershman, and Q. Cheng, *High-resolution and robust signal processing*. CRC Press, 2003. 57, 58, 60
- [308] G. Blanchet and M. Charbit, *Digital Signal and Image Processing Using Matlab*. Iste London, May 2006, vol. 4. 58, 60
- [309] D. G. Manolakis, V. K. Ingle, and S. M. Kogon, *Statistical and Adaptive Signal Processing: Spectral Estimation, Signal Modeling, Adaptive Filtering, and Array Processing*. Artech House Norwood, May 2005, vol. 46. 60, 61, 62
- [310] R. Roy and T. Kailath, “ESPRIT-estimation of signal parameters via rotational invariance techniques,” *IEEE Transactions on Acoustics, Speech and Signal Processing*, vol. 37, no. 7, pp. 984–995, July 1989. 60
- [311] K. Mahata and T. Soderstrom, “Esprit-like estimation of real-valued sinusoidal frequencies,” *IEEE transactions on signal processing*, vol. 52, no. 5, pp. 1161–1170, May 2004. 65
- [312] F.-M. Han and X.-D. Zhang, “An esprit-like algorithm for coherent doa estimation,” *IEEE Antennas and Wireless Propagation Letters*, vol. 4, pp. 443–446, December 2005. 65

REFERENCES

- [313] Y.-L. Xu, H.-S. Zhang, and J.-S. Zhan, "A signal-subspace-based esprit-like algorithm for coherent doa estimation," in *Proceedings of the 5th International Conference on Wireless communications, networking and mobile computing*. IEEE Press, 2009, pp. 2323–2326.
- [314] L. Liu, Y. Gai, H. Wang, and G. Ding, "An improved esprit-like algorithm for coherent signal and its application for 2-d doa estimation," in *2006 7th International Symposium on Antennas, Propagation & EM Theory*. IEEE, 2006, pp. 1–4.
- [315] Y. Wang, Z. Liu, Z. Yin, Q. Sun, and X. Liang, "An esprit-like algorithm for coherent angle estimation in bistatic mimo radar," in *IET International Radar Conference 2015*. IET, 2015, pp. 1–6.
- [316] Y. yang Ma, C. xiao Li, and J. Yang, "An improved algorithm based on esprit-like for coherent signals," in *Communication Technology (ICCT), 2012 IEEE 14th International Conference on*. IEEE, 2012, pp. 1072–1076.
- [317] F.-J. Chen, S. Kwong, and C.-W. Kok, "Esprit-like two-dimensional doa estimation for coherent signals," *IEEE Transactions on Aerospace and Electronic Systems*, vol. 46, no. 3, pp. 1477–1484, July 2010.
- [318] F. K. Chan, H. So, L. Huang, and L.-T. Huang, "Parameter estimation and identifiability in bistatic multiple-input multiple-output radar," *IEEE Transactions on Aerospace and Electronic Systems*, vol. 51, no. 3, pp. 2047–2056, 2015. 65
- [319] K. Mahata, "Subspace fitting approaches for frequency estimation using real-valued data," *IEEE transactions on signal processing*, vol. 53, no. 8, pp. 3099–3110, 2005. 66
- [320] A. Mariani, A. Giorgetti, and M. Chiani, "Model order selection based on information theoretic criteria: design of the penalty," *IEEE Transactions on Signal Processing*, vol. 63, no. 11, pp. 2779–2789, June 2015. 66, 67, 68, 69
- [321] P. Stoica and Y. Selen, "Model-order selection: a review of information criterion rules," *IEEE Transactions on Signal Processing Magazine*, vol. 21, no. 4, pp. 36–47, July 2004. 67

-
- [322] J.-J. Fuchs, “Estimating the number of sinusoids in additive white noise,” *IEEE Transactions on Acoustics, Speech, and Signal Processing*, vol. 36, no. 12, pp. 1846–1853, 1988.
- [323] P. M. Djurić, “A model selection rule for sinusoids in white gaussian noise,” *IEEE Transactions on Signal Processing*, vol. 44, no. 7, pp. 1744–1751, 1996. 67
- [324] A. Quinlan, J.-P. Barbot, P. Larzabal, and M. Haardt, “Model order selection for short data: An exponential fitting test (eft),” *EURASIP Journal on Applied Signal Processing*, vol. 2007, no. 1, pp. 201–201, 2007. 67
- [325] A. P. Liavas and P. A. Regalia, “On the behavior of information theoretic criteria for model order selection,” *IEEE Transactions on Signal Processing*, vol. 49, no. 8, pp. 1689–1695, August 2001. 67
- [326] T. W. Anderson, “Asymptotic theory for principal component analysis,” *The Annals of Mathematical Statistics*, vol. 34, no. 1, pp. 122–148, March 1963. 68
- [327] A. Bazzi, D. T. Slock, and L. Meilhac, “Detection of the number of superimposed signals using modified mdl criterion: A random matrix approach,” in *2016 IEEE International Conference on Acoustics, Speech and Signal Processing (ICASSP)*. IEEE, 2016, pp. 4593–4597. 69
- [328] X. Mestre, “Improved estimation of eigenvalues and eigenvectors of covariance matrices using their sample estimates,” *IEEE Transactions on Information Theory*, vol. 54, no. 11, pp. 5113–5129, 2008. 69
- [329] Q. Wu and D. R. Fuhrmann, “A parametric method for determining the number of signals in narrow-band direction finding,” *IEEE Transactions on Signal Processing*, vol. 39, no. 8, pp. 1848–1857, August 1991. 69
- [330] B. Nadler, “Nonparametric detection of signals by information theoretic criteria: performance analysis and an improved estimator,” *IEEE Transactions on Signal Processing*, vol. 58, no. 5, pp. 2746–2756, 2010. 69
- [331] S. Chaudhari *et al.*, “Spectrum sensing for cognitive radios: Algorithms, performance, and limitations,” 2012. 84

REFERENCES

- [332] M. Barkat, *Signal detection and estimation*. Artech house, 1991. 84, 92
- [333] R. D. Hippenstiel, *Detection theory: applications and digital signal processing*. CRC Press, 2001. 88, 91
- [334] M. Feder and N. Merhav, “Universal composite hypothesis testing: A competitive minimax approach,” *IEEE Transactions on information theory*, vol. 48, no. 6, pp. 1504–1517, 2002. 93
- [335] F. Y. Nan and R. D. Nowak, “Generalized likelihood ratio detection for fmri using complex data,” *IEEE Transactions on Medical Imaging*, vol. 18, no. 4, pp. 320–329, April 1999. 95
- [336] Y. Trachi, E. Elbouchikhi, V. Choqueuse, M. E. H. Benbouzid, and T. Wang, “A novel induction machine faults detector based on hypothesis testing,” *IEEE Transactions on Industry Applications*, 2016. 98
- [337] Y. Trachi, E. Elbouchikhi, V. Choqueuse, W. Tianzhen, and M. E. H. Benbouzid, “Induction machines fault detection based on constant false alarm rate detector,” in *Proceedings of the 2016 IEEE IECON*, Florence, Italy, October 2016, pp. 1–5. 102

Contribution à la Détection de Défauts dans les Machines Asynchrones à l'aide de Techniques Paramétriques de Traitement de Signal

Résumé—L'objectif de ces travaux de thèse est de développer des architectures fiables de surveillance et de détection des défauts d'une machine asynchrone basées sur des techniques paramétriques de traitement du signal. Pour analyser et détecter les défauts, un modèle paramétrique du courant statorique en environnement stationnaire est proposé. Il est supposé être constitué de plusieurs sinusoides avec des paramètres inconnus dans le bruit. Les paramètres de ce modèle sont estimés à l'aide des techniques paramétriques telles que les estimateurs spectraux de type sous-espaces (MUSIC et ESPRIT) et l'estimateur du maximum de vraisemblance. Un critère de sévérité des défauts, basé sur l'estimation des amplitudes des composantes fréquentielles du courant statorique, est aussi proposé pour évaluer le niveau de défaillance de la machine. Un nouveau détecteur des défauts est aussi proposé en utilisant la théorie de détection. Il est principalement basé sur le test du rapport de vraisemblance généralisé avec un signal et un bruit à paramètres inconnus. Enfin, les techniques paramétriques proposées ont été évaluées à l'aide de signaux de courant statoriques expérimentaux de machines asynchrones en considérant les défauts de roulements et les ruptures de barres rotoriques. L'analyse des résultats expérimentaux montre clairement l'efficacité et la capacité de détection des techniques paramétriques proposées.

Mots-Clés—Machine asynchrone, surveillance, détection des défauts, analyse du courant statorique, maximum de vraisemblance, techniques de sous-espace, sévérité des défauts, test d'hypothèses, le test du rapport de vraisemblance généralisé.

On Induction Machine Faults Detection using Advanced Parametric Signal Processing Techniques

Abstract—This Ph.D. thesis aims to develop reliable and cost-effective condition monitoring and faults detection architectures for induction machines. These architectures are mainly based on advanced parametric signal processing techniques. To analyze and detect faults, a parametric stator current model under stationary conditions has been considered. It is assumed to be multiple sinusoids with unknown parameters in noise. This model has been estimated using parametric techniques such as subspace spectral estimators and maximum likelihood estimator. A fault severity criterion based on the estimation of the stator current frequency component amplitudes has also been proposed to determine the induction machine failure level. A novel faults detector based on hypothesis testing has been also proposed. This detector is mainly based on the generalized likelihood ratio test detector with unknown signal and noise parameters. The proposed parametric techniques have been evaluated using experimental stator current signals issued from induction machines under two considered faults: bearing and broken rotor bars faults. Experimental results show the effectiveness and the detection ability of the proposed parametric techniques.

Keywords—Induction machine, condition monitoring, faults detection, stator current analysis, maximum likelihood, subspace techniques, fault severity, hypothesis testing, generalized likelihood ratio test.